BRNO UNIVERSITY OF TECHNOLOGY

VYSOKÉ UČENÍ TECHNICKÉ V BRNĚ

FACULTY OF CHEMISTRY

FAKULTA CHEMICKÁ

INSTITUTE OF MATERIALS SCIENCE

ÚSTAV CHEMIE MATERIÁLŮ

INFLUENCE OF PREPOLYMERIZATION OF MGCL2-SUPPORTED TICL4 CATALYST ON PROPENE POLYMERIZATION AND PROPERTIES OF RESULTANT POLYPROPENE POWDER

VLIV PŘEDPOLYMERACE MGCL2- NOSIČOVÉHOTICL4 KATALYZÁTORU NA POLYMERACI PROPENU A VLASTNOSTI VÝSLEDNÉHO POLYPROPENOVÉHO PRÁŠKU.

MASTER'S THESIS

DIPLOMOVÁ PRÁCE

AUTHOR
AUTOR PRÁCE

Bc. Peter Gažo

SUPERVISOR
VEDOUCÍ PRÁCE

Ing. Jan Kratochvíla, CSc.

BRNO 2018

VYSOKÉ UČENÍ TECHNICKÉ V BRNĚ
FAKULTA CHEMICKÁ

Zadání diplomové práce

Číslo práce:	FCH-DIP1172/2017
Ústav:	Ústav chemie materiálů
Student:	**Bc. Peter Gažo**
Studijní program:	Chemie, technologie a vlastnosti materiálů
Studijní obor:	Chemie, technologie a vlastnosti materiálů
Vedoucí práce:	**Ing. Jan Kratochvíla, CSc.**
Akademický rok:	2017/18

Název diplomové práce:

Vliv předpolymerace MgCl2– nosičovéhoTiCl4 katalyzátoru na polymeraci propenu a vlastnosti výsledného polypropenového prášku.

Zadání diplomové práce:

Cílem této práce bude prostudovat vliv předpolymerace na vybraný komerční MgCl2–nosičový TiCl4 katalyzátor (tzv. Zieglerův–Nattův). Výsledkem práce by mělo být nalezení optimálních podmínek, které umožní ideálně využít této techniky k modifikaci struktury a morfologie zvoleného katalyzátoru a dosažení stabilnějšího průběhu polymerace a lepších vlastností produkovaného polypropenu. U předpolymerací bude studován vliv teploty, koncentrace triethylhliníkového kokatalyzátoru a externího donoru, množství polyolefinu syntetizovaného během předpolymerace (tzv. stupeň předpolymerace) na následné chování předpolymerovaného katalyzátoru při plynofázní polymeraci propenu.

Termín odevzdání diplomové práce: 7.5.2018

Diplomová práce se odevzdává v děkanem stanoveném počtu exemplářů na sekretariát ústavu. Toto zadání je součástí diplomové práce.

Bc. Peter Gažo student(ka)	Ing. Jan Kratochvíla, CSc. vedoucí práce	prof. RNDr. Josef Jančář, CSc. vedoucí ústavu

V Brně dne 31.1.2018

prof. Ing. Martin Weiter, Ph.D.
děkan

ABSTRAKT

Cílem této práce bylo prostudovat vliv předpolymerace na vybraný komerční $MgCl_2$–nosičový $TiCl_4$ katalyzátor (tzv. Zieglerův-Nattův). Výsledkem práce bylo nalezení optimálních podmínek, které umožní ideálně využít této techniky k modifikaci struktury a morfologie zvoleného katalyzátoru a dosažení stabilnějšího průběhu polymerace a lepších vlastností produkovaného polypropenu. U předpolymerací byl studován vliv teploty, koncentrace triethylhliníkového kokatalyzátoru a externího donoru, množství polyolefinu syntetizovaného během předpolymerace (tzv. stupeň předpolymerace) na následné chování předpolymerovaného katalyzátoru při plynofázní polymeraci propenu.

ABSTRACT

The influence of pre–polymerization on the selected commercial $MgCl_2$–supported $TiCl_4$ catalyst (Ziegler–Natta) was studied. The work was focused on the evaluation of optimal conditions of pre–polymerization, which allow efficient modification of the selected catalyst and achievement of more stable process of the polymerization combined with better properties of produced polypropene. The influence of the temperature, concentration of triethylaluminum co–catalyst, external donor and amount of polyolefin synthetized during pre–polymerization (degree of pre–polymerization) on subsequent behavior of pre–polymerized catalyst in the gas-phase propene polymerization was evaluated.

KLÍČOVÁ SLOVÁ

Předpolymerace, propen, Zieglerův-Nattův kazalyzátor, plynofázní polymerace

KEY WORDS

Pre–polymerization, propene, Ziegler–Natta catalyst, gas–phase polymerization

GAŽO, P. *Vliv předpolymerace $MgCl_2$–nosičového $TiCl_4$ katalyzátoru na polymeraci propenu a vlastnosti výsledného polypropenového prášku.* Brno: Vysoké učení technické v Brně, Fakulta chemická, 2018. 80 s. Vedoucí diplomové práce Ing. Jan Kratochvíla, CSc..

DECLARATION

I declare that I wrote this Master thesis by myself and all literature sources are cited correctly and completely. This Master thesis from the point of view of content is a property of Faculty of Chemistry, Brno, University of Technology, and can be used for commercial use only with the approval of supervisor of Master thesis and dean of FCH, BUT.

.....

Student´s signature

ACKNOWLEDGEMENT

I would like to thank the company Unipetrol RPA, s.r.o. – Polymer Institute Brno, odštěpný závod, for support of my research. Also, I would like to thank the company W. R. Grace for providing the catalyst.

I would like to express sincerely thanks to my supervisors Dr. Ing. Miroslav Skoumal and Ing. Jan Kratochvíla, Csc. for their support and helpful advices and great interest in my work. Many thanks to RNDr. Igor Cejpek, Csc. for giving me helpful advices and carrying out the kinetic calculations. Also, I can not forget to thank to Jana Leonová and Marie Černohorská, who were always willing to help me with my research, teach me polymerization procedures as well as determination procedures of polymer properties.

My biggest thanks belong to my family, who always supported me during my university studies. This work is dedicated to my parents and grandparents without whom this would not be possible.

Peter Gažo
Brno, May 2018

Content

1. Introduction

Until 1950s propene polymer was considered to be useless branched low molecular weight amorphous oil, of no interest. The development in polymer science from early 1920s caused continual research of this sector. Some theories about polyolefin properties were predicted, but nobody have prepared high molecular weight polyolefins before. The effort of Karl Ziegler supported by Julio Natta (both were awarded the Nobel Prize for chemistry in 1963) to cause the growth of alkyl chains by insertion of ethylene into the Al–C bond of trialkylaluminum caused one of the biggest breakthroughs in polymer science. The high molecular weight polyethylene (PE) was first time prepared in 1953 followed by preparation of high molecular weight polypropene (PP) in March 1954 [1]. Ziegler–Natta catalysts have been used in the commercial manufacture of various polyolefin since 1956. Since this dates, the global polyolefin industry has become a tremendous business with annual production of around 131 million metric tons [2]. Polypropene becomes second largest thermoplastics by volume, ranking after polyethylene and his world demand increases. The average annual growth is forecasted at 5 – 6 %. The main reason for this success is the low price and the interesting material properties. The development of new technologies for polymerization processes and the development of catalyst systems, the scope of polyolefin products has rapidly increased and applications that used to require relatively expensive materials as polyvinylchloride (PVC) and poly–acrylonitrile–butadiene–styrene (ABS) can be with cheaper polyolefin replaced [3].

1.1 Ziegler–Natta Catalyst

A typical Ziegler–Natta (ZN) catalyst consists of the combination of the transition metals compounds IV.–VIII. group of the periodic table, usually halide or oxyhalide of titanium, vanadium or chromium and organometallic compounds of metals of I.–III. groups in periodic table – hydrides, alkyl or aryl derivatives of aluminum, lithium, zinc or magnesium using as co–catalyst are overwhelmingly preferred [4]. The most commonly ZN catalyst system consists of the combination of $TiCl_3$ or $TiCl_4$ with trialkylaluminum compounds. The titanium chloride compound has a crystal structure in which each Ti atom is coordinated to 6 chlorine atoms. On the crystal surface, Ti atom is surrounded by 5 chlorine atoms with one empty orbital. The co–catalyst donates an alkyl group to Ti atom and the Al atom is coordinated to one of the Cl atoms. Simultaneously, one Cl atom from Ti catalyst is cleaved and this process caused an empty orbital in the system. By the coordination of the co-catalyst, the catalyst is activated (**Figure 1.1.1**) [5–7].

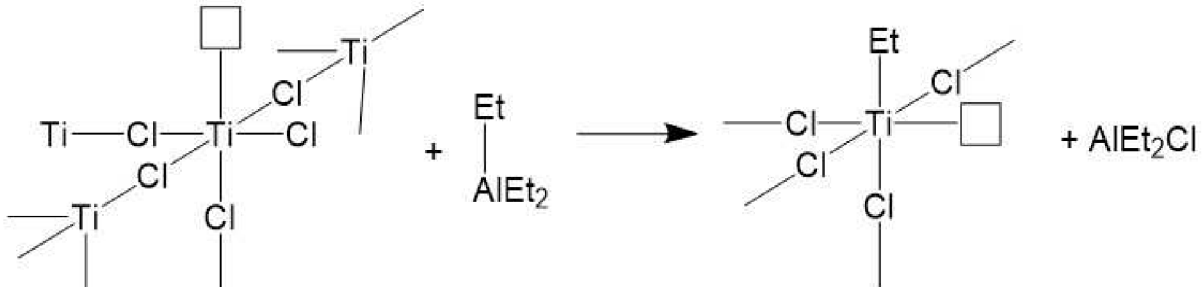

Figure 1.1.1: *Scheme of the activation of ZN catalyst system by coordination of triethylaluminum ($AlEt_3$) to Ti atom [7].*

The polymerization process is initiated by formation of alkene–metal complex. An alkene monomer, which has filled π–bonding and empty π–anti bonding orbitals can coordinate with Ti atom, with empty dxy orbital and filled $dx^2–y^2$ orbital in outermost shell, by overlapping their orbitals, i.e. π–bonding and dxy bonding orbital share a pair of electron followed by sharing another pair of electrons from π–anti bonding and $dx^2–y^2$ orbital (**Figure 1.1.2**).

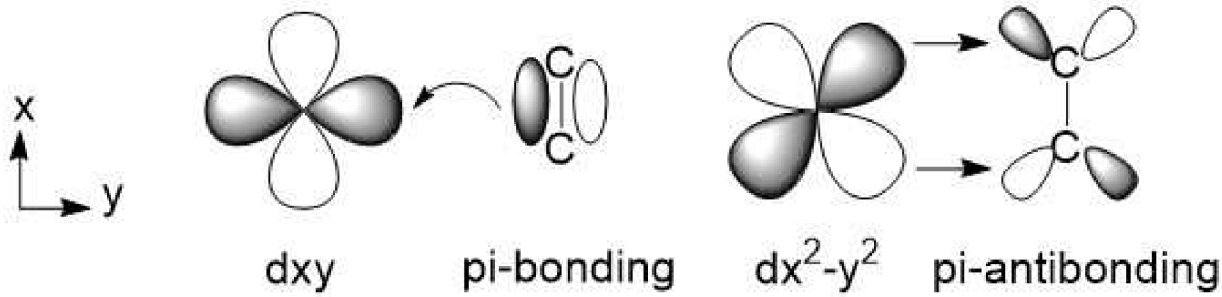

Figure 1.1.2: *Molecular orbitals representation of monomer coordinating to metal center [7].*

A several electron pairs shift their position in this complex. The electron pair from π–bond shift to form Ti–C bond, the pair of electrons from the bond between Ti and ethyl group of $AlEt_3$ shift to form bond between the ethyl group and the methyl–substituted carbon of alkene. After this, Ti atom has empty orbital again needing electrons to fill it (**Figure 1.1.3**).

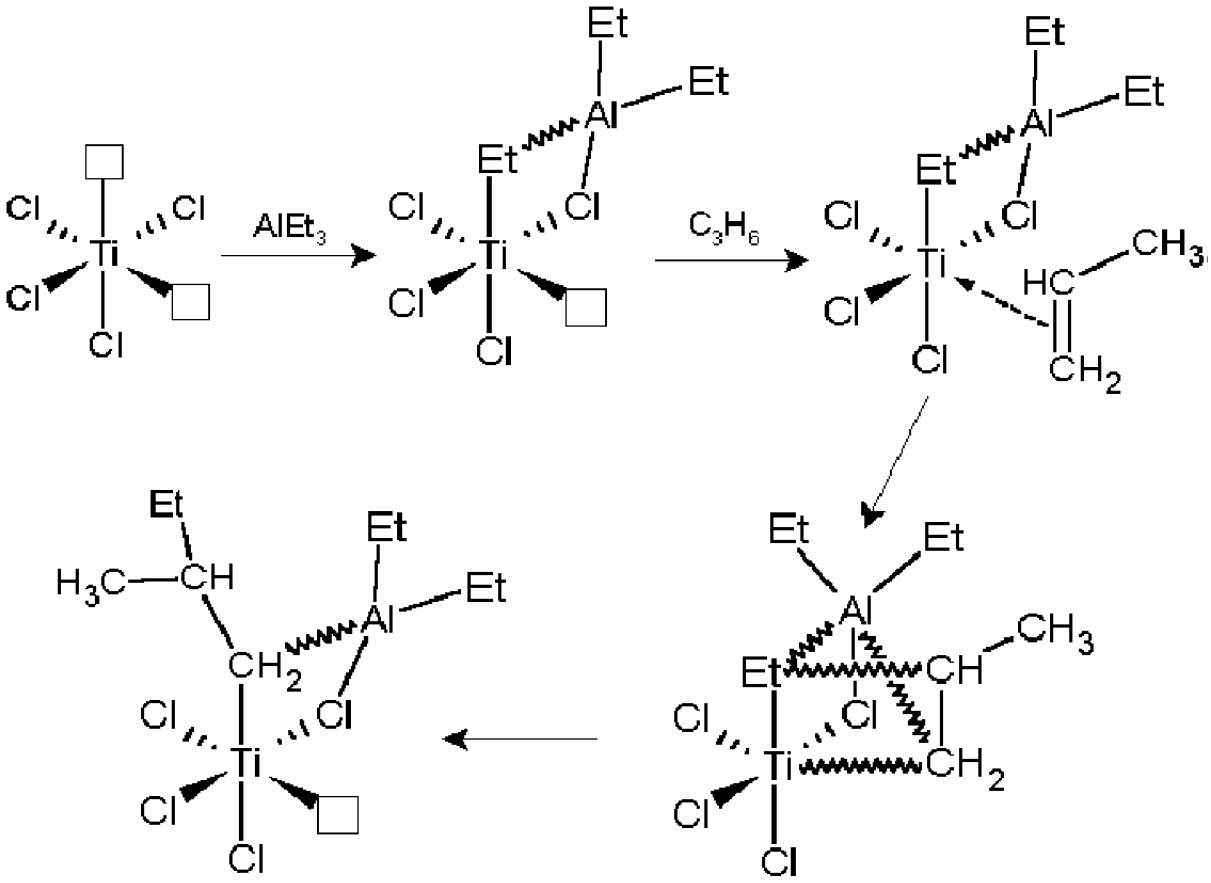

Figure 1.1.3: *Mechanism of coordination polymerization on the bimetallic active center according to Rodriguez [7].*

1.1.1 Homogeneous Ziegler–Natta Catalyst

In 1957, Breslow and Natta introduced independently soluble catalyst [8–10] based on transition metallocenes (titanocenes, zirconocenes and hafnocenes), as a bis(cyclopentadienyl) titanium dichloride ($Ti(Cp)_2Cl_2$), characterized by two bulky cyclopentadienyl (Cp) ligands with C_2 symmetry (**Figure 1.1.4**).

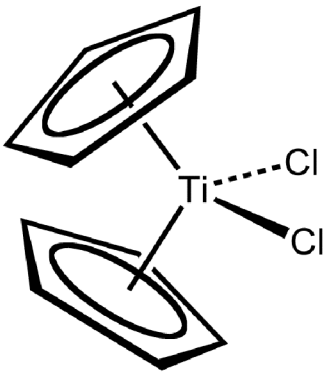

Figure 1.1.4: *Scheme of bis(cyclopentadienyl) titanium dichloride catalyst [10].*

These catalysts were activated with alkylaluminum chloride (AlR_2Cl), but it was less active in PE polymerization in comparison with heterogeneous ZN catalyst system. However, it was much better for basic research of catalyst nature. This catalyst system was not active in

propene polymerization. A further research showed that a small amount of impurities as oxygen, ether or water in catalyst system has positive effect on the activity of catalyst. Especially, the reaction between water and aluminum alkyls to produce alkylalumoxanes is significant and became the basis of methylalumoxane (MAO) as a most important co–catalyst of metallocene compounds [11,12,14]. By using this catalyst system, high activity of ethylene polymerization was obtained. However, only atactic polypropene was synthetized by using this catalyst. This problem was solved in 1980s by Brintzinger and his group [13] by preparation of catalysts as ethylene bis–indenylzirconium ($Et(Ind)_2ZrC1_2$) (**Figure 1.1.5**) also called ansa–metallocene, where two indenyl (Ind) ligands are arranged in a chiral array and connected together with chemical bonds by a bridging group. These catalyst activated by MAO were able to perform the stereoselective polymerization of propene with high activity [14].

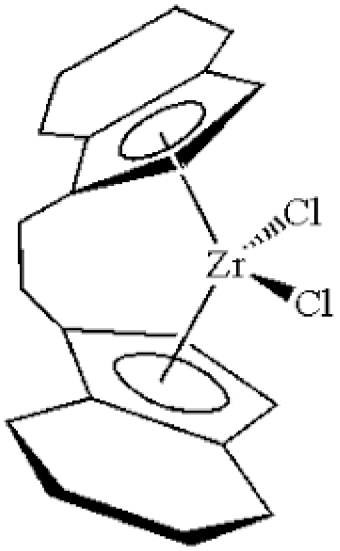

Figure 1.1.5: *$Et(Ind)_2ZrC_{12}$ able to synthetize isotactic PP[13].*

The subsequent catalyst modifications of the ligands surrounding the active center permits a correlation of catalyst structure with catalytic activity and stereospecificity. The polymerization processes in homogeneous systems are often more simple in comparison with heterogeneous, kinetic and mechanistic analyses for these systems are significantly simplified. Studies made on such metallocene compounds have increased understanding of the molecular mechanism of stereochemical control in α–olefin polymerizations.

1.1.2 **Heterogeneous Catalyst System**

This type of catalyst system dominate in industry. Mostly it is based on titanium or vanadium compounds in combination with alkylaluminum compounds as a co–catalyst. The $TiCl_3/AlEt_2Cl$ catalyst used in the earlier PP industrial process, showed a low activity and stereospecifity. Also, catalyst residues and removing of atactic polymer fraction were required. Heterogeneous, also called conventional catalysts have been continuously improved to increase their activity and stereospecificity [3].

1.1.2.1 *First Generation of ZN Catalyst*

The Natta´s group in 1957 discovered that the mixture of $TiCl_3$ and $AlCl_3$ as a catalyst is much more active in comparison with pure $TiCl_3$. Three structural modifications (α, γ and δ) out of the four possible ones for $TiCl_3$ are highly stereoselective [15]. The three modifications had a purple color and a layer lattice structure and differ in the mode of Cl^- packing (**Figure 1.1.6**) [3,16]. The presence of $AlCl_3$ causes simple replacement of Ti^{3+} by Al^{3+} ion in the crystal lattice without significantly modifying the unit cell parameters, but activities are from 2 to 7 times higher in combination with $AlEt_2Cl$ [17]. This catalyst was called AA–$TiCl_3$, where AA means Al–reduced and activated, and is considered as first generation ZN catalyst for PP. The productivity and stereospecificity were still low and removal of catalyst residues and atactic PP were required, what caused manufacturing of isotactic PP expensive [3].

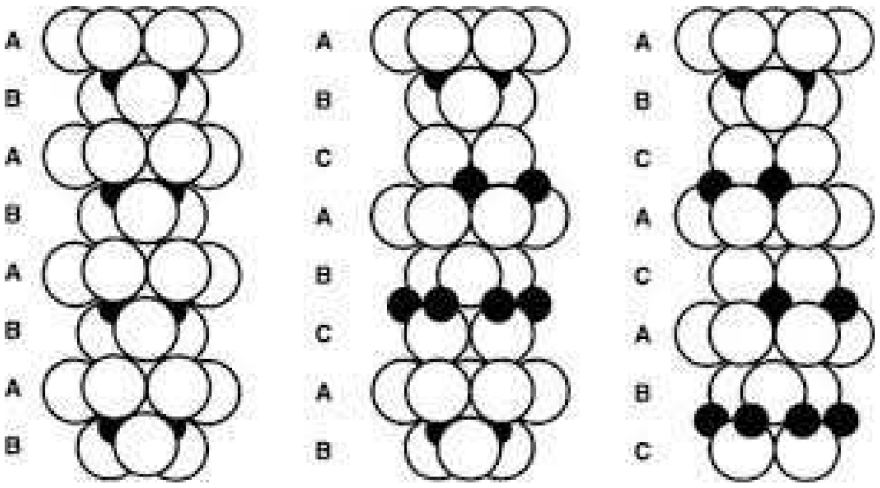

Figure 1.1.6: *Modifications of $TiCl_3$ α–hexagonal form (left) ,γ–cubic form (center) and δ–random succession of hexagonal and cubic form (right)[16].*

1.1.2.2 *Second Generation of ZN Catalyst*

Solvay in 1970s developed $TiCl_3$ catalyst with much higher surface area (>150 $m^2 \cdot g^{-1}$) than previous AA–$TiCl_3$ (30–40 $m^2 \cdot g^{-1}$) [18]. This „Solvay" catalyst has spherical shape with porous surface with diameter of micropores at about 200 Å, almost fivefold activity (1900 $g_{PP} \cdot g_{TiCl3}^{-1}$) and isotactic index at about 95 %. The catalyst surface modification with diethylaluminum chloride (DEAC) as co–catalyst can be considered as the beginning of second generation of ZN catalyst. Subsequently, this catalyst was improved by addition of alkoxysilanes as a third component what further increased higher activity and isotactic index. However, the removal of catalyst residues was still required.

1.1.2.3 *Third Generation of ZN Catalyst*

The effort to improve catalyst system led to support the $TiCl_3$ active species on the surface of inorganic materials with chemical reaction. In this time, the concentration of $TiCl_3$ active species was less than 0.1 wt.%, what was the reason for replacing of internal $TiCl_3$ with inorganic support. The history of third generation of ZN catalyst began in 1960s, when $MgCl_2$

as a support material for $TiCl_4$, was patented [18]. $MgCl_2$ is effective support, because it has similar crystalline structures and values of ionic radius as $TiCl_4$. Many authors [20–22] described two crystalline modifications of $MgCl_2$, α-$MgCl_2$ with commercial use and less stable β–form. However, the most suitable form for this catalyst generation is δ–form, also called activated form, which has disordered structure originating from the rotation and translation of the structural Cl–Mg–Cl layers producing high surface area (**Figure 1.1.7**). According to Gianinni and his team [24], Mg^{2+} atoms are coordinated with 4 or 5 Cl^- atoms on preferential lateral cleavage surfaces. These lateral cuts are responsible for (110) and (100) faces of $MgCl_2$, which can coordinate with bridged dinuclear Ti_2Cl_8 species and after contact with an appropriate co–catalyst, these species are reduced to Ti_2Cl_6 in which the environment of the Ti atoms are chiral, suitable for isospecific polymerization. The influence of different conditions on preparation of $MgCl_2$–supported catalyst has been described by Garoff et. al. [25].

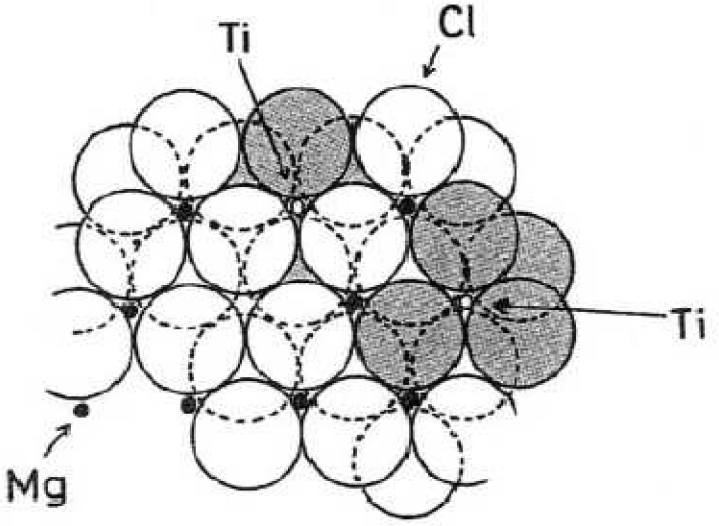

Figure 1.1.7: *Model for surface of an $MgCl_2$–supported $TiCl_4$ [20].*

The research performed by Norio Kashiwa [19] brought drastically increased specific surface area to 292 $m^2 \cdot g^{-1}$. He found out that this catalyst activated with triethylaluminum (TEA) has activity more than 100 times higher in comparison with former catalyst generations, but the stereoregularity was very low. Kashiwa noticed that an addition of third compound called an electron donor, which could coordinate on the $MgCl_2$ surface can improve low stereospecificity and allow manufacturers to control the active species structure. The electron donors could be classified into 2 types. The role of internal donor (ID) is to stabilize small primary crystallites of $MgCl_2$ and control the amount and distribution of $TiCl_4$ in the final catalyst. Without ID, $TiCl_4$ will coordinate to both faces of $MgCl_2$, but presence of ID cause competition between donor and $TiCl_4$ for the available coordination sites, but because of high acidity of the coordination sites on the (100) face, the coordination of the donor on these sites will avoid the formation of Ti species with poor selectivity. The role of external donor (ED) is to prevent loss of ID as a result of alkylation or complexation reactions with co–catalyst by replacing the catalyst component with ED. The absence of ED leads to poor selectivity due to increased mobility of the Ti species on the catalyst surface.

The presence of electron donor also influence the molecular weight [23,25–28]. **Table 1.1.1** shows the progress of catalyst system.

Table 1.1.1: *Progress in ZN catalyst system development [1,27].*

	I.I. [wt.%]	Activity [$g_{PP} \cdot g_{cat}^{-1}$]
$TiCl_3$–Et_2AlCl	90	1
$MgCl_2/TiCl_4$–Et_3Al	30	250
$MgCl_2/TiCl_4$/EB–Et_3Al/EB	94	140

1.1.2.4 *Fourth Generation of ZN Catalyst*

In the early 1980s, the combination of alkylphthalates as ID and alkoxysilanes as ED was discovered. Especially a combination of di-i-butyl phthalate (DIBP) as ID and di-i-butyldimethoxysilane (DIBDMS) or cyclohexylmethyldimethoxysilane (CHMDMS) as ED exhibits a much better productivity and isotacticity [8,27,31]. The combination of ED and ID with catalyst system was called as ”super–active third generation” but due to some confusions this catalyst system was renamed to fourth generation catalyst [29]. Better polymerization properties are probably caused by similar interaction between the oxygen atoms of diesters or alkoxysilanes and Mg^{2+} atoms and to their higher basicity, which is important for ID replacement on the $MgCl_2$ faces removed from the catalyst by the TEA during polymerization process [30]. Sacchi and his group proposed these exchanges as follow [31].

$$\mathrm{CatID} + \mathrm{AlEt_3} \rightarrow \mathrm{Cat-[\ \ ]} + \mathrm{AlEt_3ID} \quad (1)$$

$$\mathrm{Cat-[\ \ ]} + \mathrm{AlEt_3} \rightarrow \mathrm{CatAlEt_3} \quad (2)$$

$$\mathrm{AlEt_3} + \mathrm{ID} \rightarrow \mathrm{AlEt_3ID} \quad (3)$$

$$\mathrm{Cat-[\ \ ]} + \mathrm{AlEt_3ID} \rightarrow \mathrm{CatID} + \mathrm{AlEt_3} \quad (4)$$

where $\mathrm{Cat-[\ \ ]}$ is free site.

1.1.2.5 *Fifth Generation of ZN Catalyst*

The discovery of 1,3–diethers as new type of ID in 1988 is considered to be beginning of the fifth generation of ZN catalyst system. The extremely high activities and isotacticities without addition of any ED are possible to reach by using this type of catalyst. Many studies about interaction of 1,3–diethers and $MgCl_2$ have been published, but exact mechanism of interaction is still not clear [32–34]. In the end of 20th century, the succinate as ID was developed with addition of alkoxysilane as ED. The performance of this catalyst is similar to fourth generation, but PP has significantly broader molecular weight distribution. Succinates have longer space between the oxygen atoms, thus they can adopt more variety of conformations, when coordinating to Mg atoms. This leads to the higher configurational diversity of active species in comparison with diethers with shorter space. Some people consider this catalyst system as sixth generation [3,35].

1.2 Polymerization Kinetics of α–Olefins with $MgCl_2$–Supported Catalyst

Polymerization process with heterogeneous nature of $MgCl_2$–supported catalysts is in unsteady states, because the reaction rate changes with time. A typical kinetics profile of $MgCl_2$–supported catalysts shows a fast activation period within 0.1 s caused by formation of active sites by reaction with co–catalyst [36,38]. After fast activation, catalyst exhibits the typical high initial activities followed by rapid polymerization rate decreasing (**Figure 1.2.1**).

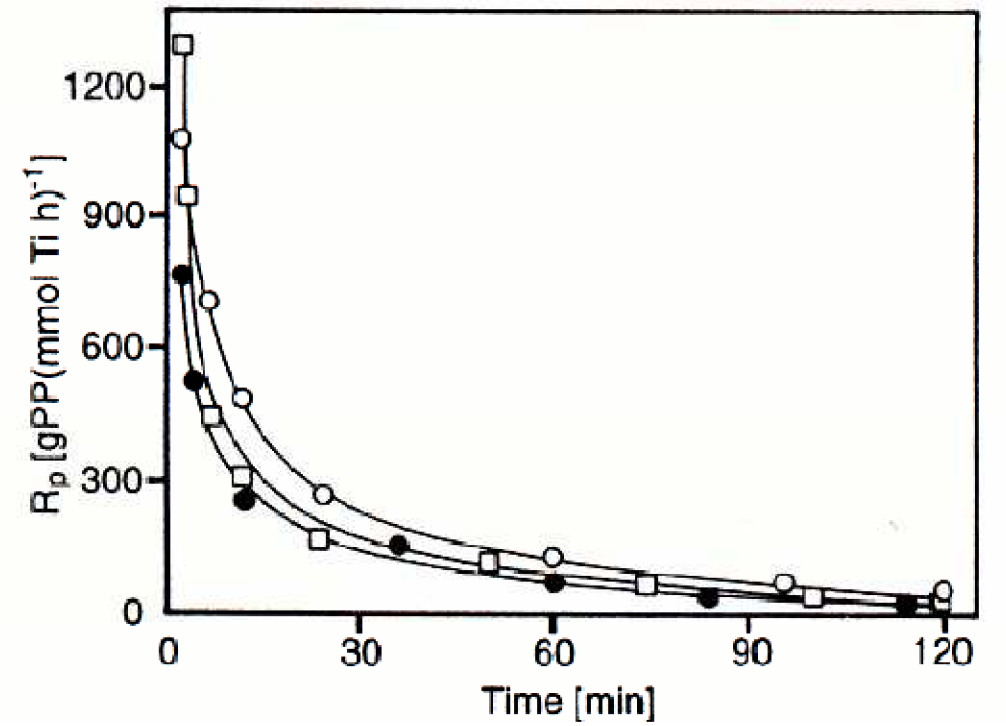

Figure 1.2.1: *Typical decelerating kinetic profiles of $MgCl_2$ (ball milled)/EB/$TiCl_4$-TEA catalytic system in propene polymerization expressed by plotting of polymerization rate as a function of time. Polymerization conditions: temperature 60 °C; pressure 1 bar; TEA/Ti molar ratio = 176 [37].*

One of the reasons for high reaction rate can be destabilization of titanium–polymer bond by withdrawing an electron leading to igher propagation rate constant. Some scientist assumed that the $MgCl_2$ electron donating effect on the more electronegative titanium stabilizes the coordination of the monomer resulting in an acceleration of the monomer insertion [3,39,40]. Many theories explaining the rapid rate decreasing have been published. The rapid rate decreasing can be caused by monomer flux diffusion limitation due to the encapsulation of the catalyst in the polymer layer [41]. Keii et al. [42] proposed the rate decreasing is caused by interaction between catalyst and alkylaluminum causing reduction of Ti^{3+} to lower oxidation states, mainly Ti^{2+}, which are inactive in propene polymerization, but active in ethylene polymerization [43]. A further possible reason is poisoning with ethylaluminum dichloride (EADC), which is formed during interaction between catalyst and TEA [44]. Most likely reason for the activity decay in propene polymerization is the irregular (2,1)–monomer insertion into the growing chain [45]. It is generally accepted that (2,1)–

inserted propene units slow down the chain propagation, due to the steric hindrance of the methyl group close to the Ti atom (**Figure 1.2.2**).

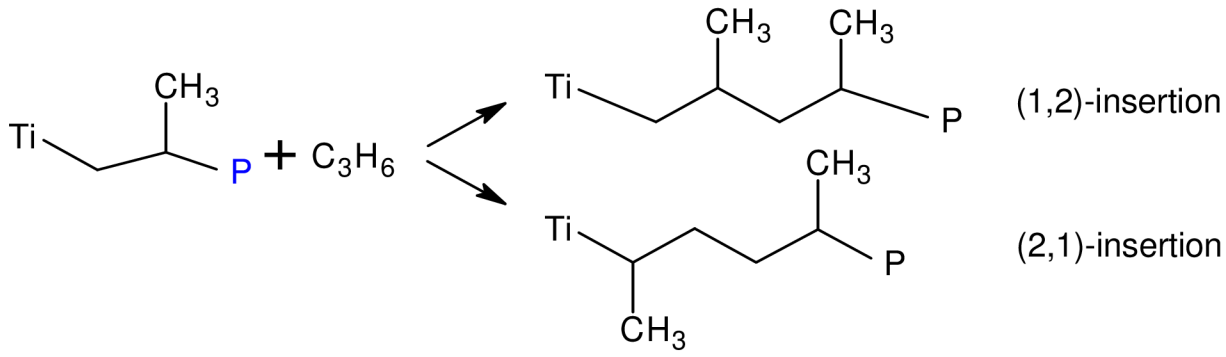

Figure 1.2.2: *Regiorregular (1,2) and regioirregular (2,1) insertion of propene.*

1.3 Ziegler–Natta Catalyst Pre–polymerization

A term pre–polymerization implies separation of the catalyst activation stage from the actual polymerization stage defined by precisely controlled polymerization step under the mild condition, especially relatively low temperature and low monomer concentration, carried out before the main polymerization step [46]. When using Ti based catalysts supported on $MgCl_2$ magnesium chloride, a pre–polymerization step is often used. Two main methods are used for the ZN catalysts pre–polymerization: isothermal (IPP) and non–isothermal (NIPP). In the first case, i.e. IPP method, the ZN catalyst components are injected into reactor containing monomer at low temperature. After the defined time, the reactor temperature is raised to main polymerization temperature as soon as possible. The IPP method has the advantage that the pre–polymerization temperature is constant, thus the effect on properties of final polymer are not depended on this parameter. In the second case, i.e. NIPP method, the reactor containing monomer is also cooled to low temperature. However, after the injection of all catalyst components, the temperature is gradually raised to the main polymerization temperature in the defined time. During NIPP, the catalyst is exposed to rapid change of temperature and pressure, which could cause lower catalyst activity compared to IPP method. The polymerization process of both types of pre–polymerization is shown in **Figure 1.3.1**. The low reaction rate during the pre–polymerization allows the catalyst particle to fully activate, helps to prevent thermal effect, provides controlled fragmentation of the catalyst and influences polymer isotacticity [48,52].

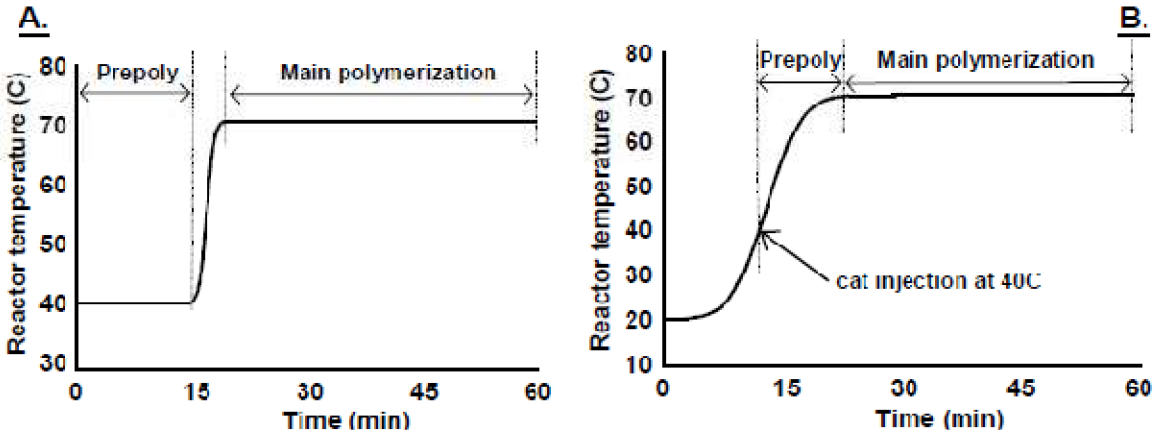

Figure 1.3.1: *Process of pre–polymerization for IPP (A) and NIPP (B) [52].*

1.3.1 **Thermal Effect**

During the initial phase of polymerization, the growing particle has small surface area causing poor heat exchange at high reaction rate. If the monomer concentration and temperature are too high, the rate of the heat production in the growing polymer particle could cause thermal overheating of the particle resulting in undesired thermal catalyst deactivation and melting of produced polymer. These events will adversely affect the powder morphology. Thus, the pre–polymerization step is often used to avoid thermal runaway on the catalyst particle during the initial phase of the polymerization by increasing the surface area [47–50].

1.3.2 **Fragmentation of ZN Catalyst System**

It is assumed that the fragmentation of the ZN catalyst is the determining step for the final particle morphology and can be used to control polymer particle structure. In the early 1990s, Ferrero and Chiovetta have worked intensively on the implementation of the fragmentation step in the single particle models and proposed fragmentation model. They assumed that the fragmentation process proceed layer by layer starting from the surface of the particle to the core of the catalyst macroparticle (**Figure 1.3.2**) [51]. Now, it is known that the fragmentation of the ZN catalyst is complex process depending on number of variables as local initial polymerization rate and crystallization rate of the polymer product. Due to the high internal pressure and stress exerted by the producing polymer on the support of the ZN catalyst the break–up of the particles could occur leading to the creation of undesired polymer fines. This event can be eliminated by the application of pre–polymerization step, where the thin layer of polymer on the ZN catalyst particle is produced, which subsequently protects the particle against the breakage under the main polymerization conditions. The catalyst support will break up significantly slower and form regular and compact structures, which replicate the original shape of the catalyst particle [47,48,52].

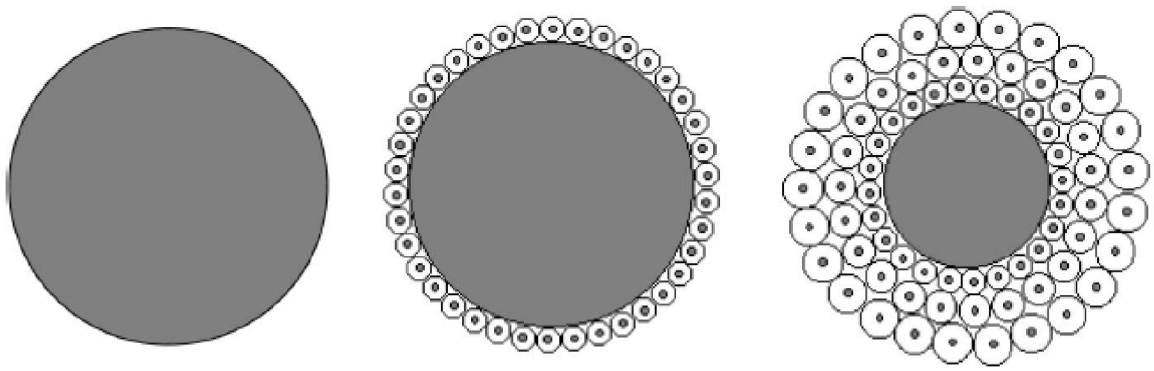

Figure 1.3.2: *Scheme of fragmentation model proposed by Ferrero [51].*

1.3.3 **Influence on Polymer Properties**

The injection of the non–activated catalyst into the environment containing monomer, co–catalyst and electron donor leads to competition between catalyst activation and polymerization [53]. The outer active sites are producing polymer, the inner sites might not be fully activated. This event might cause the formation of an obstacle to the larger electron donor and co–catalyst molecules in reaching the potential active sites. The pre–polymerization step leads to more complete catalyst activation and activation of active sites in more desirable ways leading to improvement of final polymer properties [54]. Taromi et al. [52] found out that the pre–polymerization temperature strongly influence the catalyst activity, isotacticity and morphology (**Figure 1.3.3**). They determined that the optimal pre–polymerization temperature is in the range 25 – 30 °C, because higher pre–polymerization temperatures decreased subsequent catalyst activity in main polymerization. Beside this also at lower pre–polymerization temperature better polymer particle morphology was obtained.

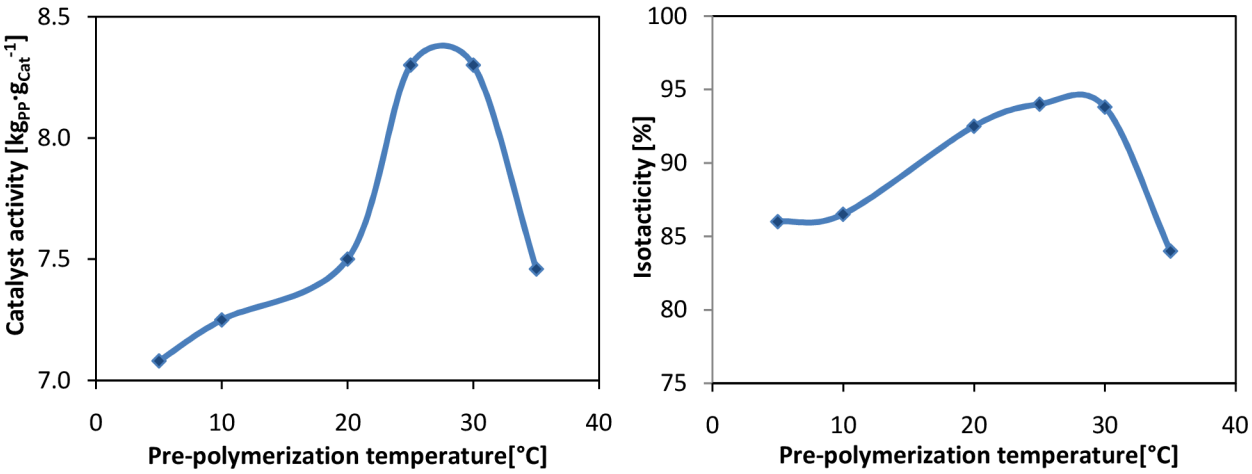

Figure 1.3.3: *Effect of pre–polymerization temperature on catalyst activity and isotacticity [52].*

1.4 Pre–polymerization of ZN Catalyst in Industrial Process

The pre–polymerization is useful tool for improving ZN catalyst performance and properties. Thus, some of the most important industrial technologies utilize it, but in different ways. **Table 1.4.1** shows the most important industrial technologies with description of the pre–polymerization step.

Table 1.4.1: *Summarization of most important technologies for PP production (adjusted for current volume estimates) [55–60].*

Process			Pre–polymerization	
Process	Owner	Annual production (MMT/year)	Pre–polymerization	Medium
Spheripol®	LyondellBasell	19.20	Yes, continuous	Liquified propene
Unipol® PP *	W. R. Grace	11.85	None	–
Novolen®	CB&I	6.77	None	–
Hypol®	Mitsui	2.26	Yes, batch	Inert hydrocarbon
Bostar®	Borealis AG	2.26	Yes, continuous	Liquified propene
Innovene®PP	INEOS Technologies	5.08	none	–

**UNIPOL® is a trademark of The Dow Chemical Company or an affiliated company of Dow. W.R. Grace & Co.-Conn. and/or its affiliates are licensed to use the UNIPOL® trademark in the area of polypropylene.*

One of the disadvantages of the pre–polymerization is the requirement of extra reactor, which increase the price of the polymerization process. The need to use the pre–polymerization step depends on the behavior of the catalyst system applied in the polymer synthesis procedure. Some catalysts do not show the initial inhibition which has moderating influence. Typically, these catalysts exhibit high initial polymerization rates and/or have insufficient morphology, so in such case the pre–polymerization is suitable to prevent such effects. However, the pre–polymerization is not suitable for all the technologies and reactors. For example, the application of the pre–polymerization step in the case of continuous stirred–tank reactor (CSTR) has the disadvantage of relatively broad residence time distribution leading to the inability to control the pre–polymerization degree. Another option is to use hydrocarbon solvent and pre–polymerize the ZN catalyst in solution in batch operation. However, this option is even more expensive than the continuous pre–polymerization process due to its discontinuity and requirement of the separation of the inert hydrocarbon and pre–polymerized catalyst. For the technologies, which are not equipped with pre-polymerization facilities, the ZN catalyst producers as LyondellBasell offers catalysts, which are already pre-polymerized [55–60]. Of course, also in this case is evident that the price of pre–polymerized

catalyst will be higher than the price of catalyst, which is not modified by pre–polymerization. However, on the other side, it is also clear that the performance of the pre–polymerized catalyst in the production reactor is better and that the possibility of any adverse effects as reactor overheating, polymer particles agglomeration, fines formation etc. is minimized. For such reason quite often it is worth for PP producers using the pre–polymerized catalysts despite its higher price [55–60].

2. Experimental part

2.1 Chemicals

All propene polymerizations were performed by using commercial high activity $MgCl_2$–supported $TiCl_4$ catalyst (2.6 wt.% of Ti and 19.0 wt.% of Mg in dry catalyst) with dialkylphthalate as ID. The catalyst was slurried in mineral oil with density ρ(25°C) = (0.86 – 0.88) g·cm^{-3} and stored in special glass vessel covered by flow of pure nitrogen.

Polymerization grade propene was purchased from Unipetrol RPA in Litvínov, Czech Republic. Propene was further purified by passing through six columns to decrease the content of impurities (CO, COS) below 10 ppb and content of H_2O and O_2 below 1 ppm.

Triethylaluminium (TEA) co–catalyst was obtained from Chemtura (Germany). TEA was diluted by pure *n*–heptane and kept in glass vessel covered by flow of pure nitrogen.

Diisobutyl dimethoxy silane (DIBDMS) external donor was purchased from Evonik (Germany). DIBDMS was diluted by pure *n*–heptane and kept in glass vessel covered by flow of pure nitrogen.

n—Heptane (99 % spectrophotometric grade) used also as pre–polymerization medium was obtained from Sigma Aldrich. Due to possible presence of impurities, *n*–heptane was treated as follow – about 10 wt.% of *n*–heptane was distilled out from vessel by flow of high purity nitrogen (70°C, 30 min) to remove H_2O and O_2.

o–Xylene (reagent grade, ≥98.0 %) for the determination of portion of PP soluble in cold xylene (i.e. Xylene Solubles) was purchased also from Sigma Aldrich.

Calcium stearate and butylated hydroxytoluene antioxidants were purchased from BASF, Switzerland and were used as stabilizers for prepared PP samples.

2.2 Pre–polymerization

2.2.1 Pre–polymerization Apparatus

A low pressure pre–polymerization apparatus with a glass reaction vessel was used for propene pre–polymerization. All the connecting tubes were made of stainless steel. The apparatus was equipped with an automatic mass flow controller (Bronkhorst High–Tech B.V., The Netherlands) for the adjustment of desired propene flow in the range 0 – 250 mg·min^{-1} with accuracy ± 0.5 % of reading. The glass reaction vessel was fixed to an analytical shaker (IKA MS3, Germany). During the pre–polymerization the reaction medium was shook by 500 rpm. Between the individual experiments, the reaction vessel was purified by the flow of high purity nitrogen (at 250 °C for 30 min). After the purification the inner volume of the reaction vessel was protected against the air contamination by the nitrogen flow.

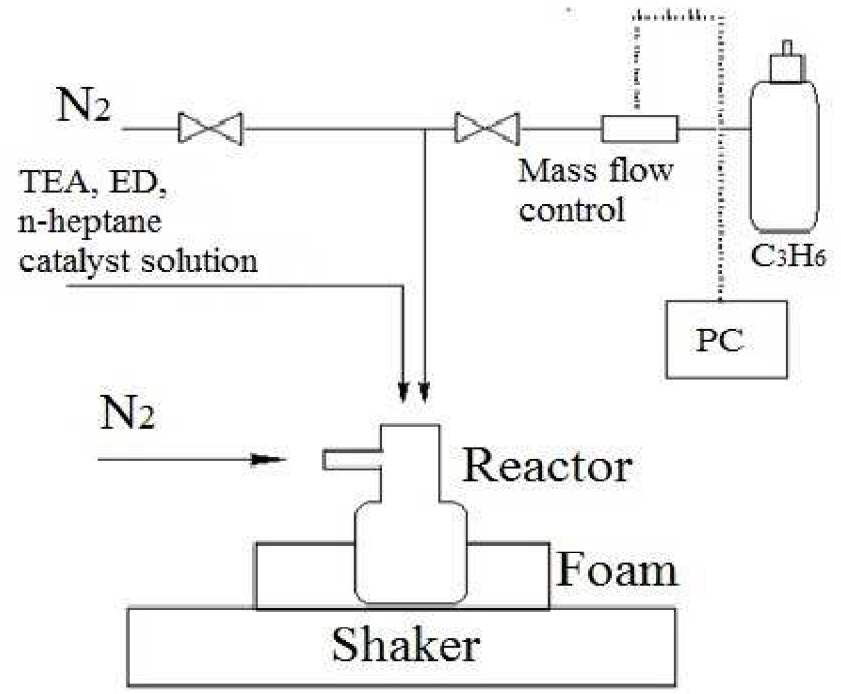

Figure 2.2.1: *Schematic illustration of pre–polymerization apparatus.*

2.2.2 **Pre–polymerization Procedure**

All the catalyst pre–polymerizations were carried out in 2.3 ml of previously purified *n*–heptane. The pre–polymerization temperature was 23 °C. All the experiments were performed with presence of external donor (DIBDMS) and without addition of hydrogen. The propene flow was set to 20 mg·min^{-1} and shaking speed was set to 500 rpm.

First of all, an empty, clean and dry reaction vessel was weighed. Then, the vessel was filled up with 2.3 ml of purified *n*-heptane and weighted again. Subsequently, the exact amount of DIBDMS and TEA was added by micropipette and weighted again. Then, catalyst in mineral oil was injected by Microman®micropipette and inlet of propene was attached close to the surface of the reaction solution. Before the start of shaking the catalyst was separated from TEA co–catalyst and external donor DIBDMS by diffusion barrier, which was present between mineral oil and *n*–heptane. The start of shaking was considered as the beginning of catalyst activation. Shaking speed 500 rpm was enough to homogenize the solution in very short time. After defined time of activation, the propene was added by flow of 20 mg·min^{-1} up to desired amount. The end of pre–polymerization was considered 1 min after addition of defined amount of monomer. This time was enough to let react whole amount of introduced propene monomer. After the pre–polymerization, the reaction vessel was weighted again. The pre–polymerized catalyst was decanted 3 times with purified *n*–heptane. Subsequently, 2.3 ml of previously purified mineral oil was added. Then the residues of *n*–heptane were removed by bubbling the suspension of pre–polymerized catalyst with nitrogen at laboratory temperature for 30 min. The presence of mineral oil facilitated subsequent addition of pre–polymerized catalyst into the main reactor. The weight concentration of the

pre–polymerized catalyst in MO was 25 mg·ml^{-1}. During the components injecting, the reaction vessel inner volume was covered by nitrogen flow and during each weighting, vessel was closed by special valve with Teflon® sealing. The exact degree of pre–polymerization was calculated according to the equation:

$$\frac{m_3 - m_2}{m_1} = \frac{m_{PP}}{m_{cat}} \qquad (5)$$

where m_3 is weight of reactor with *n*-heptane, ED, TEA, MO, catalyst and polymer (i.e. after pre–polymerization); m_2 is weight of reactor with *n*–heptane, ED, TEA, MO and catalyst (i.e. before pre–polymerization) and m_1 is weight of catalyst.

2.3 Main Polymerization in Gas–Phase

2.3.1 Polymerization Facility

A gas–phase polymerization of propene was performed in a stainless steel reactor with a volume of 2–litre equipped with a spiral–shaped stirrer driven by an electric motor via a magnetic clutch (see the scheme of the reactor in **Figure 2.3.1**). The reactor was connected to a thermostatic circuit allowing the regulation of the temperature, which is controlled by the external PID regulator. The amount of added propene before and during polymerization was measured according to the change of weight of storage pressure cylinder with propene monomer. The flows of propene and hydrogen were controlled by Bronkhorst mass flow controllers. Then the amount of added hydrogen was determined by integration of the flow. The pressure in the reactor was measured using a digital manometer from PMA GmbH and the temperature in the lower (Tr) and upper part (Tr2) of the reactor was measured by E type thermocouples from Omega. The operation of mass flow controllers and data acquisition was ensured by an external microprocessor managed by operating software on PC.

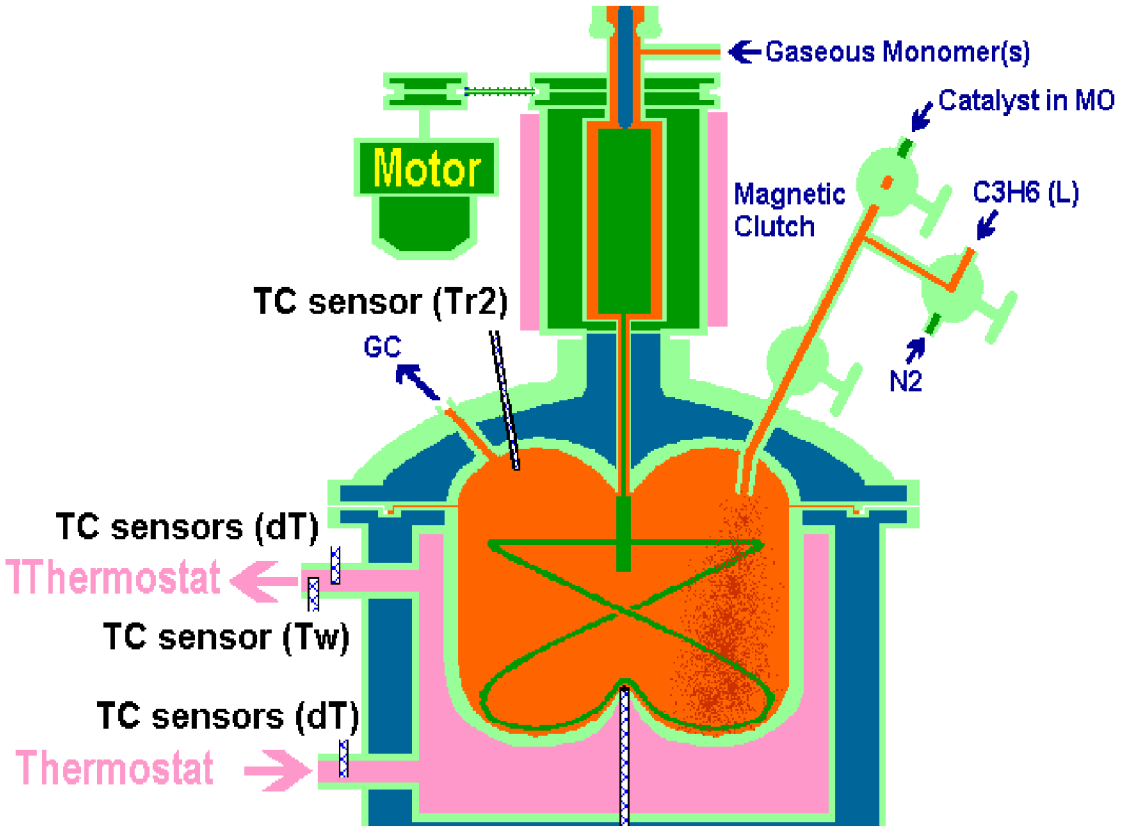

Figure 2.3.1*: Scheme of 2–litre stainless steel polymerization reactor.*

2.3.2 **Polymerization procedure**

All gas phase polymerizations were carried out in 2–litre stainless steel reactor. Polymerization parameters are shown in **Table 2.3.1**. Prior the polymerization, the reactor inner volume was dried by flow of nitrogen (95 °C, 30 min). Subsequently, the leakage test was performed at 95 °C and pressure 3.0 MPa of propene for 30 min. After successful pressure test, the reactor was depressurized and flushed by nitrogen for next 15 min followed by reactor cooling down to temperature of TEA and DIBDMS injection. After reaching constant desired temperature, TEA and DIBDMS diluted in pure *n*-heptane were dosed by using Microman®micropipette. After dosing of both components, reactor was closed and pressured with propene up to 0.8 MPa followed by hydrogen addition. Subsequently, the pressure was increased with propene monomer up to 1.3 MPa and temperature was increased up to the temperature of the catalyst injection. The appropriate amount of catalyst suspension was sampled by Microman®micropipette and injected into the catalyst charging device under the nitrogen blanket. The catalyst slurry was shortly after charging flushed into the reactor with ca. 45 g of liquid propene. The total propene amount in the 2–litre reactor after the catalyst introduction was 90 g.

After the catalyst injection, the reactor temperature was increased up to the polymerization temperature (75 °C). The moment of reaching 85 % of polymerization temperature was considered as beginning of gas–phase polymerization. During the polymerization, temperature and pressure were maintained constant.

After 60 min, the polymerization was terminated by the reactor depressurization. The produced polypropene powder was dried in vacuum oven at 70 °C for 60 min.

Table 2.3.1: *Main polymerization conditions.*

P [MPa]	T [°C]	T (TEA and ED injection.) [°C]	T (Catalyst injection) [°C]	Polym. Time [min]	H_2 [mmol]	Cat. [mg]	TEA/Ti [mol·mol^{-1}]	DIBDMS/Ti [mol·mol^{-1}]
2.2	75	40	40	60	20	5	120	12

2.3.3 Polymerization Conditions and Procedure of 2nd Catalyst Injection

The TEA co–catalyst and external donor solutions in n–heptane were dosed into the purified empty reactor at 40 °C and atmospheric pressure (TEA/Ti molar ratio 120). Subsequently, the suitable amount of hydrogen and 45 g of propylene were charged into the closed reactor. During the polymerization period the concentration of hydrogen was kept constant by continuous hydrogen feeding.

The catalyst was dosed as mineral oil slurry. The 1st catalyst dose was charged by Microman®micropipette into the charging device and flushed into the pressurized reactor (40 °C, 2.2 MPa) by liquid propene (45 g). The total amount of propene present in the reactor after the 1st catalyst introduction was 90 g. Consequently, 3 – 5 min temperature rise to the polymerization temperature followed. The polymerization was carried out in gas phase at 75 °C and 2.2 MPa (g) with 0.1 MPa of nitrogen partial pressure.

After 30 min of 1st catalyst dose polymerization the flow of propylene was set on low constant flow 20 g·h^{-1} (only for protection of bearings in magnetic clutch). This propylene flow was not sufficient to maintain constant pressure during the polymerization, thus the pressure in the reactor started to decrease. The rate of pressure decrease depended on actual catalyst activity. Such conditions were maintained for 10 min. Then similar amounts of TEA and ED as charged in 1st dose were introduced into the catalyst charging device and flushed into the reactor by 10 g of propylene. 2 – 3 min after the 2nd TEA+ED dose the 2nd catalyst dose (same catalyst amount as in 1st dose) was introduced into the reactor, flushed by propylene amount suitable for reaching pressure 2.2 MPa (g). Total polymerization time was 100 min (40 min last polymerization of 1st catalyst dose and 60 min last polymerization 1st and 2nd catalyst dose together).

2.4 Analytical Methods

2.4.1 Melt Flow Rate (MFR)

The melt flow rate (MFR) of polypropene was measured according to ISO 1133-1 standard at 230 °C and load 21.6 N on a Dynisco LMI 5000 instrument. 20 g of polypropene powder were stabilized with 0.1 g calcium stearate and 0.03 g butylated hydroxytoluene dissolved in heptane. Then PP powder was dried in vacuum oven at 70 °C for 60 min. Subsequently, 5 g of stabilized powder were utilized for one measurement on Dynisco LMI 5000 plastometer.

The melt mass-flow rate is defined as a mass of polymer melt in grams flowing through a capillary of specific diameter (2.095±0.005 mm) and length (8.000±0.025 mm) by pressing the piston by defined load for defined period of time. MFR unit is g·(10 min)$^{-1}$. Before the measurement the polypropene sample was kept for 5 min at 230 °C. Then the defined load

factor was applied (2.16 kg), which was considered as start of measurement. Subsequently, MFR was calculated according to the following equation:

$$MFR = \frac{427 \cdot l \cdot \rho}{t} \qquad (6)$$

where l means the distance, which the piston passed, ρ means the density of melted polypropene and t means time of measurement.

2.4.2 Bulk Density (B.D.)

Polymer powder bulk density was determined according to the standard ISO 60. Bulk density is defined as amount of powder material, which could be filled into one liter volume, so unit is $kg \cdot m^{-3}$.

20 g of polypropene powder were poured in 200 ml of Slovasol to eliminate static charge, which could adversely influence the determination of bulk density. After 30 min, polypropene powder was filtered and dried in vacuum oven at 70°C for 60 min. Subsequently, the dry PP powder was cooled down to ambient temperature and bulk density was measured by pouring the polypropene powder into the glass vessel with exact volume and weighted.

2.4.3 Xylene Solubles (X.S.)

The content of polypropene soluble in cold xylene was determined by using FIPA Viscotek TPA instrument (Malvern Panalytical) as an alternative to standard method ISO 16152.

25 ml of *o*–xylene were poured into a glass vessel with 0.5 g of polypropene powder. The glass vessel was equipped with a magnetic stirrer. The PP sample was stirred in *o*-xylene for 60 min at 135 °C, which led to the complete dissolving of the whole PP material. Subsequently, the glass vessel was put into a water bath with 25 °C for 60 min. During this period PP insoluble in xylene, which is mainly crystalline PP, precipitated. Then 2.0 ml sample of *o*–xylene with PP material, which remained dissolved, was filtered via syringe filter with pore size 0.2 µm. The sample of filtrate was closed in 2.0 ml glass vial with Teflon® sealing. Subsequently, sample was put into sample holder in FIPA instrument and run the analysis. The instrument has to be calibrated before analysis. The X.S. content is determined by using computer program SW OmniSEC.

2.4.4 PP Powder Porosity

The testing is performed in accordance with ISO 4608 based on the amount of dioctyl phthalate (DOP) retained by the PP powder

First of all, blank samples were measured to be able to calculate the amount of DOP retained by the cotton wool. The piece of cotton wool (100 ± 2) mg was weighed, placed into the adjusted test tube and slightly pressed down. Tube with cotton wool was weighed (m_1). 4.0 ml of DOP was added from the burette into the tube and left stand for 10 min. Subsequently, tubes were put into the holder and placed into the centrifuge. The centrifugation was performed at laboratory temperature for 60 min and the revolutions were = 3 800 rpm. After centrifugation, the tubes were weighed and the amount of DOP absorbed by cotton wool was determined (m_0).

The powder porosity was determined as follow. Tube and cotton wool was prepared as before in blank measurement and weighed (m_1). Then, 2.0 g of polymer powder was weighed into the prepared tube (m_2). From the burette 4.0 mL of DOP were poured into the tube and left stand for 10 minutes. Tube was put into the holder and placed into the centrifuge as before. After 60 min of centrifuging, the tube was cleaned to remove all DOP present on the outside walls of the tube and the tube was weighed (m_3). Porosity of the powder was expressed as amount of DOP absorbed by 100 g of polymer powder according to equation:

$$\frac{(m_3 \cdot m_0) - m_2}{m_2 - m_1} \cdot 100 = g\ DOP \cdot (100\ g)^{-1}\ PP \qquad (7)$$

2.4.5 **Particle Size Distribution (PSD)**

The method is based on ISO 1624. 10 g of polypropene powder were sieved through the set of screens with following mesh diameters (mm): 4.00, 3.15, 2.50, 2.24, 2.00, 1.80, 1.50, 1.25, 1.00, 0.80, 0.50, 0.20, 0.10, 0.05 and frit S3. The sieving was performed in ethanol starting with the screen with highest mesh size. The powder fraction on each screen was dried in vacuum oven at 70 °C for 60 min. Then, during next 60 min it was cooled down to ambient temperature and subsequently weighed.

2.4.6 **Mathematical Processing Method for Polymerization Kinetic Profile Evaluation**

The evaluation of kinetic polymerization profile was performed by using computational method, which optimizes eight parameters of mathematical equation (8) defined by Cejpek (Polymer Institute Brno, 2003)

$$A(t)8p = A_1 e^{(-kd_1 t)} + \left\{1 - e^{\left[-(\frac{t}{ka_2})^{pow}\right]}\right\} \cdot \left\{A_2 e^{-(kd_2 \cdot t)} + A_3 \cdot e^{-kd_3 t}\right\} \qquad (8)$$

Where A(t)8p is instant polymerization rate, A_1, A_2, A_3, Ka_2, pow, kd_1, kd_2 and kd_3 are empirical parameters which are optimized during the computation process, polymerization time since condensed propene evaporation.

This computational method utilized the automated optimization procedure of program „VYH9P01.PAS" developed by a team of authors Cejpek, Peroutka and Jelen (Polymer Institute Brno) based on the applied simplex optimization method. The calculation procedure optimized the values of all eight parameters simultaneously with the numerical procedure according to the propene consumption empirically corrected to the actual phase state in the reactor.

3. Results and Discussion

3.1 Development of Pre–polymerization Procedure

The three techniques were examined in order to find out the most appropriate way of stirring the components during the catalyst pre–polymerization. All experiment were performed under the same conditions, i.e. TEA/Ti = 3.0 $mol \cdot mol^{-1}$, DIBDMS/Ti = 0.15 $mol \cdot mol^{-1}$, 1 min activation, pre–polymerization degree (DPP) = 3.0 $g_{PP} \cdot g_{cat}^{-1}$ and 30 min ageing of pre–polymerized catalyst before the start of main polymerization. The scheme of different stirring techniques is shown in **Figure 3.1.1**. The conditions applied in main polymerization are indicated in **Table 2.3.1**.

As first, the glass reaction vessel with a straight bottom and octagonal–shaped magnetic bar with pivot ring around the center was utilized. The pivot ring reduced the contact surface of the stirrer with glass vessel bottom and enables the stirrer to adopt the optimum stirring position (**Figure 3.1.1a**). Next experiment was performed in glass vessel with a round bottom and egg–shaped magnetic stirring bar (**Figure 3.1.1b**). In this case the stirring bar perfectly copied the glass vessel bottom. The third experiment was performed in glass vessel with round bottom without stirring bar. This vessel was placed into the foam attached to the laboratory shaker, which provided the stirring motion (**Figure 3.1.1c**). All the pre–polymerized catalysts were evaluated in standard gas–phase polymerizations performed in 2–litre stainless steel reactor. The prepared PP powders were also compared with reference powder prepared with catalyst, which was not pre–polymerized.

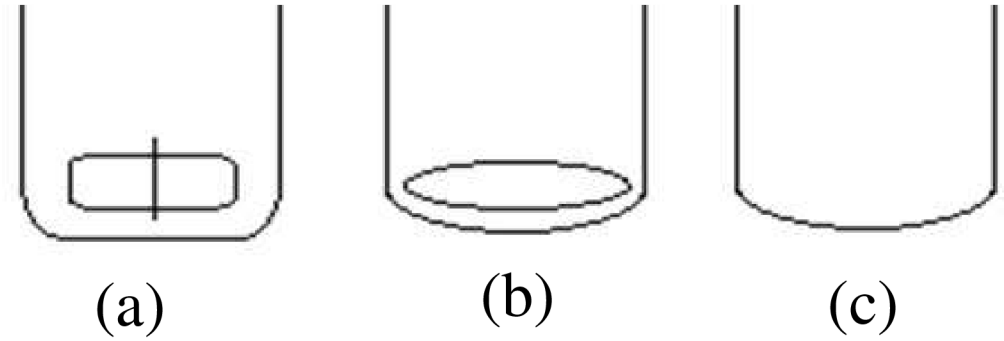

Figure 3.1.1: *Scheme of different types of stirring during catalyst pre–polymerization in glass reaction vessel, (a) octagonal-shaped stirring bar, (b) egg-shaped stirring bar and (c) stirred by shaking without stirring bar*

The significant difference between polymer morphologies was observed (**Figure 3.1.2**). It is obvious that not pre–polymerized catalyst system underwent fragmentation at demanding conditions of gas–phase polymerization. **Figure 3.1.3** shows the particle size distribution of the prepared polymer powders. It is evident that any type of stirring bar present inside the glass vessel during the pre–polymerization is not suitable and led to the production of polymer powders with noticeable amount of broken particles. Especially, the egg–shaped stirring bar evidently damaged the catalyst particles during the pre–polymerization, because high portion of broken particles was produced in subsequent gas–phase polymerization. **Figure 3.1.3** and **Table 3.1.1** shows that the highest amount of fine powder, i.e. particles with

diameter smaller than 1.0 mm, was produced in polymerization with catalyst pre–polymerized with the egg–shaped stirring bar. The reason for poor polymer morphology could be explained by the fact that all the studied stirring bars caused fragmentation of catalyst particles with active centers into smaller pieces, which subsequently led to production of smaller pre–polymerized catalyst particles. The fragmentation continued during the main polymerization in 2–litre stainless steel reactor and resulted in fragmentation even higher than was observed in reference experiment with not pre–polymerized catalyst. The experiments performed within this study revealed that the most suitable stirring way is the using of analytical shaker, which provided the polymer powder with good morphology, lowest amount of fine particles (i.e. particles smaller than 1.0 mm) and highest fraction of particles with diameter bigger than 2.0 mm.

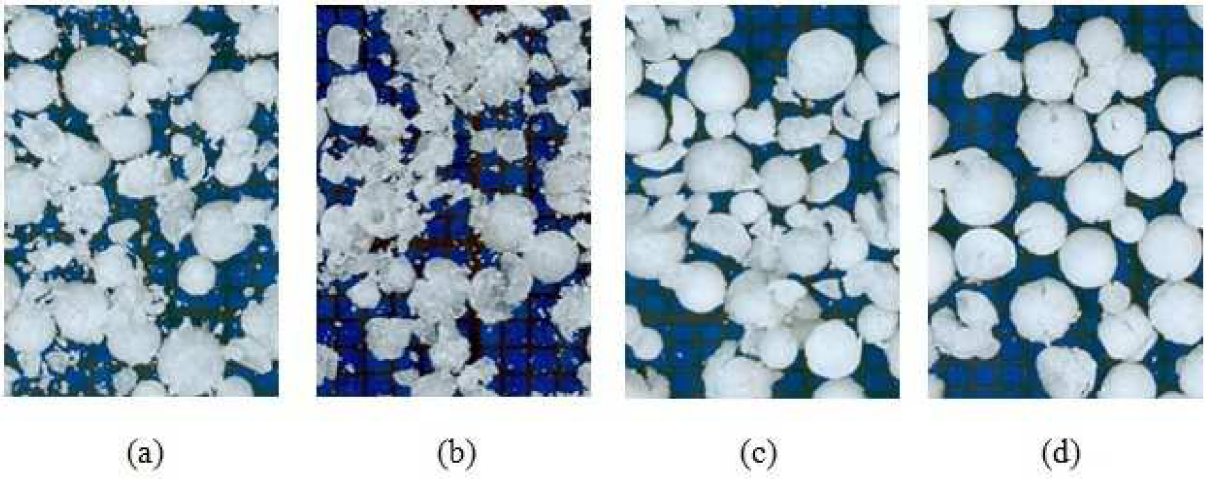

Figure 3.1.2: *Pictures of final polymer powders produced in main polymerization with catalysts pre–polymerized by using (a) not pre–polymerized catalyst (b) oval egg–shaped stirring bar, (c) octagonal–shaped stirring bar and (d) stirred by analytical shaker.*

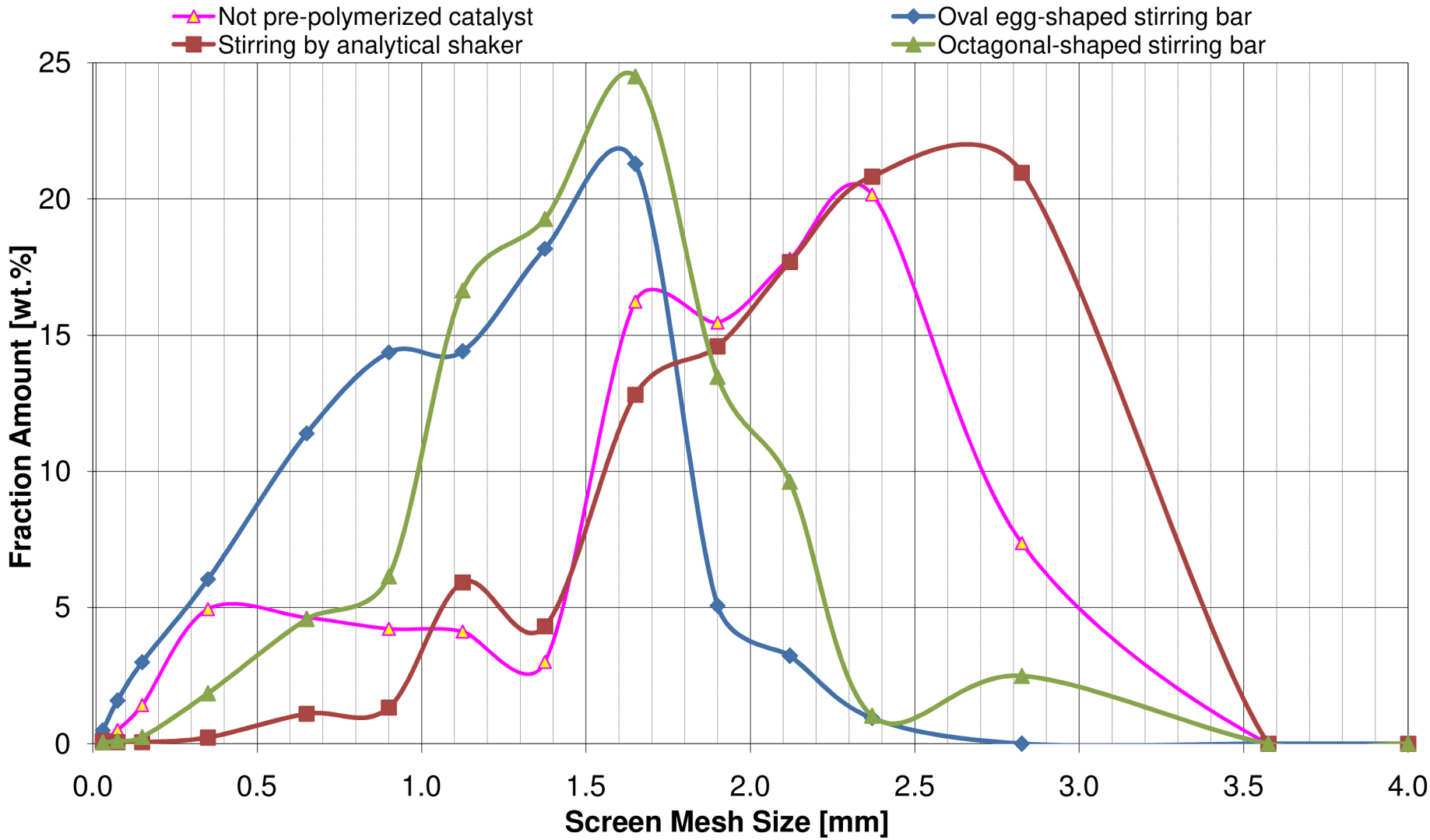

Figure 3.1.3: *Particle size distribution of final polymer powders produced in main polymerization with catalysts pre–polymerized by using different techniques of stirring during pre–polymerization process.*

3.2 Effect of Time of Catalyst Activation

The activation time is other important parameter in the ZN catalyst pre–polymerization step. Series of experiments were performed in order to study the influence of the activation time on final polymer powder morphology and find out the most appropriate activation time for studied ZN catalyst. Within thus study the catalyst was prepared without pre–polymerization step due to possibility to clearly see effect of adverse reactions in catalyst system. The pre–polymerizations were performed with TEA/Ti = 3.0 mol·mol^{-1}, DIBDMS/Ti = 0.15 mol·mol^{-1} and catalyst ageing for 30 min. The activation times and polymers properties are shown in **Table 3.2.1**. The main polymerization conditions are shown in **Table 2.3.1.**

Table 3.2.1: *Final properties of polymer powders with different activation times. Pre–polymerization conditions: TEA/Ti = 3.0 mol·mol^{-1}, DIBDMS/Ti = 0.15 mol·mol^{-1},30 min ageing, temperature of pre–polymerization 23 °C, pressure 1 bar.*

Activation [min]	Activity [kg·g^{-1}·h^{-1}]	B.D. [kg·m^{-3}]	MFR(2.16kg load) [g·(10min)$^{-1}$]	X.S. [wt.%]	Porosity [g_{DOF}·(100g_{PP})$^{-1}$]
No activated	33.6	431	8.5	1.79	2.80
1	41.7	427	6.7	1.56	2.70
5	41.1	420	7.0	1.66	2.64
15	37.0	418	7.0	1.70	2.76
30	36.6	413	6.8	1.92	2.60

The series of polymerizations with activated catalysts revealed that the longer pre–contacting time is applied, the less activity the catalyst exhibits (**Figure 3.2.1**). The kinetic profiles shown in **Figure 3.2.2** revealed that the decrease of polymerization activity with prolongation of activation period before pre–polymerization is related mainly to the decrease of the initial polymerization rate. It is evident that longer activation times led to the deactivation of mainly the unstable highly active centers. It is assumed that the unstable active centers were deactivated by the over reduction with TEA. The Ti^{3+} form is further reduced to Ti^{2+}, which is not able to polymerize propene [64]. From the industrial point of view, the elimination of high initial activities by longer activation period could be considered as positive feature, because could prevent polymer particles overheating and production of agglomerates and/or fine polymer particles. Other positive feature of longer activation period is that the studied ZN catalyst exhibited more stable kinetic profile with less deactivation during main polymerization period in comparison with the reference not activated and pre–polymerized catalyst system.

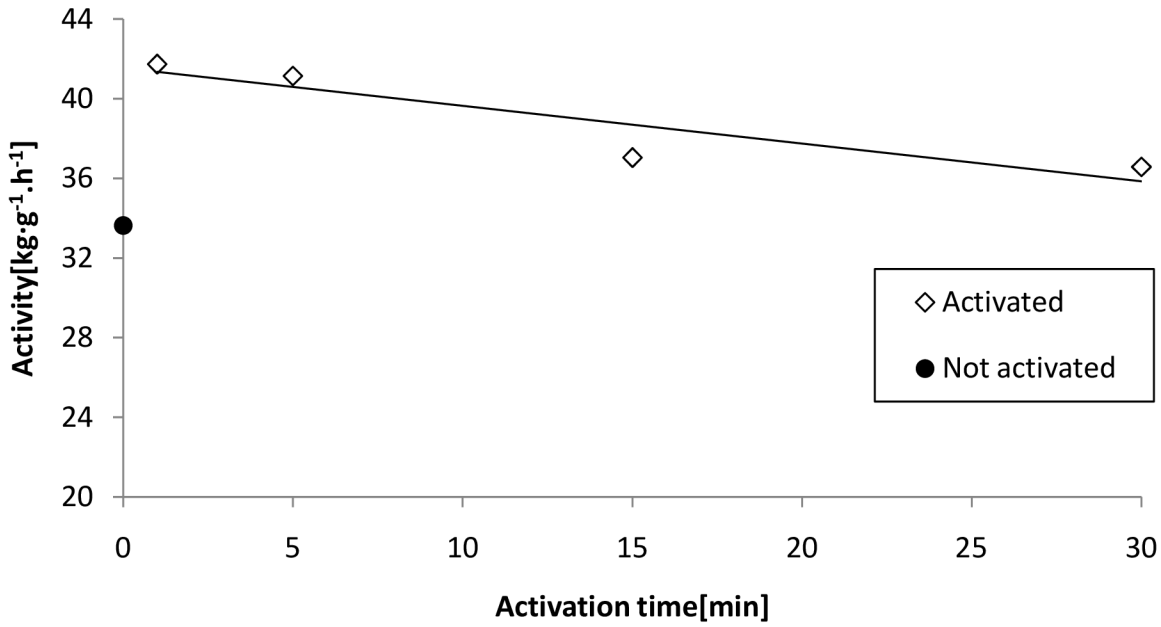

Figure 3.2.1: *Dependence of catalyst activity on activation time.*

Table 3.2.1 and **Figure 3.2.1** further show that not activated and not pre–polymerized catalyst system exhibited noticeably lower polymerization activity in comparison with the experiments performed with the activated catalysts. It is known that during the activation period the catalyst components as TEA and DIBDMS had enough time to diffuse inside the primary catalyst particles and activate all the possible centers. According to the experiments performed by Coutinho et al. [65], which were based on the ZN catalyst pre–polymerizations with different monomers, it is presumed that the activated as well as the pre–polymerized catalyst particles have exposed also the occluded catalyst centers, which lead to the catalyst activity enhancement.

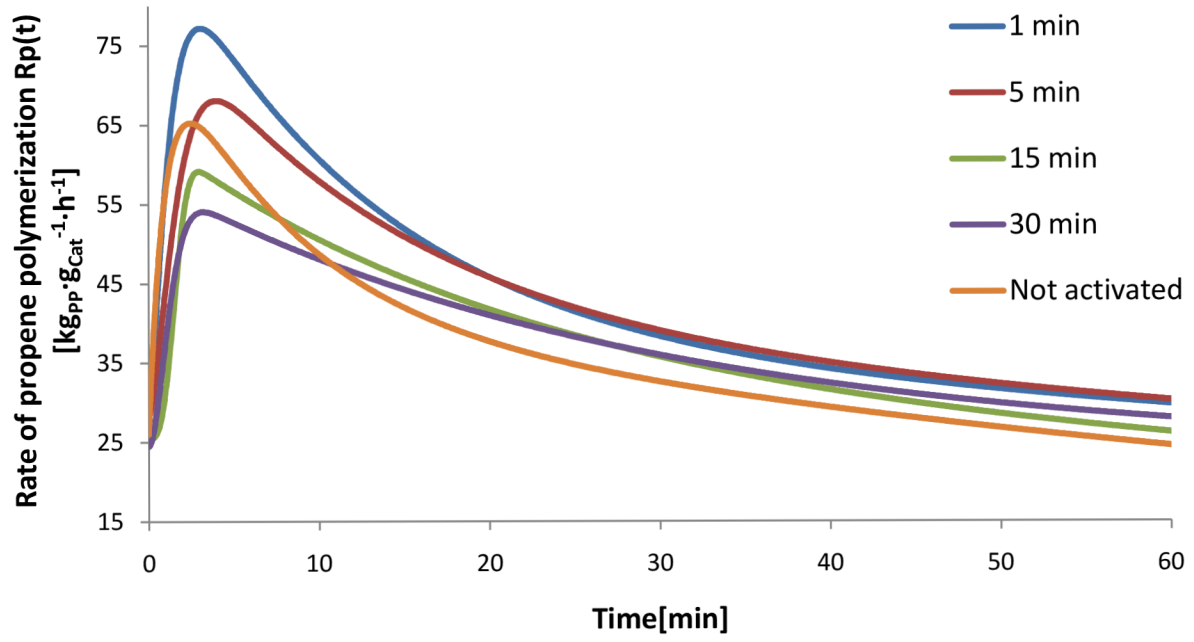

Figure 3.2.2: *Propene polymerization kinetics of catalysts with different activation times.*

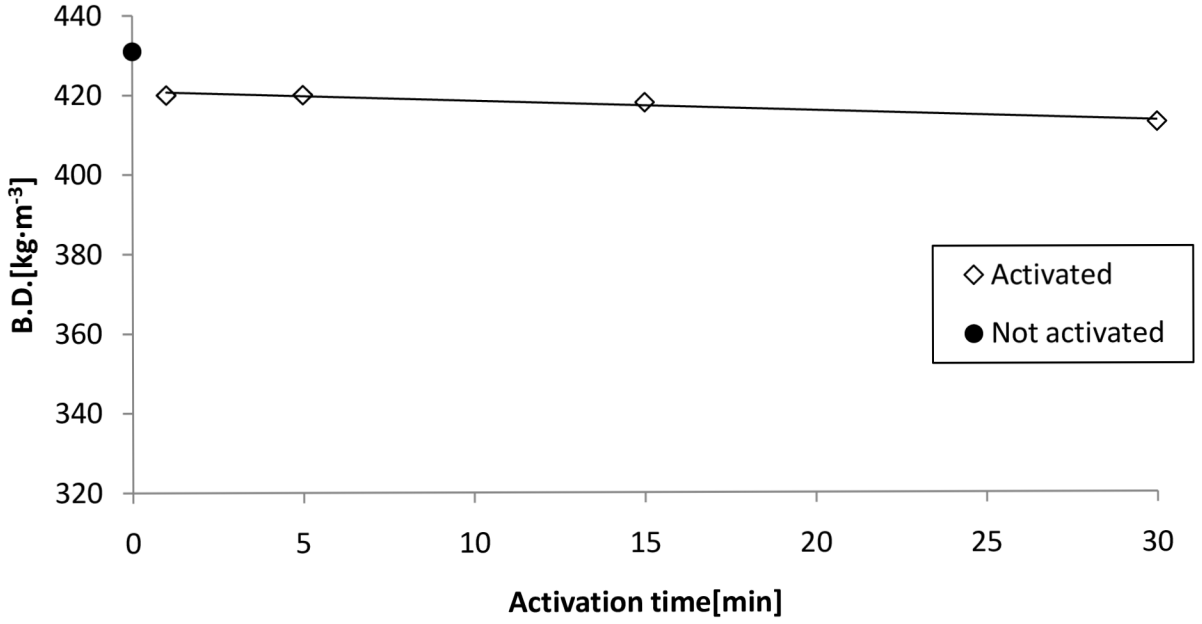

Figure 3.2.3: *Dependence of bulk density on activation time.*

Figure 3.2.3 shows the dependence of bulk density as a function of activation time. No significant change was observed in activated catalysts. According to theories mentioned by Taromi [52] , there are two possible explanations of the different morphology of not activated and not pre–polymerized catalyst. First theory claims that morphology is adversely influenced by local propene boiling related to higher initial polymerization rates compared to activated and pre–polymerized catalyst. It is possible that higher polymerization rate causes particle overheating due to insufficient heat transfer. This negative effect could lead to sudden

formation of gas bubbles. The force of the gas expansion can cause that on the particle surface more open structure is formed. The second suggested theory is about the rate of fragmentation, which could be also related to higher initial polymerization rates. High polymerization rate lead to the creation of internal pressure of polymer on the pore wall. If the pressure is increasing fast enough, the catalyst support undergoes uncontrolled fragmentation resulting in lower bulk density and morphology similar as shown in **Figure 3.2.4a**. The pre–polymerization as well as activation of catalyst help to prevent these negative phenomenons. This observation is also confirmed by polymer powder pictures presented in **Figure 3.2.4b–e**, where changes in particles morphology was not observed in the case of activated and pre–polymerized catalyst.

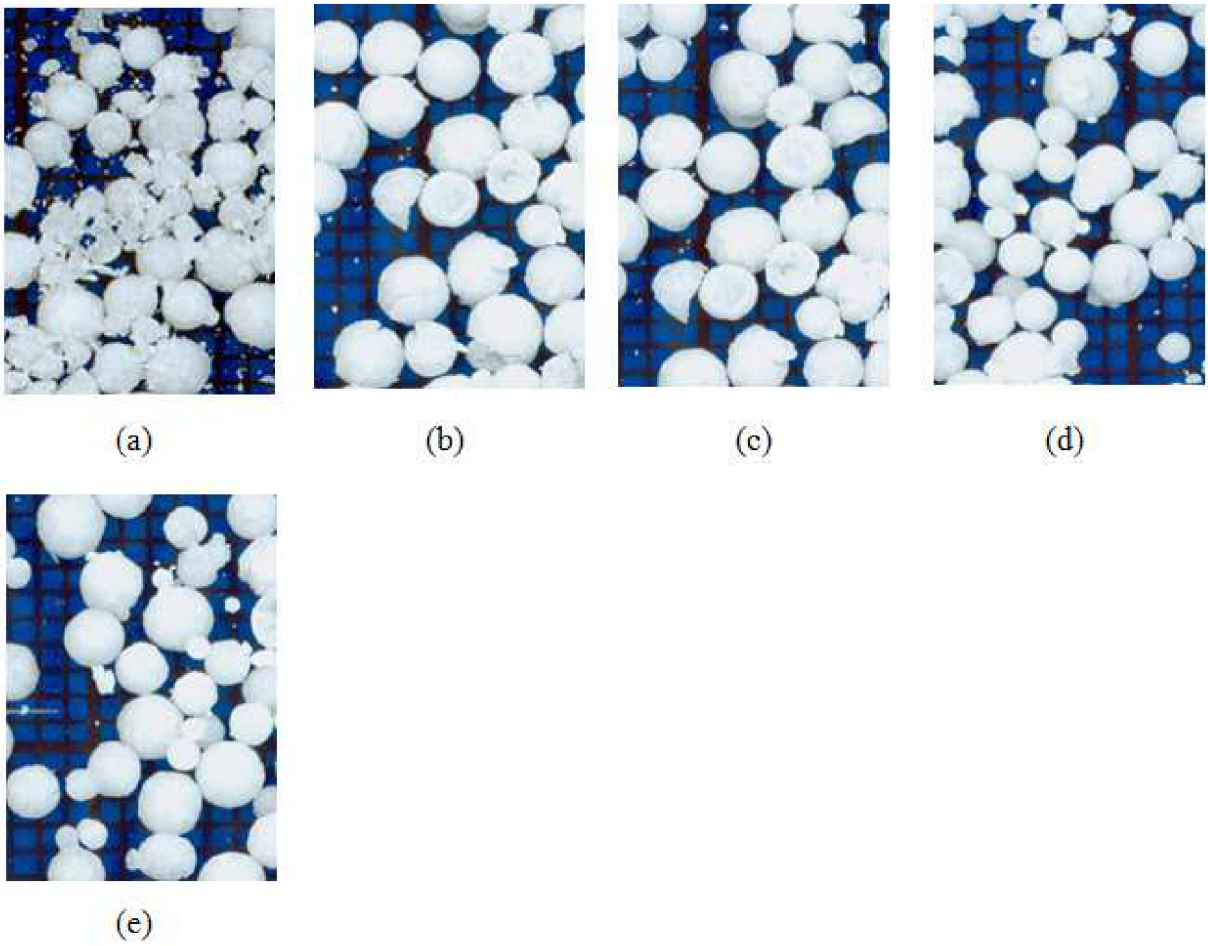

Figure 3.2.4: *Pictures of polymer powder with different activation periods a)no activated b) 1 min, c) 5 min, d) 15 min and e) 30 min activation.*

Figure 3.2.5 shows the dependence of porosity on the activation time. The slightly decreasing trend with longer activation was observed. The higher porosity was observed also in the case of PP powder produced with reference not activated catalyst. During the catalyst activation TEA has enough time to penetrate into the internal parts of catalyst. Then, in comparison with not activated catalyst, the activated one produces more compact polymer particles with lower porosity [70].

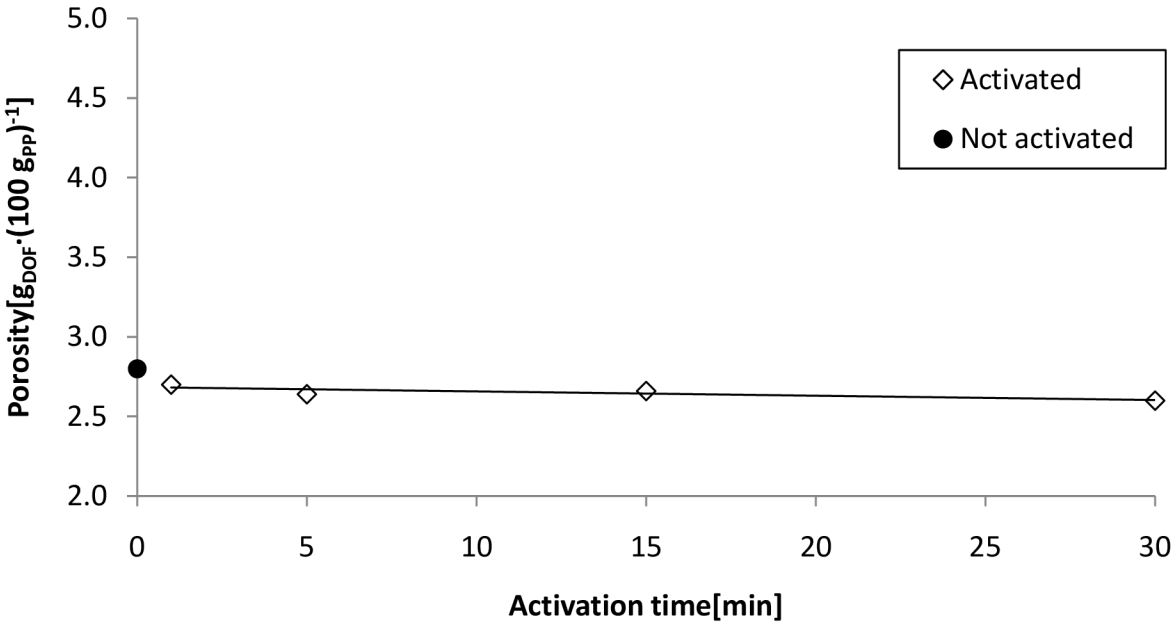

Figure 3.2.5: *Dependence of porosity on of activation time.*

The dependence of MFR on activation time is shown in **Figure 3.2.6**. Evidently, no changes in MFR were observed with activation time prolongation. This means that the activation time did not affected hydrogen response of active centers and average molar mass of the produced polymer. However, noticeably higher MFR of polymer prepared with not activated catalyst was observed. The noticeable difference between the activated/pre–polymerized and not activated/not pre–polymerized catalyst could be explained as follows. The not pre–polymerized catalyst underwent fragmentation into the smaller subparticles during initial phase of main polymerization. Growing polymer shell around all subparticles formed diffusional barrier for the transport of monomer and mainly hydrogen to the active centers located in the center of the growing polymer particle. The concentration gradient in the particle caused that longer polymer chains were produced on active centers located inside the particle than on active centers located close to the particle surface [61]. As the pre–polymerization step prevents fragmentation, the produced polymer particles are bigger and the concentration gradient plays more significant role than in the case of not pre–polymerized catalyst, where the fragmentation occurred. So, based on this theory the fragmentation in the case of not pre–polymerized catalyst increased MFR.

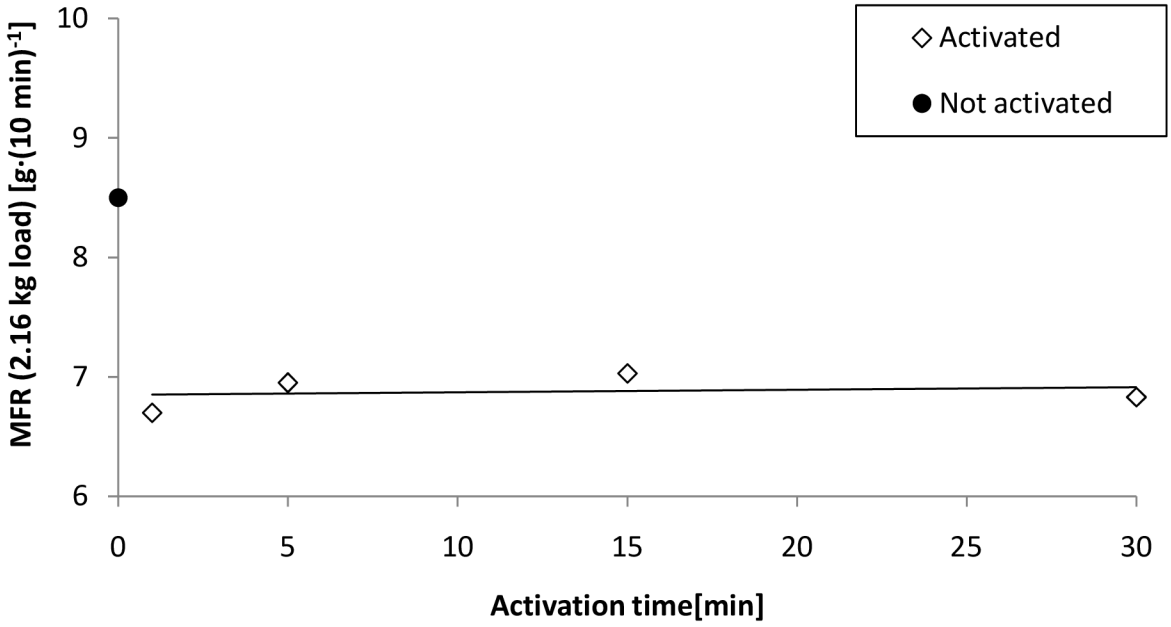

Figure 3.2.6: *Dependence of MFR (2.16 kg load) on activation time.*

The activation time has also noticeable influence on X.S. value. The linear increase of X.S. with the prolongation of activation time is depicted in **Figure 3.2.7**. The reason for the change of the catalyst stereoselectivity can be explained as follows. When the catalyst system is brought into contact with TEA, significant portion of ID is extracted from the catalyst surface by alkylation or complexation reactions with TEA [64]. Of course, the ED is present during activation, but it seems that its efficiency is decreasing with activation time prolongation. The influence of different amounts of ED on the pre–polymerization will be discussed later. Higher X.S. value of no pre–polymerized catalyst is observed.

It is clear that catalyst system in 2–litre gas–phase polymerization reactor did not have enough time to activate all possible polymerization centers. As a result of this fact, the polymer with poorer isotacticity is produced.

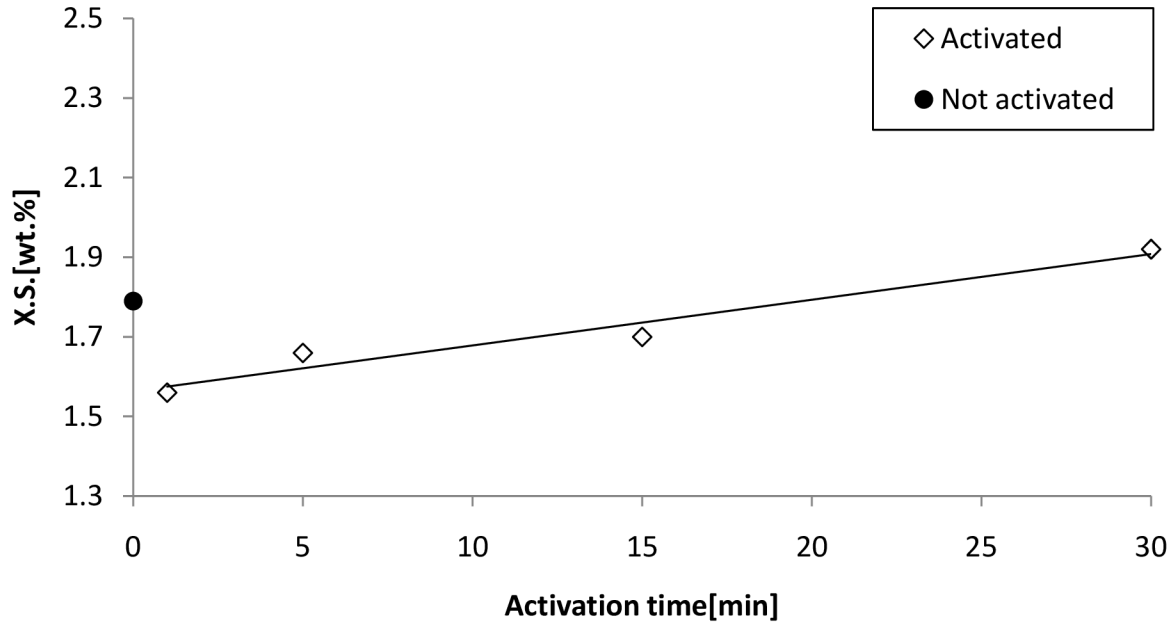

Figure 3.2.7: *Dependence of X.S. on activation time.*

3.3 The influence of Degree of Pre–polymerization (DPP)

The parameter DPP could be explained as the weight ratio of the amount of polypropene produced on active centers during the pre–polymerization to the total amount of catalyst (unit $g_{PP}{\cdot}g_{cat}^{-1}$). The series of the pre–polymerizations experiments were performed to different DPP levels (0.5, 3.0 and 9.0 $g_{PP}{\cdot}g_{cat}^{-1}$) to obtain information about the influence of DPP on the catalyst performance in main polymerization and polymer properties of produced PP. The catalyst, which was only activated and not pre–polymerized, was considered as catalyst with DPP = 0 $g_{PP}{\cdot}g_{cat}^{-1}$. The time of the catalyst activation was 1 min, TEA/Ti = 3.0 $mol{\cdot}mol^{-1}$, DIBDMS/Ti = 0.15 $mol{\cdot}mol^{-1}$ and after the pre–polymerization the catalyst was aged for 30 min before the injection into the 2–litre reactor. The main polymerizations were carried out under the conditions shown in **Table 2.3.1**. The final polymer powder properties are shown in **Table 3.3.1.**

Table 3.3.1.: *Final properties of polymer powders made with catalysts pre–polymerized to different pre–polymerization degrees. TEA/Ti = 3.0 mol·mol^{-1}, DIBDMS/Ti = 0.15 mol·mol^{-1}, temperature of pre–polymerization 23 °C, 1 min activation, 30 min ageing, pressure 1 bar.*

DPP [$g_{pp}{\cdot}g_{cat}^{-1}$]	Activity [$kg{\cdot}g^{-1}{\cdot}h^{-1}$]	B.D. [$kg{\cdot}m^{-3}$]	MFR (2.16 kgload) [$g{\cdot}(10\ min)^{-1}$]	X.S. [wt.%]	Porosity [$g_{DOF}{\cdot}(100g_{PP})^{-1}$]
no activated and no ppol	33.6	431	8.5	1.79	2.82
no ppol, only activated	41.7	420	7.0	1.56	2.74
0.5	40.7	415	7.3	1.55	2.73
3.0	36.0	421	7.5	1.58	2.75
9.0	29.2	425	6.8	1.40	2.65

Figure 3.3.1 shows the dependence of the catalyst activity on DPP. The linear catalyst activity decrease with increase of DPP was observed. In comparison with reference experiment performed with not activated and not pre–polymerized catalyst, the catalyst which was only activated or slightly pre–polymerized exhibited noticeably higher polymerization activity.

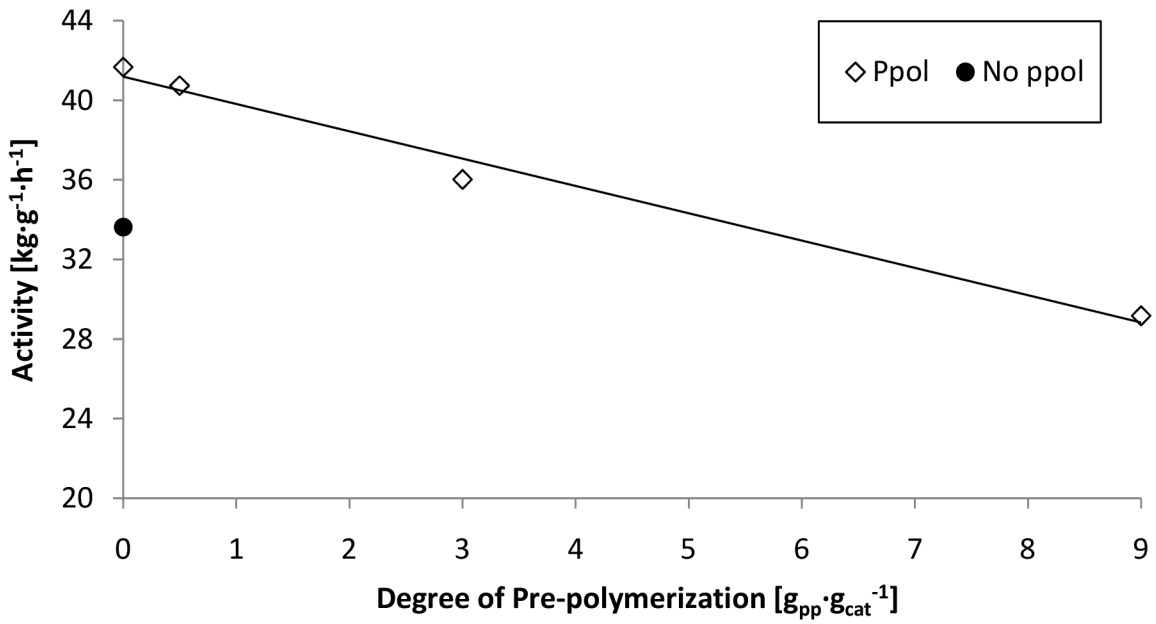

Figure 3.3.1: *Dependence of catalyst activity on pre–polymerization degree.*

As you can see in **Figure 3.3.2**, the increase of DPP caused noticeable decrease of the initial, but also the overall, polymerization rate. This implies that the catalyst pre–polymerization to higher DPPs caused, beside the deactivation of the unstable active centers, also partial deactivation of the stable centers, which is shown by the overall decrease of kinetics profile. As was mentioned before, the high level of the initial activity followed by the rapid deceleration is negative phenomenon, which is related to the intensive heat releasing. The intensive heat release could cause polymer particles overheating and adverse changes in the particle morphology. The polymerization kinetics show that the high initial polymerization rates could be treated, beside the time of activation, also by the pre–polymerization of the catalyst. However, in the case of the pre–polymerization to higher degrees you will also lose part of the stable active centers.

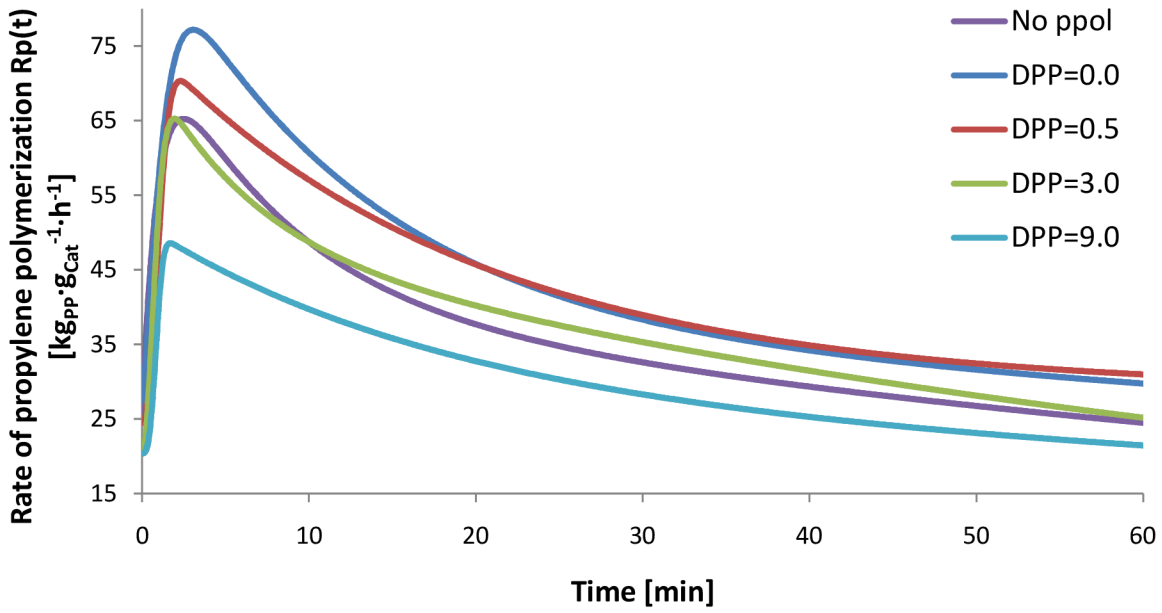

Figure 3.3.2*: Propene polymerization kinetics with catalyst pre–polymerized to different degrees.*

The possible explanations of catalyst activity decrease with increasing DPP could be following. The encapsulation of the active centers by the polymer layer could cause limitation of monomer flux diffusion to active center [41]. Next possible explanation is proposed by Pater et al. [47]. The studied catalyst could be sensitive to 2,1–monomer insertion, which cause the formation of the dormant state of active centers. So, the increase of DPP could increase number of active centers blocked by 2,1–irregular insertion, which cause the decrease of catalyst activity due to the steric hindrance of the methyl group close to the Ti atom.

The dependence of bulk density on DPP is shown in **Figure 3.3.3**. No significant difference between the pre–polymerized and not pre–polymerized catalyst was observed. So, it seems that the studied range of DPP was too narrow to see any effects on B.D., because some authors found that DPP could have noticeable influence on polymer powder bulk density [54,66]. According to their results the catalysts with lower DPPs are associated with higher initial polymerization rates and produce polymer particles with lower bulk densities. They assumed that the higher DPP pre–polymerization step protected catalyst particles against higher initial polymerization rates and fragmentation, which led to the improvement of polymer particle morphology and bulk density.

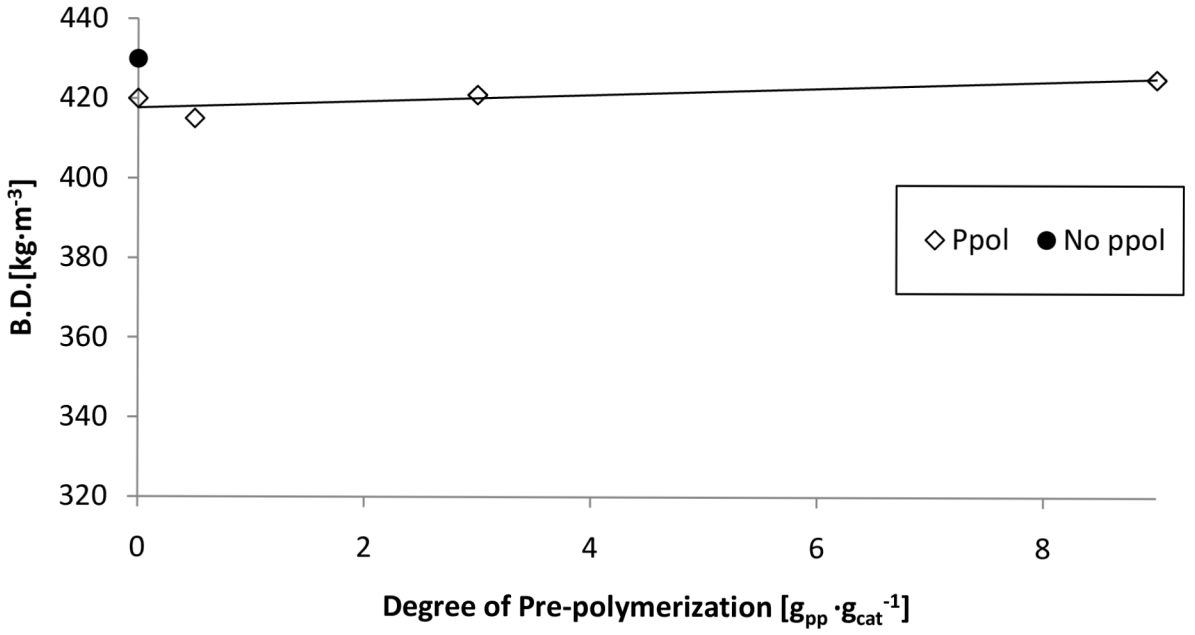

Figure 3.3.3: *Dependence of bulk density on DPP.*

Figure 3.3.4 shows, no significant differences in polymer particle morphology, which was prepared in main polymerization with catalyst pre–polymerized to different DPPs. It is clear that not pre–polymerized catalyst (**Figure 3.3.4a**) produced particles with poor morphology. As was mentioned in Chapter 3.2 during the pre–polymerization step polymer shell was created, which protected catalyst particle against fragmentation, thus the final polymer particles had evidently better shape.

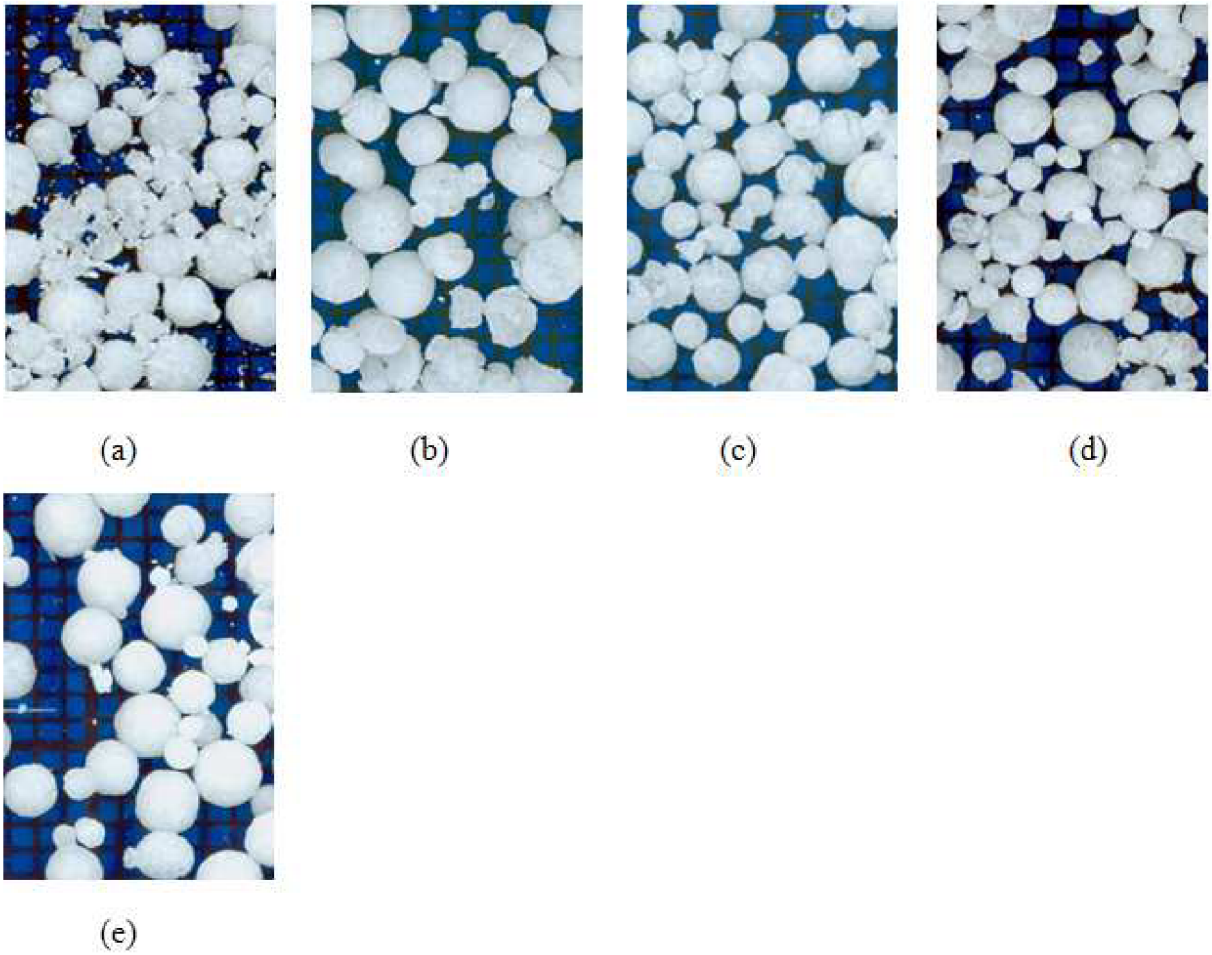

Figure 3.3.4: *Pictures of polymer powders produced in main polymerization in 2–litre reactor with catalysts pre–polymerized to different DPPs:(a) no activation and pre–polymerizated to (b) only activation (DPP = 0.0), (c) DPP = 0.5, (d) DPP = 3.0 and (e) DPP = 9.0* $g_{pp} \cdot g_{cat}^{-1}$.

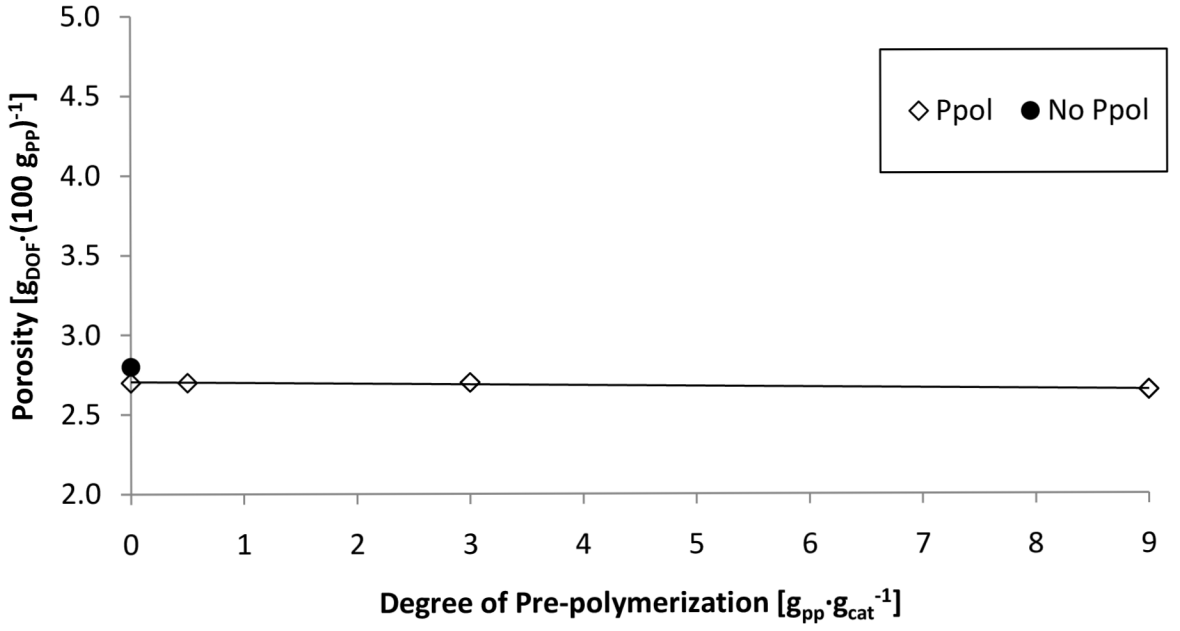

Figure 3.3.5: *Dependence of polymer particle porosity on DPP.*

The fact that the change of catalyst DPP in narrow range $0.0 - 9.0$ $g_{PP} \cdot g_{cat}^{-1}$ has no significant influence on polymer particle morphology produced in main polymerization is proven also by the dependence of polymer particle porosity, where no changes are observed (**Figure 3.3.5**).

Figure 3.3.6 shows the dependence of melt flow rate on DPP. The noticeable difference between the pre–polymerized catalyst and without activation and pre–polymerization was observed. It is clear that changing DPP has no effect on final polymer MFR. Higher MFR of no pre–polymerized catalyst is explained in Chapter 3.2.

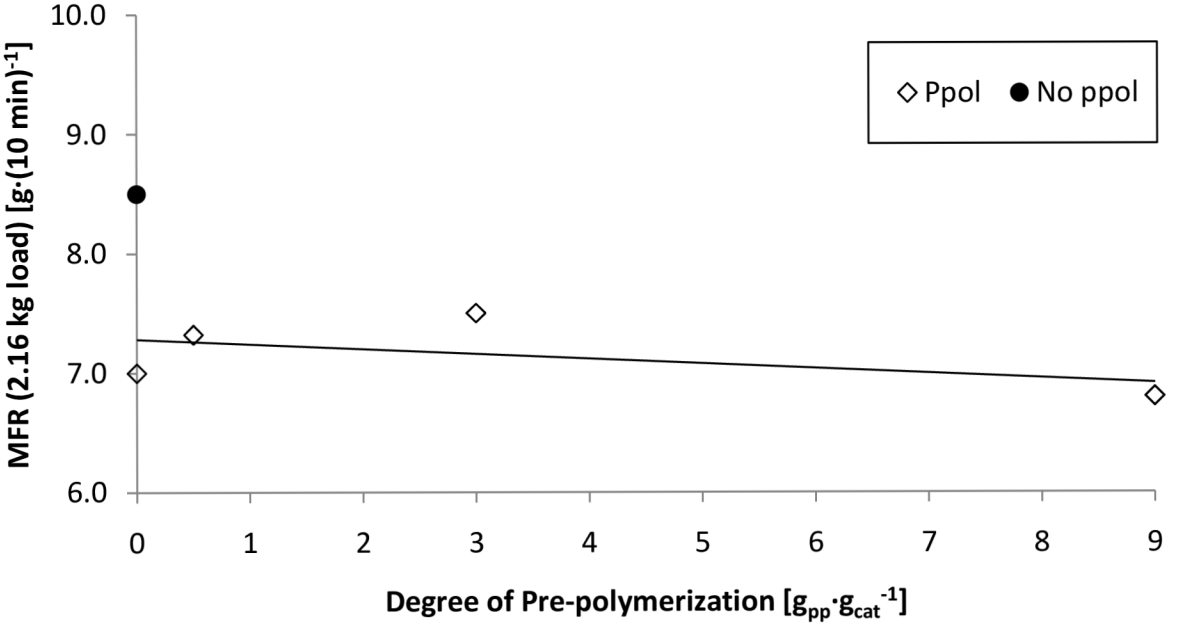

Figure 3.3.6: *Dependence of melt flow rate on DPP.*

Finally, **Figure 3.3.7** shows the dependence of X.S. on DPP. Only slight decrease of X.S. was observed in the case of PP material prepared with catalyst pre–polymerized to highest studied DPP = 9.0 $g_{PP}{\cdot}g_{cat}^{-1}$. So, it could be postulated that, on contrary to duration of catalyst activation, within the studied range the DPPs no effect on catalyst stereospecificity was observed.

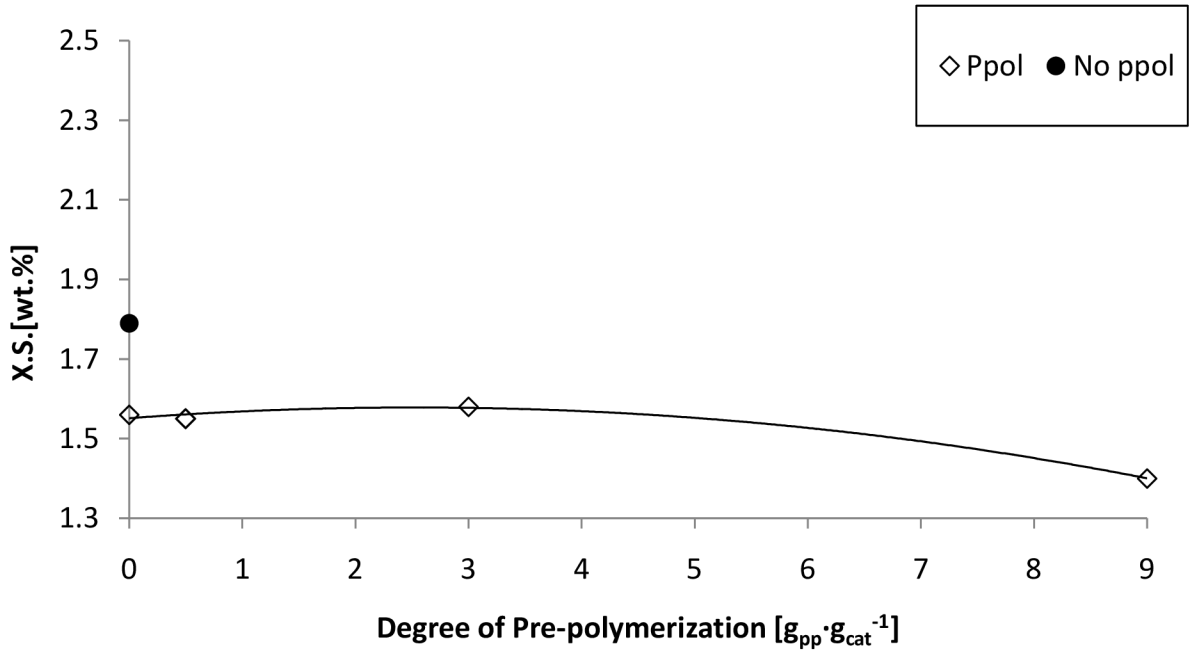

Figure 3.3.7: *Dependence of X.S on DPP.*

3.4 Effect of Ageing on Pre–polymerized Catalyst

It is clear that the pre–polymerized catalyst contain reactive actives centers, which could further react with TEA (over reduction of Ti) or some polar impurities (H_2O, R–OH, O_2, CO_2, CO etc.). Such reactions create different products, which are not able to polymerize propene. The study, which is presented in this Chapter, was focused on the evaluation of effect of ageing on the pre–polymerized catalyst performance. The catalyst was pre–polymerized under the following conditions: 1 min activation, TEA/Ti = 3.0 $mol{\cdot}mol^{-1}$, DIBDMS/Ti = 0.15 $mol{\cdot}mol^{-1}$, DPP = 3.0 $g_{PP}{\cdot}g_{cat}^{-1}$. Subsequently, the pre–polymerized catalyst was washed by heptane three times and diluted by mineral oil to suitable concentration. Then, after the defined time of the ageing the catalyst was injected into the 2–litre reactor and evaluated in main gas–phase polymerization. The final catalyst activities and polymer powder properties in the dependence on ageing time are shown in **Table 3.4.1**. The main polymerizations were carried out under the conditions shown in **Table 2.3.1**.

Table 3.4.1: *Final polymer powder properties made with pre–polymerized catalyst after defined ageing. TEA/Ti = 3.0 mol·mol^{-1}, DIBDMS/Ti = 0.15 mol·mol^{-1}, DPP = 3.0 g_{PP}·g_{cat}^{-1}, 1 min activation, temperature of pre–polymerization 23 °C, pressure 1 bar*

Ageing [h]	Activity [kg·g^{-1}·h^{-1}]	B.D. [kg·m^{-3}]	MFR(2.16 kg load) [g·(10 min)$^{-1}$]	X.S. [wt.%]	Porosity [g_{DOF}·(100 g_{PP})$^{-1}$]
–(no ppol)	33.6	431	8.5	1.79	2.81
1.5	33.5	430	7.2	1.64	2.53
4.5	32.9	426	7.0	1.66	2.52
23.5	31.3	427	6.9	1.59	2.64
47.5	31.0	425	7.1	1.60	2.65
168	29.4	424	6.9	1.61	2.75
336	29.2	424	6.8	1.41	2.76

It was found out that the ageing of the pre–polymerized catalyst is important parameter. The negative exponential profile of the catalyst activity decrease with longer ageing time was observed (**Figure 3.4.1**). Then the kinetic profiles shown in **Figure 3.4.2** again revealed the evident effect of pre–polymerization on the initial polymerization rate. The activity of the pre–polymerized catalyst is noticeably decreasing during first ca. 24 hours, then the decrease of activity with prolongation of ageing became less significant. **Figure 3.4.2** further shows that the kinetic profiles of pre–polymerized catalyst after different times of ageing have similar shape, but the profiles are shifted to lower levels. This implies that the catalyst active centers were deactivated.

Enrico Magni et al. [62] found out that the reaction of $TiCl_4$ with liquid TEA for long time lead to complete reduction of Ti^{4+} and formation of surface centers of stoichiometry $TiClEt_n$ (n = 1 or 2), which confirmed the possibility of ZN catalyst active centers deactivation by TEA over reduction, because it is known that Ti^{2+} and lower oxidation states are not able to polymerize propene. Of course, we have to consider also the presence of polar impurities and their possible reactions with catalyst system.

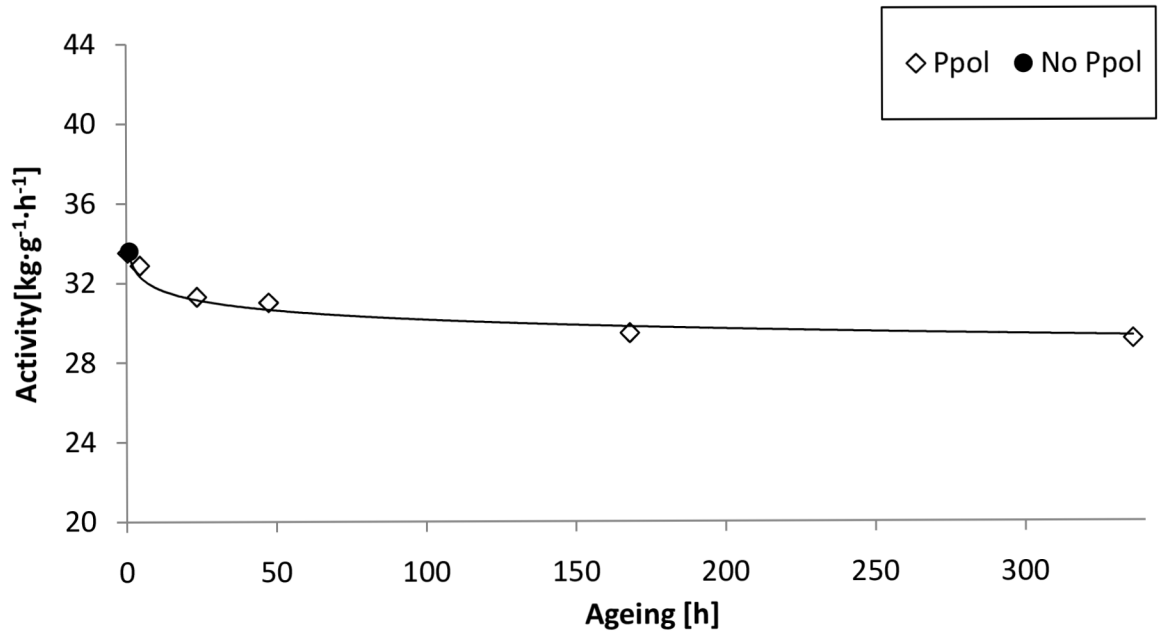

Figure 3.4.1: *Dependence of catalyst activity in main polymerization on pre–polymerized catalyst ageing.*

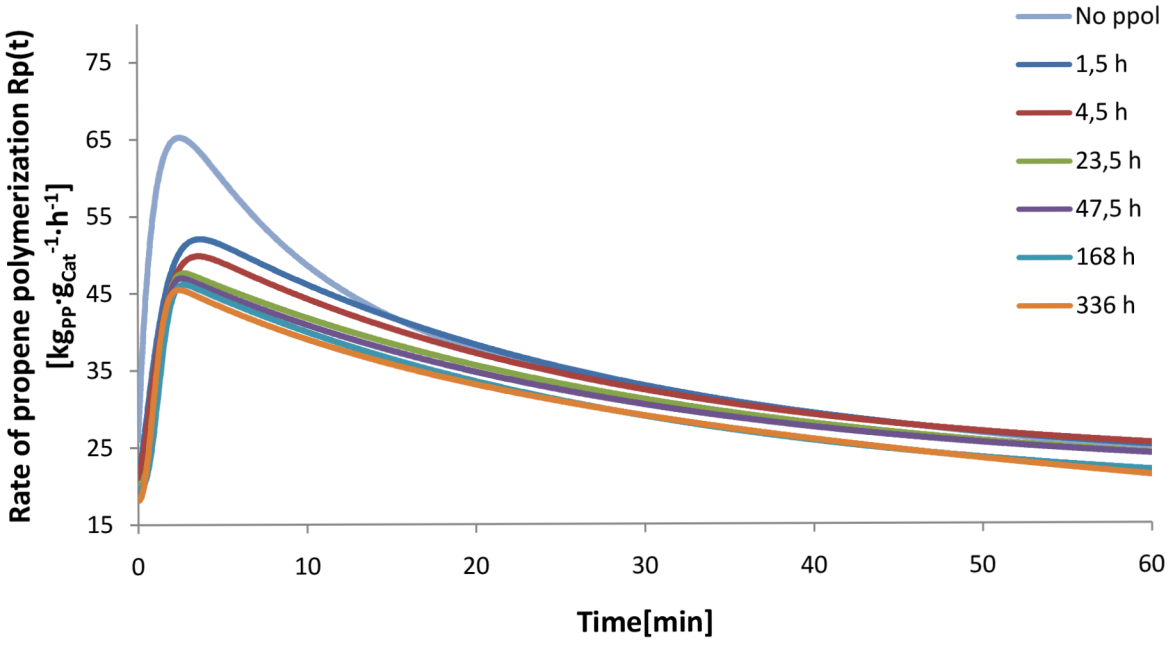

Figure 3.4.2: *Kinetic profiles of main polymerization with pre–polymerized catalyst aged for different times and compared also with reference not pre–polymerized catalyst.*

Figure 3.4.3 shows the dependence of the bulk density on the ageing of the pre–polymerized catalyst. It is evident that the ageing did not influence this polymer powder property. Also, no differences in polymer powder morphologies were observed, see **Figure 3.4.4**.

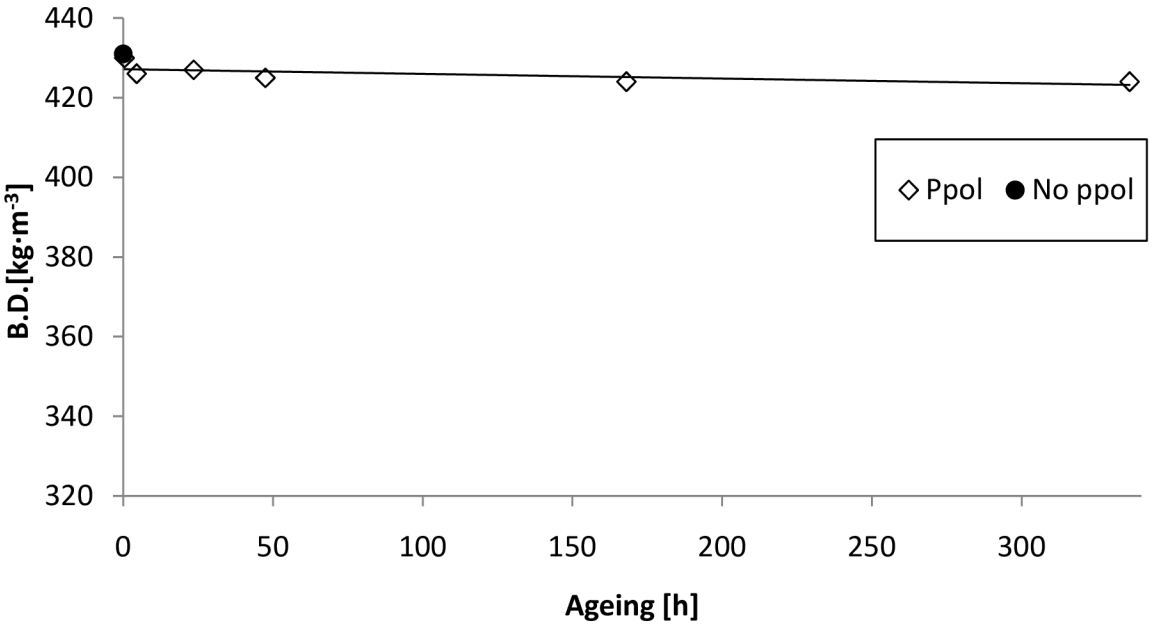

Figure 3.4.3: *Dependence of final polymer bulk density on pre–polymerized catalyst ageing.*

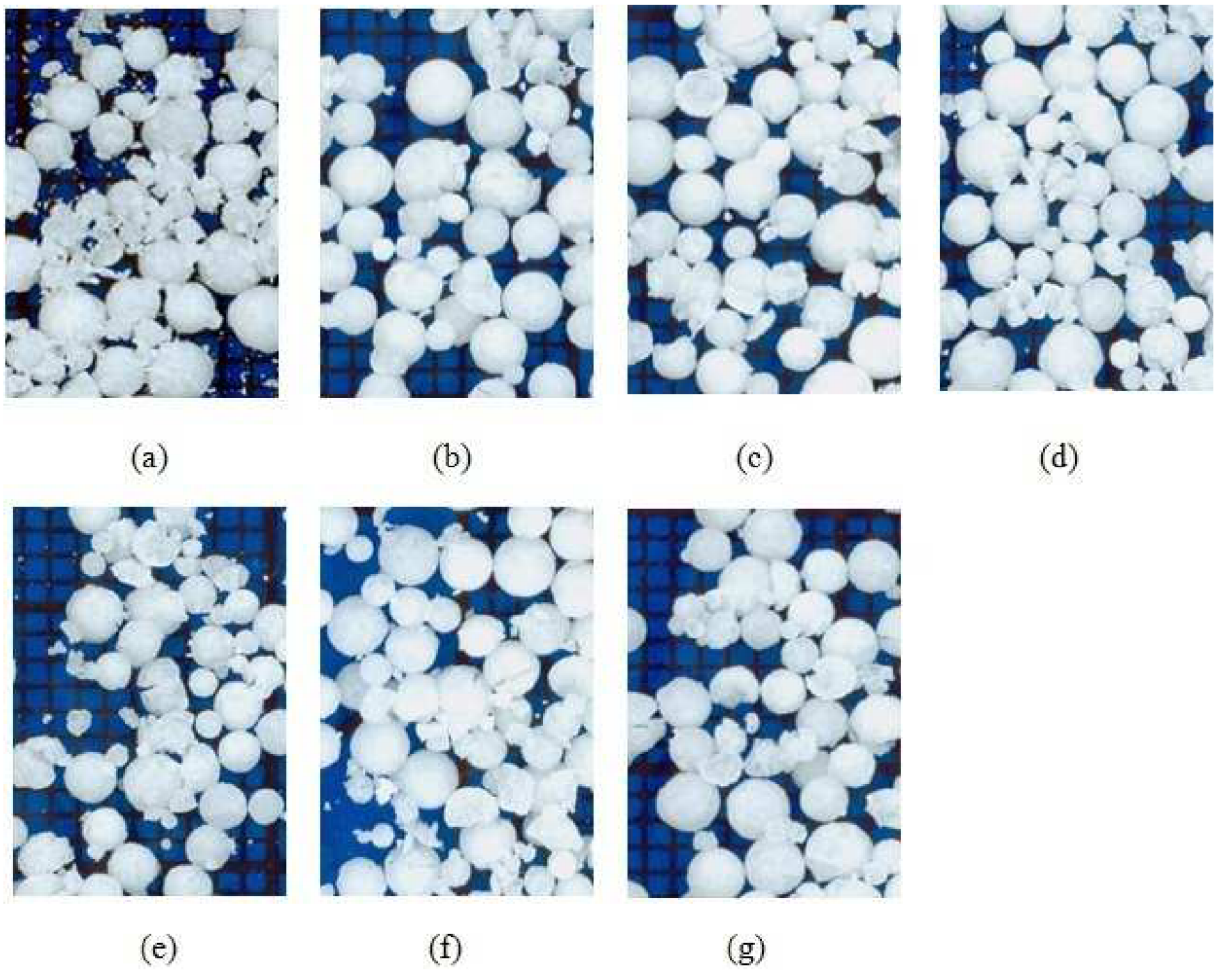

Figure 3.4.4: *Pictures of final polymer powders produced with: (a) not pre–polymerized catalyst and pre–polymerized catalyst after ageing for (b) 1.5 h, (c) 4.5 h, (d) 23.5 (e) 47.5 h, f) 168 h and h) 336 h.*

The dependence of porosity on pre–polymerized catalyst ageing is shown in **Figure 3.4.5**. It was observed that during first ca. 24 hours the porosity of produced polymer particles slightly increases. Of course, higher porosity of not pre-polymerized catalyst powder is again noticed. The results suggest that the polymer powder porosity is related to the decrease of catalyst activity, i.e. number of active centers. With decreasing catalyst activity the porosity is increasing. This fact is probably caused by formation of less dense particles due to the titanium over reduction with TEA.

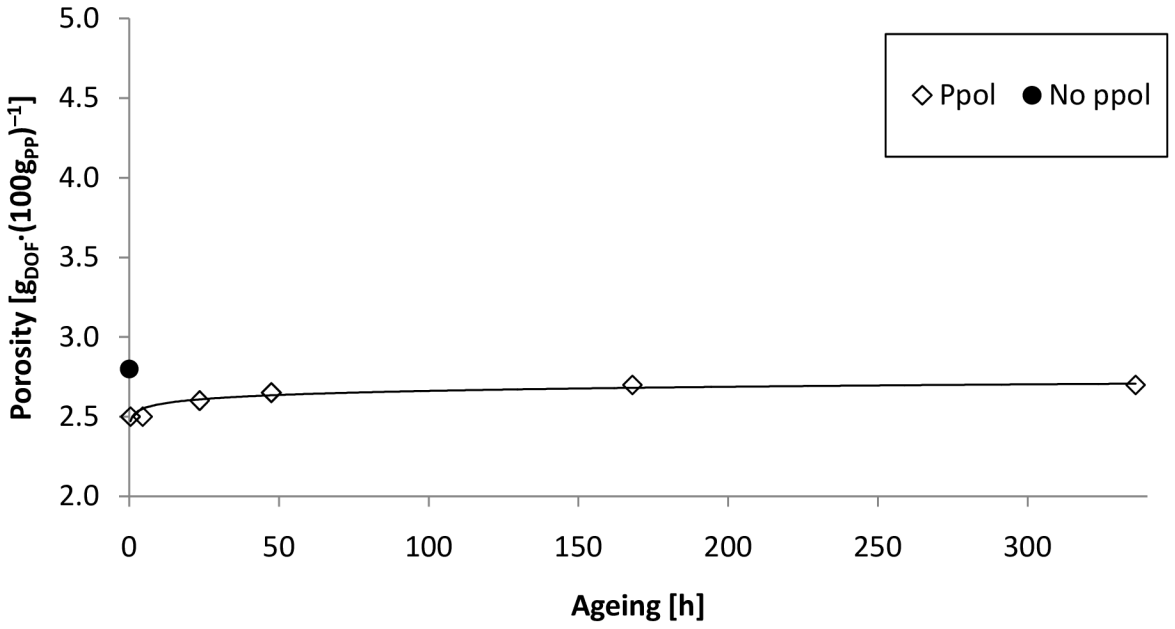

Figure 3.4.5: *Dependence of final polymer porosity on pre–polymerized catalyst ageing.*

The dependence of final polymer MFR on the pre–polymerized catalyst ageing is depicted in **Figure 3.4.6**. There are no significant changes. The reason for higher MFR of not pre–polymerized catalyst was explained in Chapter 3.2.

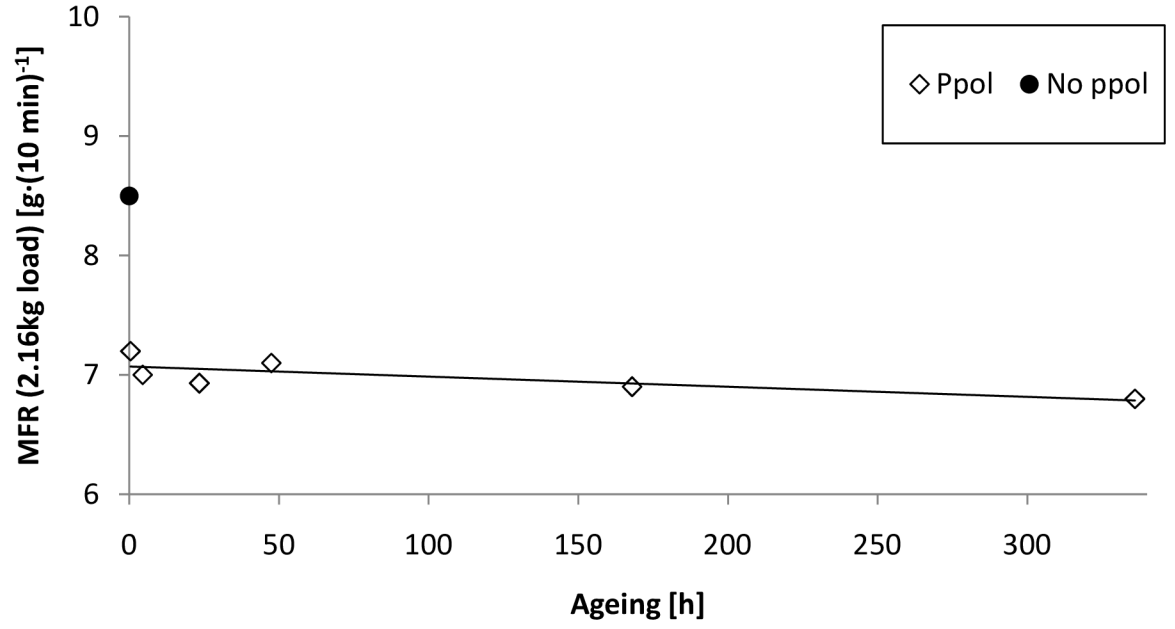

Figure 3.4.6: *Dependence of melt flow rate (2.16 kg load) of final polymer on pre–polymerized catalyst ageing.*

The slight decrease of X.S. values of the final polymer in dependence on the pre–polymerized catalyst ageing was observed and it is shown in **Figure 3.4.7**. This observation

probably mean that during the catalyst ageing mainly the active centers with poorer stereoselectivity were deactivated.

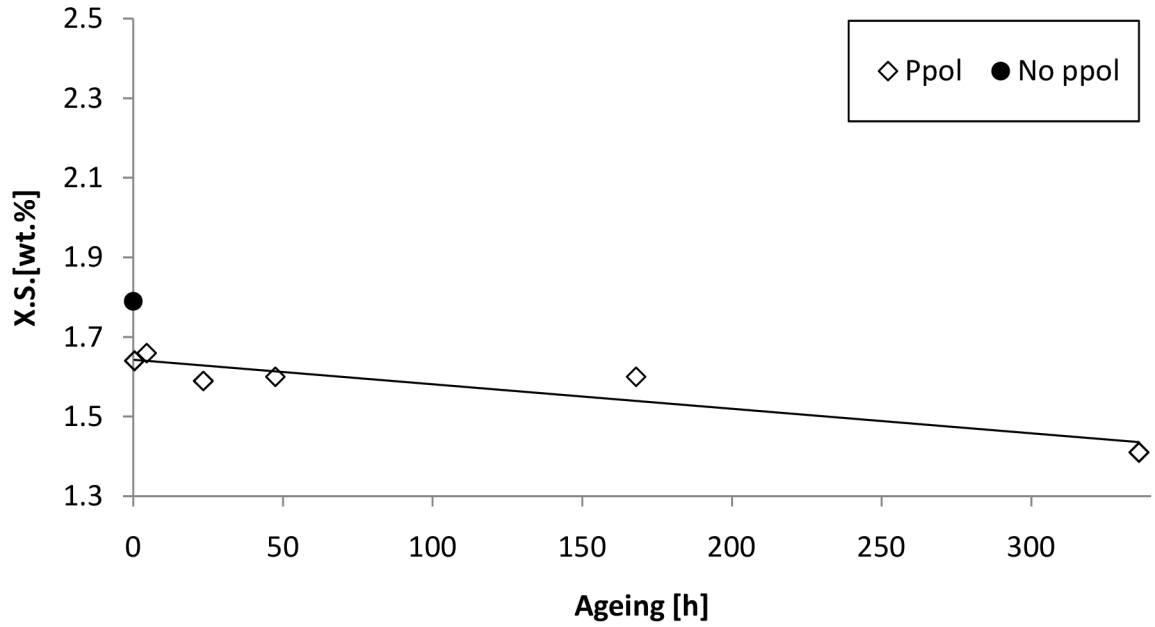

Figure 3.4.7: *Dependence of xylene solubles of final polymer on pre–polymerized catalyst ageing.*

3.5 Influence of TEA/Ti Molar Ratio on ZN Catalyst Pre–polymerization

Triethylaluminum (TEA) is the most common co-catalyst for the ZN catalysts activation. It plays the key role in the active centers formation for α-olefins polymerization. This Chapter was focused on the evaluation of the influence of the different TEA concentrations on pre–polymerized catalyst performance. All the pre–polymerizations were carried out under the following conditions: 1 min activation, 30 min ageing, DIBDMS/Ti = 0.15 mol·mol^{-1}, DPP = 3.0 g_{PP}·g_{cat}^{-1}. Studied TEA/Ti molar ratios and final polymer properties are shown in **Table 3.5.1**. Main polymerizations were carried out under the conditions mentioned in **Table 2.3.1**.

Table 3.5.1: *Final polymer powder properties made of pre–polymerized catalyst with different TEA/Ti molar ratios. DIBDMS/Ti = 0.15 mol·mol^{-1}, DPP = 3.0 g_{PP}·g_{cat}^{-1} ,1 min activation, 30 min ageing ,temperature of pre–polymerization 23 °C, pressure 1 bar*

TEA/Ti [mol·mol^{-1}]	Activity [kg·g^{-1}·h^{-1}]	B.D. [kg·m^{-3}]	MFR(2.16kg load) [g·(10 min)$^{-1}$]	X.S. [wt.%]	Porosity [g_{DOF}·(100 g_{PP})$^{-1}$]
3.0(no ppol)	33.6	431	8.5	1.79	2.81
1.0	39.2	410	7.6	1.53	2.62
3.0	36.2	435	7.2	1.67	2.54
5.0	34.8	419	7.0	1.78	2.61
10.0	30.7	430	6.6	1.78	2.45

Figure 3.5.1 shows the dependence of catalyst activity in main polymerization on the TEA concentration in the pre–polymerization step. As this figure shows, catalyst activity in main polymerization linearly decrease with increasing TEA/Ti molar ratio applied in pre–polymerization. As was mentioned above, TEA transforms the inactive centers in active ones by reducing the inactive Ti^{4+} to active Ti^{3+}. The only decreasing profile of the dependence of catalyst activity in main polymerization on TEA concentration applied in pre–polymerization step indicates that even at the lowest TEA/Ti molar ratio 1.0, the catalyst was fully activated and all the possible active centers were formed. Then the further increase of TEA/Ti ratio to higher excess to Ti promoted the adverse over reduction of active Ti^{3+} centers to Ti^{2+} and lower oxidative states, which are not able to polymerize propene. This study revealed that the molar ratio TEA/Ti 1.0 seems to be sufficient for the pre–polymerization step.

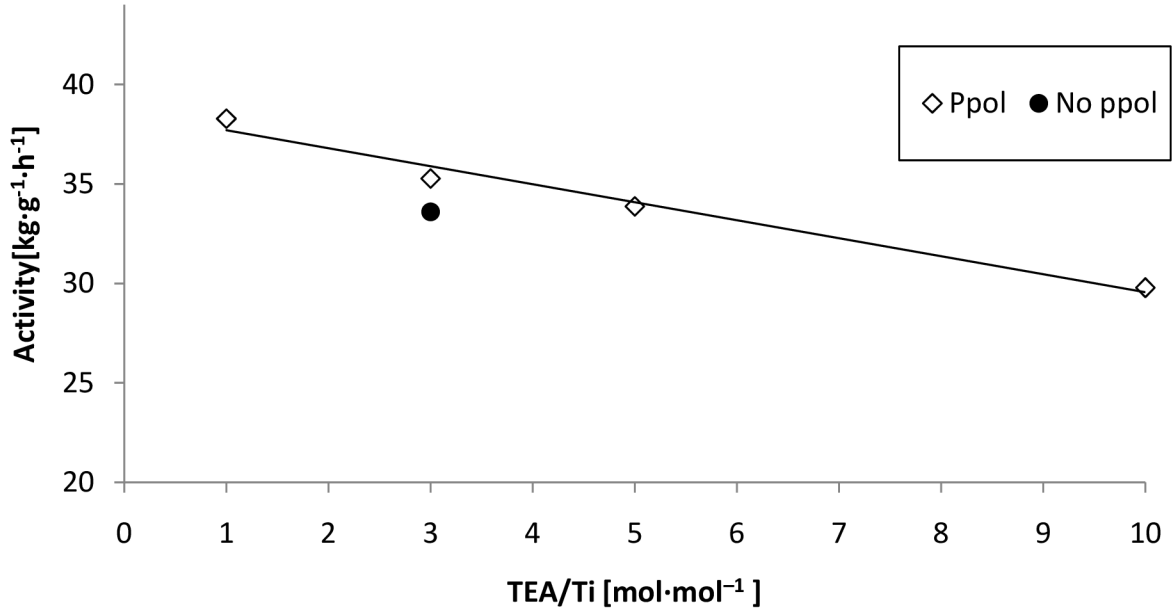

Figure 3.5.1: *Dependence of catalyst activity in main polymerization on TEA concentration in pre–polymerization step.*

Figure 3.5.2 shows the influence of TEA concentration applied in the pre–polymerization step on main polymerization kinetics. As expected, the catalyst activity as well as the polymerization rate decreased due to deactivation of the active centers by Ti^{3+} over reduction.

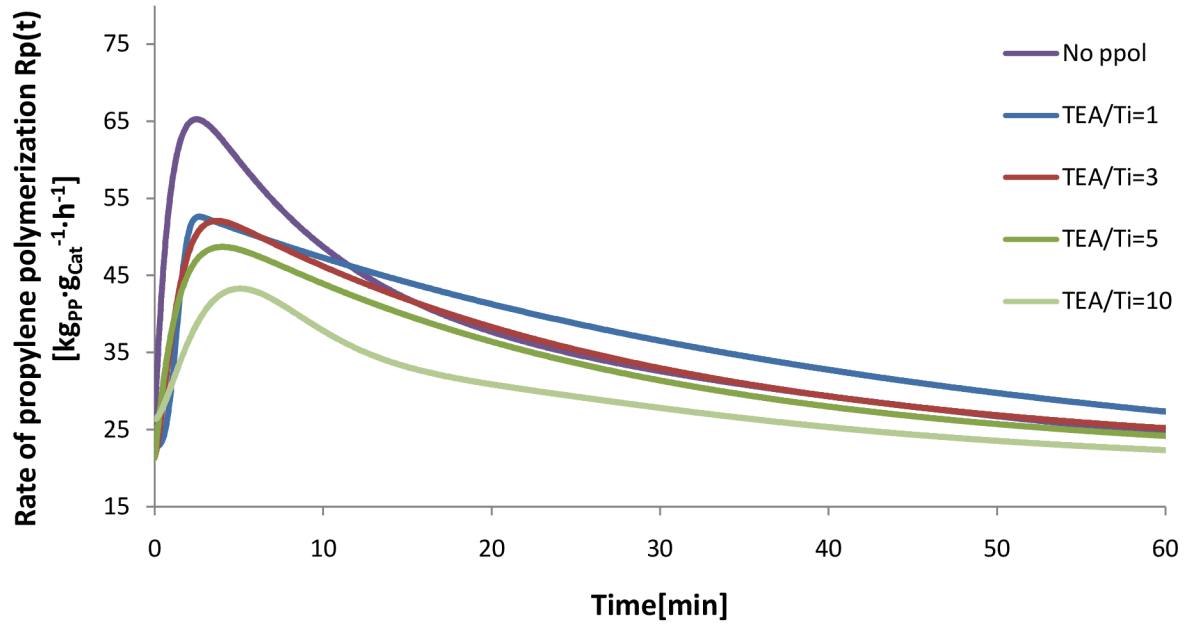

Figure 3.5.2: *Kinetic profiles of main polymerizations with catalysts pre–polymerized at different TEA/Ti molar ratios and compared also with catalyst, which was only activated, but not pre–polymerized.*

Figure 3.5.3 shows that slightly increase of B.D. occurred between TEA/Ti molar ratios 1.0 and 3.0. Higher molar ratio release the same bulk density as TEA/Ti molar ratio 3. It is clear that TEA/Ti has not any significant influence on final polymer morphology. Also, this fact is confirmed by **Figure 3.5.4b-e**, where no changes are observed.

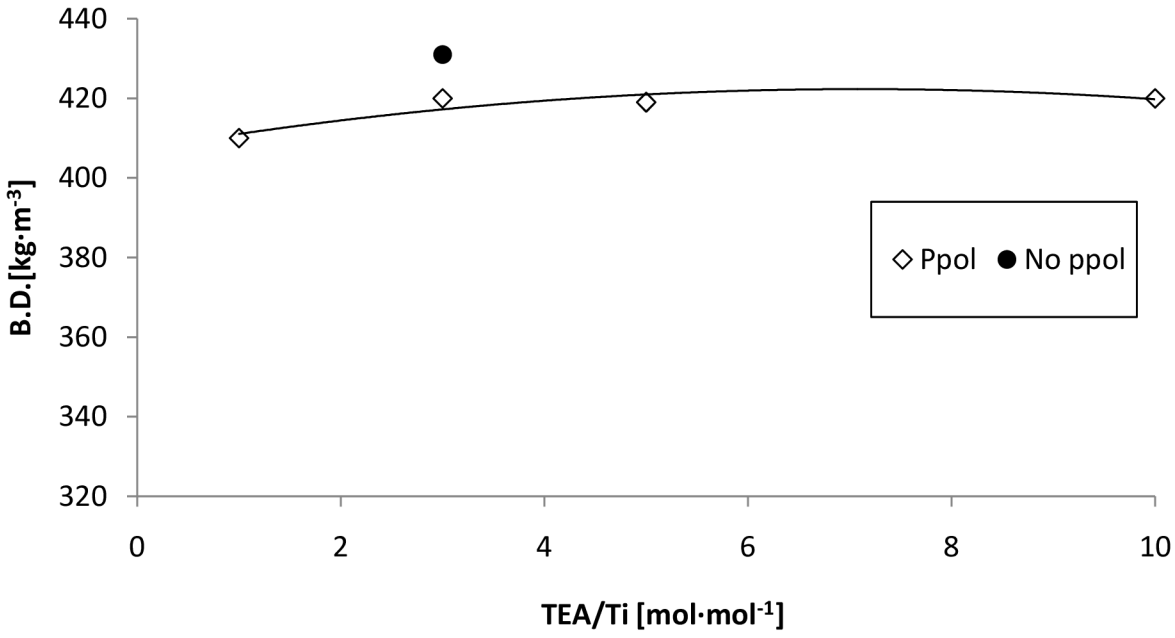

Figure 3.5.3: *Dependence of bulk density of final PP powder on TEA/Ti molar ratio applied in pre–polymerization step.*

(a) (b) (c) (d)

(e)

Figure 3.5.4: *Pictures of final polymer powders of (a) not pre–polymerized catalyst and with catalysts pre–polymerized at TEA/Ti ratios (b) 1.0, (c) 3.0,(d) 5.0 and (e) 10.0 mol·mol^{-1}.*

The effect of TEA/Ti ratio on porosity is shown in **Figure 3.5.5**. Only slight decrease of porosity was observed with increasing TEA/Ti molar ratio applied in pre–polymerization step.

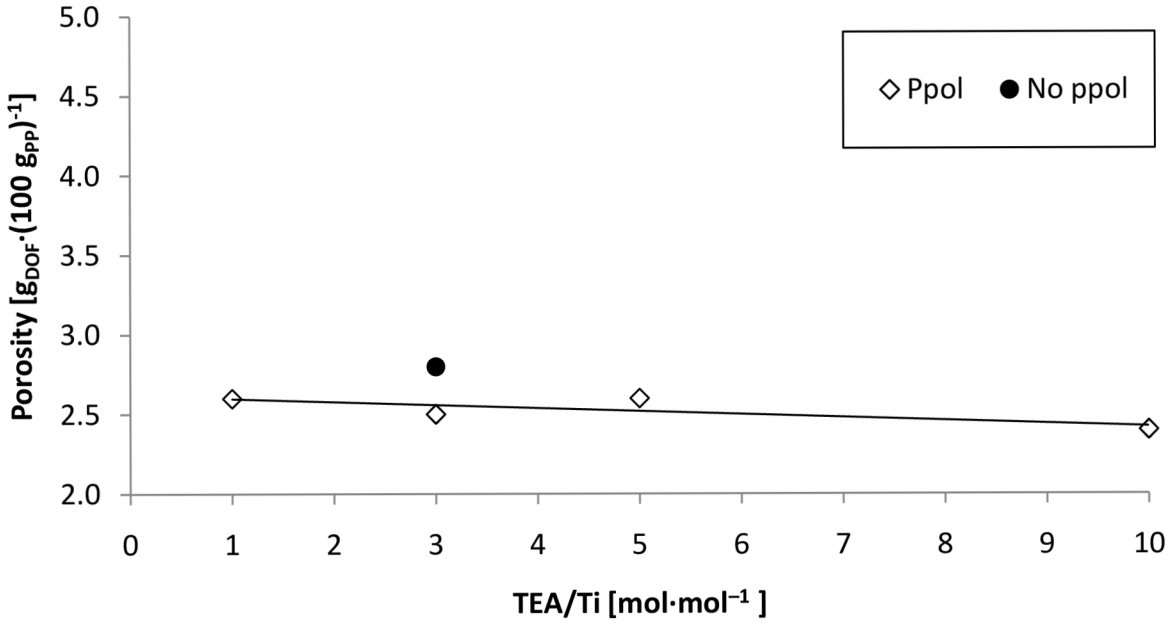

Figure 3.5.5: *Dependence of porosity of final polymer powder on TEA/Ti molar ratio applied in pre–polymerization step*

The decreasing trend of MFR in dependence to TEA/Ti ratio is shown in **Figure 3.5.6**. It is clear that MFR is related to particles fragmentation as was mentioned in Chapter 3.2.

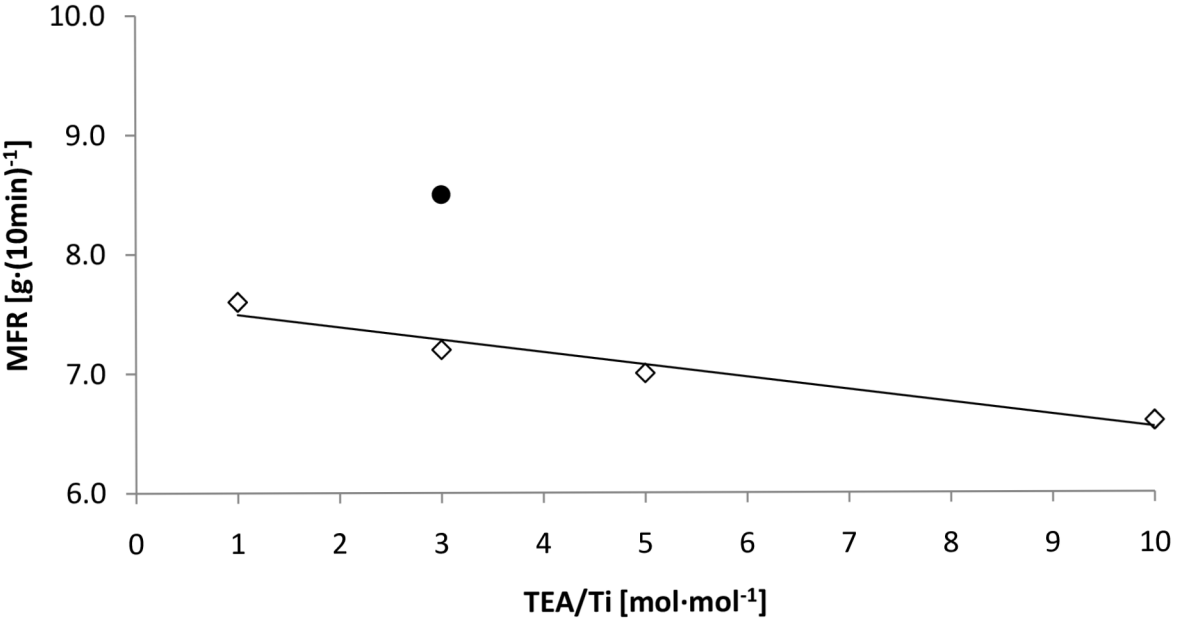

Figure 3.5.6: *Dependence of MFR (2.16 kg load) of final polymer powder on TEA/Ti molar ratio applied in pre–polymerization step.*

The effect of TEA/Ti molar ratio, which was applied in the pre–polymerization, on X.S. is depicted in **Figure 3.5.7**. Up to TEA/Ti molar ratio 5.0, X.S. is increasing. Then higher molar

ratio did not further increase X.S. value. It seems that TEA/Ti molar ratio 5 is sufficient to improve stereospecificity of all active centers.

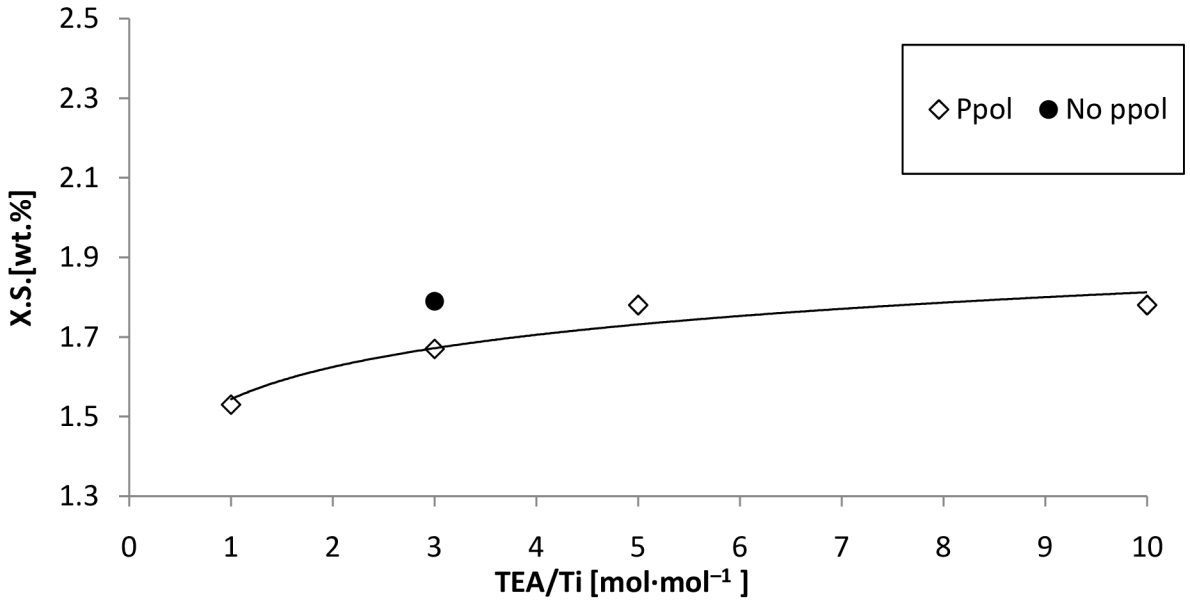

Figure 3.5.7: *Dependence of X.S. of final polymer on TEA/Ti molar ratio applied in pre–polymerization step.*

3.6 Influence of DIBDMS/Ti Molar Ratio on ZN Catalyst Pre–polymerization

It is generally accepted that the using of Lewis bases as external donors can noticeably influence the catalyst activity, polymerization kinetics and stereospecificity of active centers of 4th ZN catalyst generation [23,27,28,30].

The series of polymerizations were carried out to investigate the influence of different concentrations of DIBDMS external donor in pre–polymerization step. The studied DIBDMS/Ti molar ratios are mentioned in **Table 3.6.1** together with the properties of polymer materials produced in the subsequent main polymerization. The pre–polymerization conditions were set to TEA/Ti = 3.0 mol·mol^{-1}, DPP = 3.0 g_{pp}·g_{cat}^{-1}, 1 min activation and 30 min ageing. The main polymerizations were carried out according to the conditions mentioned in **Table 2.3.1.**

Table 3.6.1: *Final polymer powder properties with different DIBDMS/Ti molar ratio in pre–polymerization step. TEA/Ti = 3.0 mol·mol^{-1}, DPP = 3.0 g_{PP}·g_{cat}^{-1}, 1 min activation, 30 min ageing, temperature of pre–polymerization 23 °C, pressure 1 bar*

DIBDMS/Ti [mol·mol^{-1}]	Activity [kg·g^{-1}·h^{-1}]	B.D. [kg·m^{-3}]	MFR(2.16 kg load) [g·(10 min)$^{-1}$]	X.S. [wt.%]	Porosity [g_{DOF}·(100 g_{PP})$^{-1}$]
0.15(No ppol)	33.6	431	8.5	1.79	2.81
0.00	33.8	429	7.9	1.78	2.42
0.15	35.3	410	7.7	1.80	2.64
0.30	32.7	408	7.6	1.78	2.52
0.50	33.8	405	7.4	1.77	2.65
0.80	33.0	402	7.3	1.75	2.87

The dependence of the catalyst activity on the increasing concentration of DIBDMS is in **Figure 3.6.1**. The results show that the different amounts of DIBDMS have no significant effect on catalyst pre–polymerization. This is also supported by propene polymerization kinetics shown in **Figure 3.6.2**. The recent study [69] revealed that external donors can cause the deactivation of parts of active centers, but in our case the catalyst pre–polymerized without using DIBDMS shows almost similar properties compared to different DIBDMS concentrations. This indicates that soft conditions under which the pre–polymerizations were carried out caused that external donor was not necessary, because during the pre–polymerization the extraction of internal donor by TEA was limited.

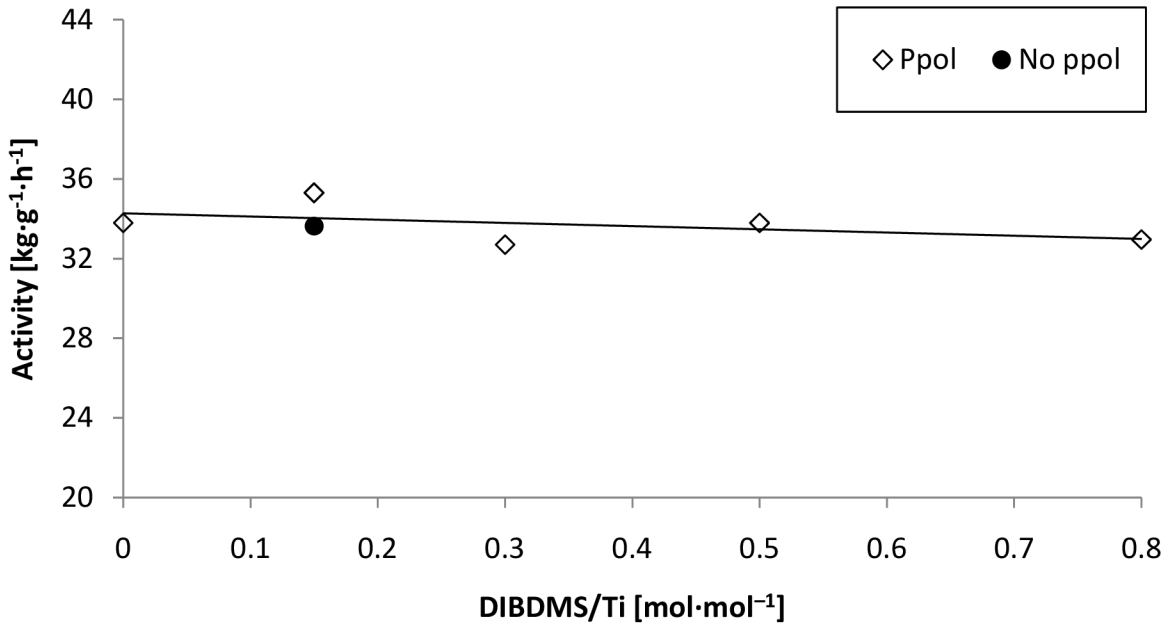

Figure 3.6.1: *Dependence of catalyst activity in main polymerization on increasing amount of DIBDMS external donor in pre–polymerization step.*

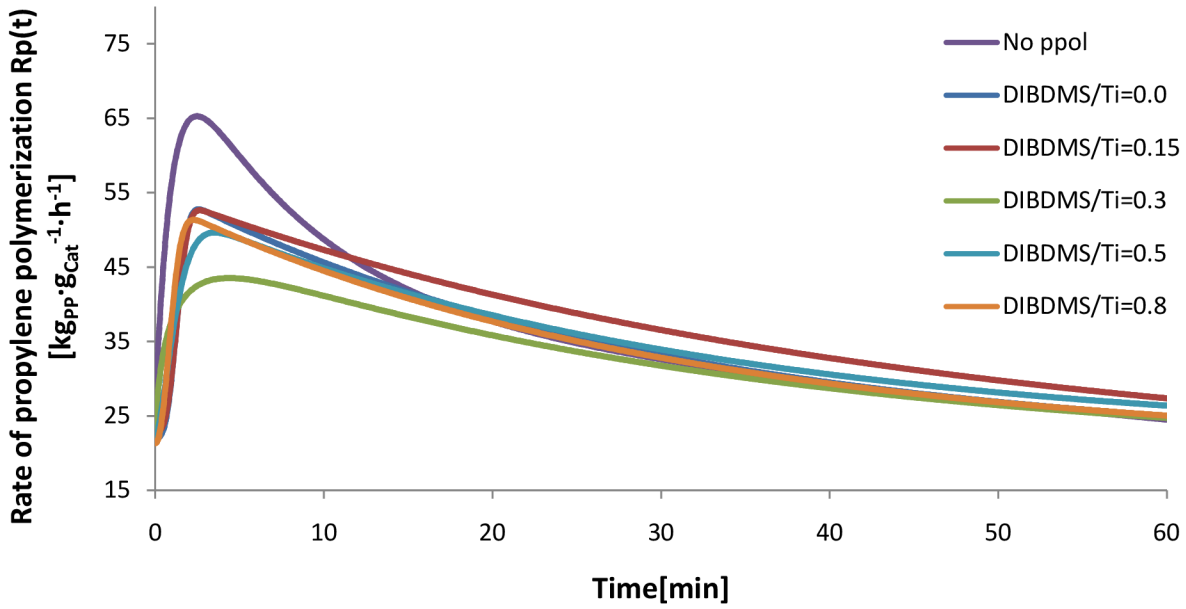

Figure 3.6.2: *Kinetics profiles of pre-polymerized catalysts with different DIBDMS/Ti ratios compared to not pre-polymerized catalyst*

In **Figure 3.6.3** the effect of different DIBDMS concentrations on bulk density is plotted. No significant changes were observed. Only experiment without DIBDMS shows higher bulk density, which is equal to the not pre–polymerized catalyst. Next, **Figure 3.6.4** shows the pictures of polymer particles. This also confirmed the fact that no significant changes in polymer particles morphology occured. On the other side, evident increase of polymer particle porosity with increasing DIBDMS concentration was observed as it is shown in **Figure 3.6.5**. The reason explaining this fact is not clear and requires more experiments.

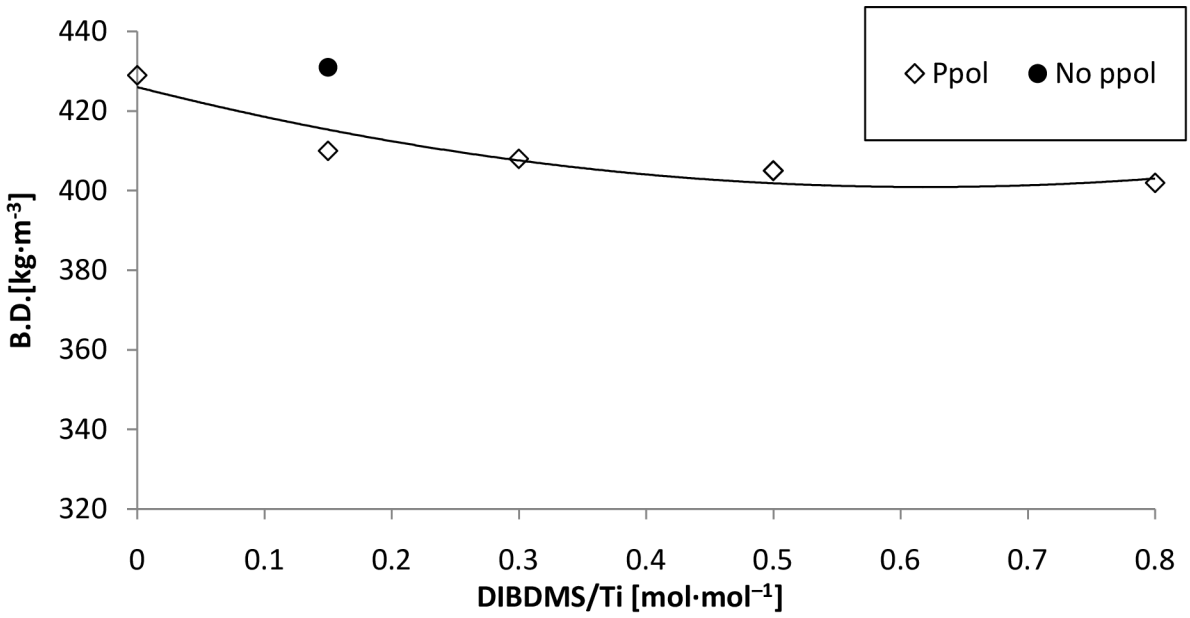

Figure 3.6.3: *Dependence of final polymer bulk density on DIBDMS/Ti molar ratio applied in pre–polymerization step.*

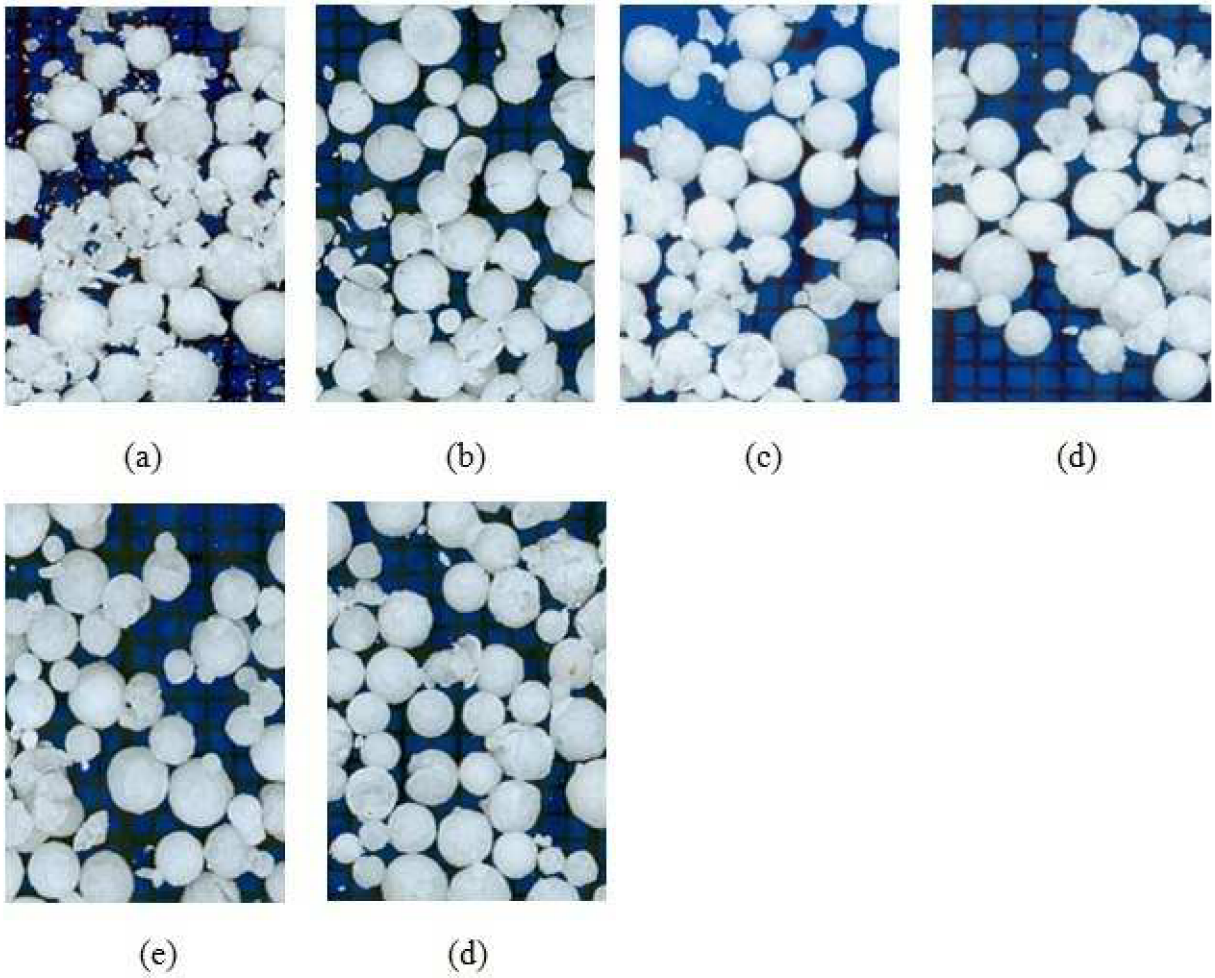

Figure 3.6.4: *Pictures of polymer powders of (a)not pre–polymerized catalyst and pre–polymerized catalysts with DIBDMS/Ti molar ratios: b) 0.0 (only activation), c) 0.15, d) 0.3, e) 0.5 and f) 0.8 mol·mol^{-1}*

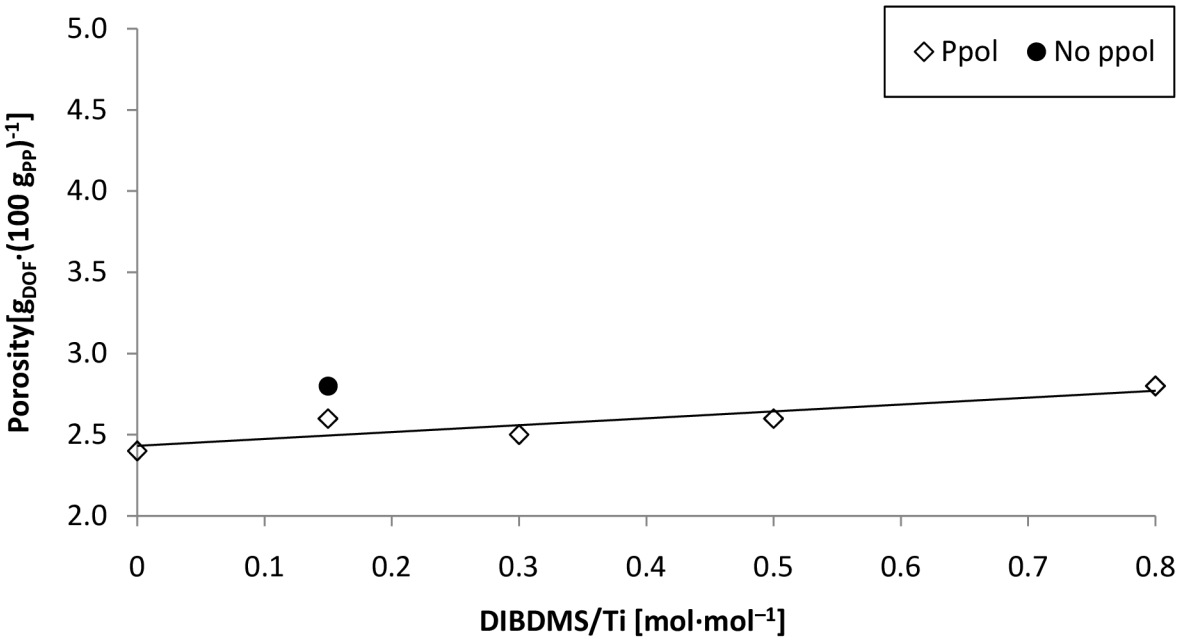

Figure 3.6.5: *Dependence of main polymer porosity on DIBDMS/Ti molar ratio applied in pre–polymerization step.*

Figure 3.6.6 shows almost negligible linear decrease of final polymer MFR (2.16 kg load) with increasing concentrations of DIBDMS in pre–polymerization step.

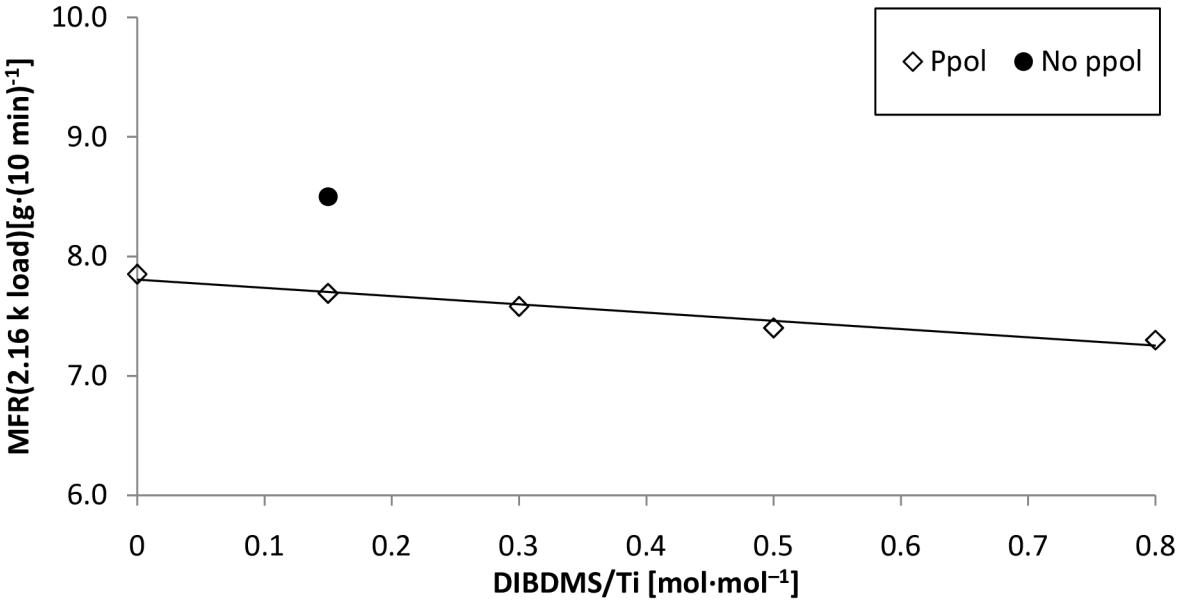

Figure 3.6.6.: *Dependence of main polymer MFR(2.16kg load) on DIBDMS/Ti molar ratio in applied pre–polymerization step.*

The observation that different amounts of DIBDMS do not have any significant effect on the pre–polymerization step is also confirmed by the results presented in **Figure 3.6.7**,where X.S. values are plotted in dependence on DIBDMS/Ti molar ratio.

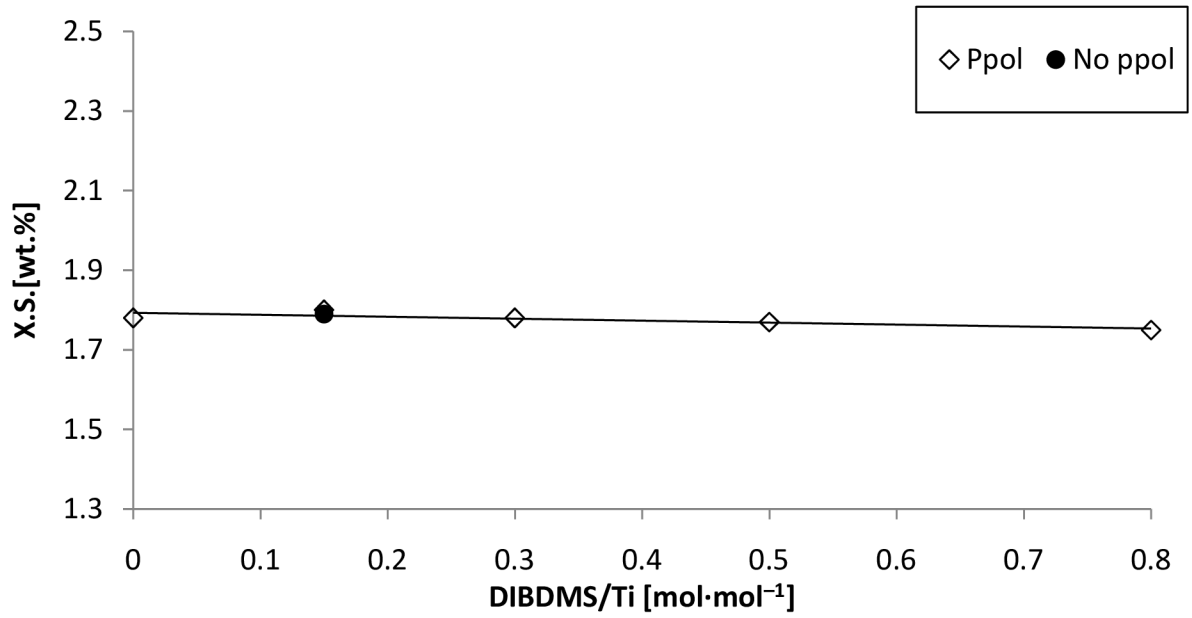

Figure 3.6.7: *Dependence of final polymer X.S. on DIBDMS/Ti molar ratio applied in pre–polymerization step.*

3.7 Influence of Temperature of Pre–polymerized Catalyst Injection into Main Polymerization

The series of experiments were carried out in the 2–litre reactor focused on the evaluation of the influence of the injection temperature on the catalyst performance in main gas–phase polymerization and final polymer particle morphology. Within this study the not pre–polymerized and pre–polymerized catalysts were compared at injection temperatures selected from the range 40 to 70 °C. The pre–polymerization step was carried out under following conditions: TEA/Ti = 3.0 mol·mol^{-1}, DIBDMS/Ti = 0.15 mol·mol^{-1}, 1 min activation, DPP = 3.0 g_{pp}·g_{cat}^{-1} and 30 min of ageing. The main polymerizations were carried out according to **Table 2.3.1** only the temperature of catalyst injection was changed. The studied catalyst injection temperatures and final polymer powder properties are shown in **Table 3.7.1**.

Table 3.7.1: *Properties of final polymer powders produced in main polymerizations with pre–polymerized and not pre–polymerized catalysts. Evaluation of effect of different temperatures of catalyst injection. TEA/Ti = 3.0 mol·mol^{-1}, DIBDMS/Ti = 0.15 mol·mol^{-1}, DPP = 3.0 g_{PP}·g_{cat}^{-1}, 1 min activation, 30 min ageing, temperature of pre–polymerization 23 °C, pressure 1 bar*

	Injection Temp. [°C]	Activity [kg·g^{-1}·h^{-1}]	B.D. [kg·m^{-3}]	MFR (2.16 kgload) [g·(10 min)$^{-1}$]	X.S. [wt.%]	Porosity [g_{DOF}·(100g_{PP})$^{-1}$]
No ppol	70	23.3	333	9.7	2.32	4.91
	60	27.5	339	9.1	2.11	3.92
	50	31.5	384	8.1	1.76	3.14
	40	33.6	431	8.5	1.79	2.84
Ppol	70	27.5	374	8.0	1.92	3.26
	60	31.2	397	7.4	1.85	3.00
	50	31.0	410	7.4	1.64	2.51
	40	33.1	415	6.8	1.68	2.42

According to **Figure 3.7.1** the temperature of catalyst injection has evident effect on catalyst activity. Up to 50 °C the not pre–polymerized and pre–polymerized catalysts exhibits similar activities. Subsequently, at higher injection temperatures sharper decrease of catalyst activity of not pre–polymerized catalyst was observed. **Figure 3.7.2** and **Figure 3.7.3** shows the polymerization kinetics of both types of catalysts. In both cases higher temperature of catalyst injection led to lower initial polymerization rates. It seems that higher temperature accelerates catalyst deactivation due to overheating. In **Figure 3.7.4** is shown the comparison of polymerization kinetics of not pre–polymerized and pre–polymerized catalysts injected into main polymerization at 40 and 70 °C. Again it is obvious that the pre–polymerization step decrease the initial polymerization rate. Furthermore, it is also obvious that pre–polymerization stabilizes the catalyst, which is then more resistant against overheating and catalyst could better survive the injection into the reactor at higher temperature.

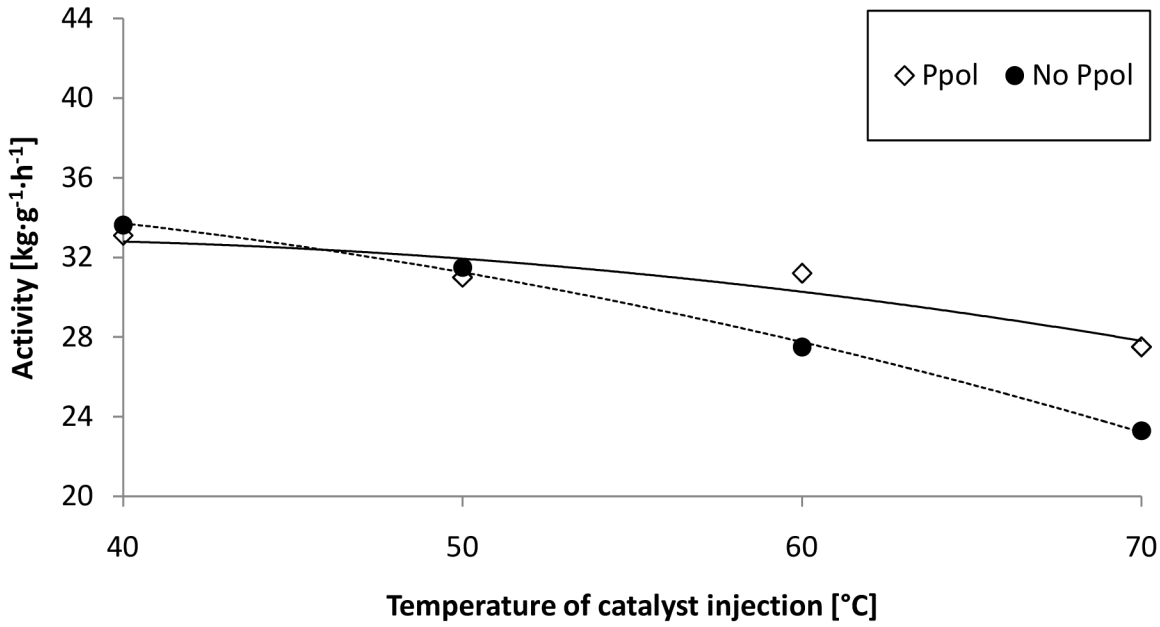

Figure 3.7.1: *Dependence of catalysts activity in main polymerization on temperature of catalyst injection into 2–litre reactor. Comparison of pre–polymerized and not pre–polymerized catalysts.*

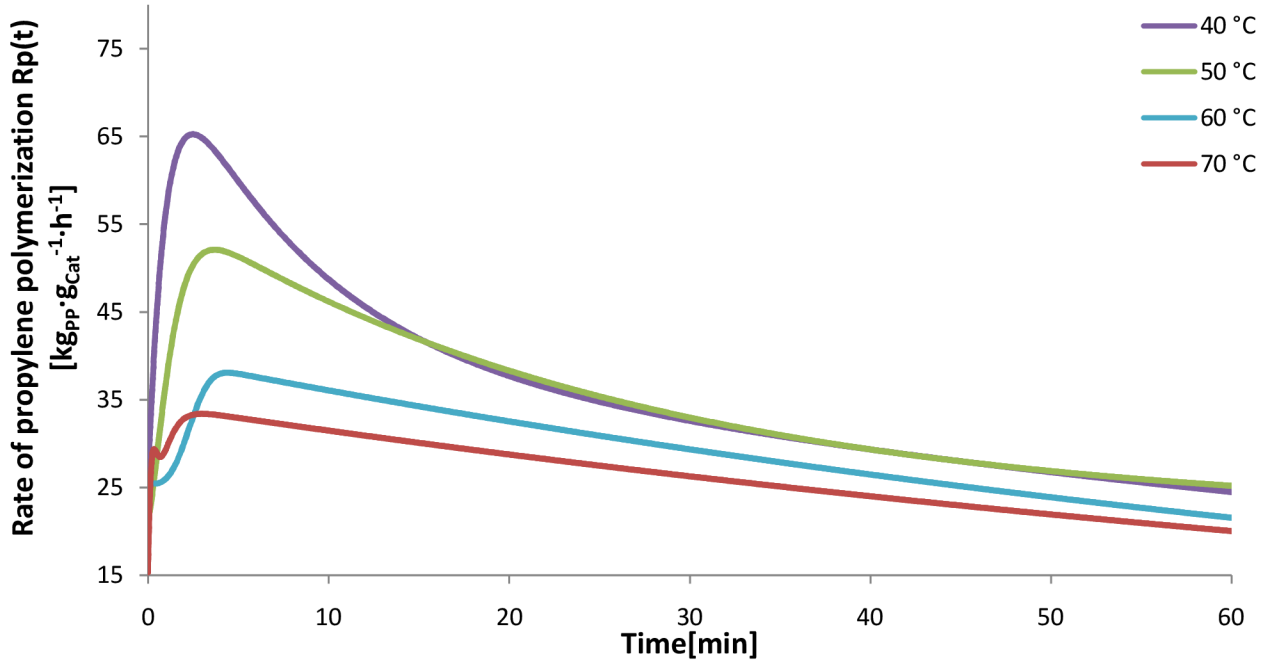

Figure 3.7.2: *Polymerization kinetics of not pre–polymerized catalyst. Effect of different temperatures of catalyst injection into main polymerization.*

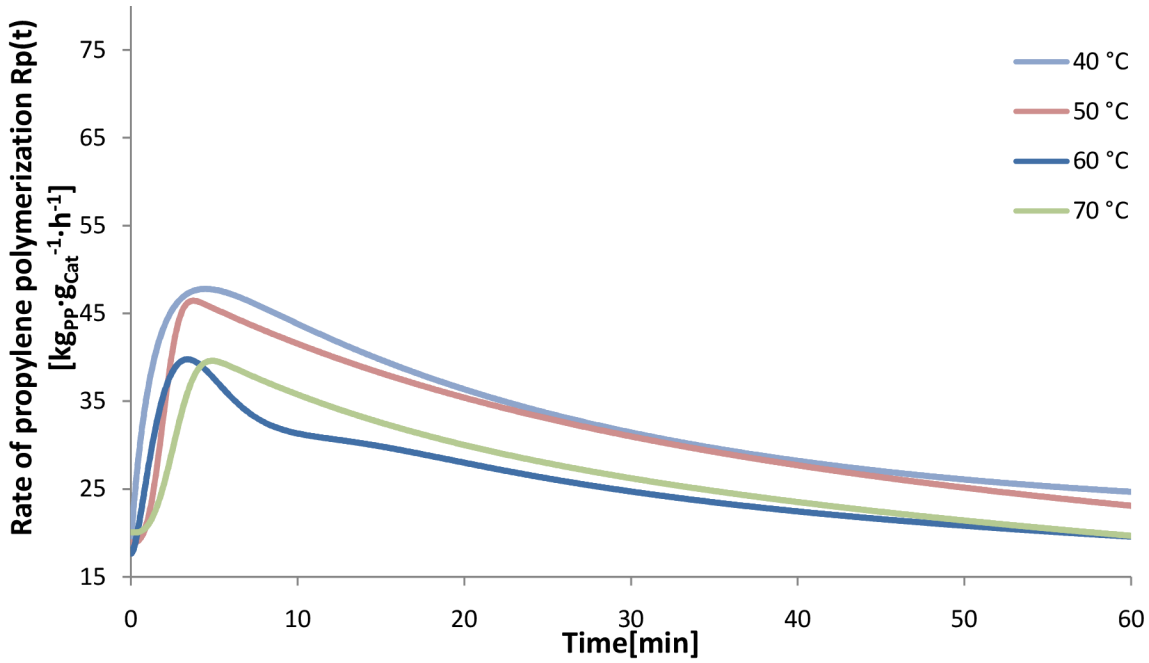

Figure 3.7.3: *Polymerization kinetics of pre–polymerized catalyst. Effect of different temperatures of catalyst injection into main polymerization.*

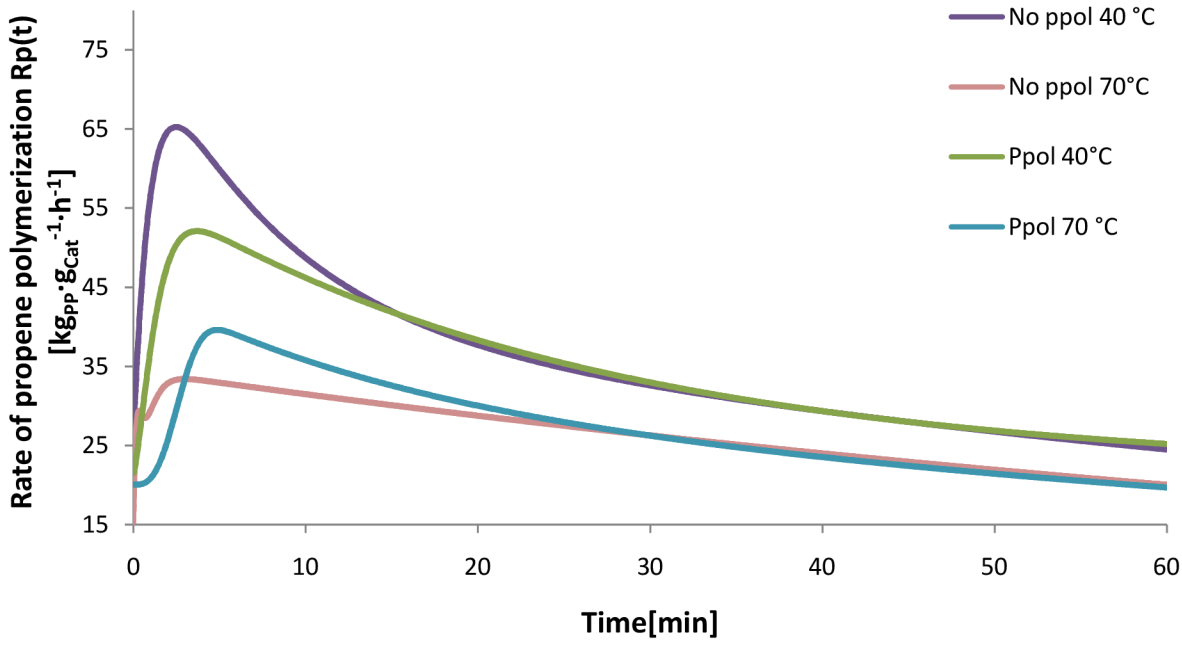

Figure 3.7.4: *Comparison of polymerization kinetics of pre–-polymerized and not pre–polymerized catalysts at 40 and 70 °C.*

It is clear that the morphology of the final polymer particles is strongly dependent on the temperature of catalyst injection. The higher injection temperature was applied, the lower polymer bulk density was obtained (**Figure 3.7.5**). At higher temperatures of catalyst injection the pre–polymerized catalyst produced polymer powder with noticeably higher bulk density in comparison with not pre–polymerized sample. **Figure 3.7.6** further show that the

final polymer particle morphology deteriorates more significantly in the case of not pre–polymerized catalyst. In these cases, we have to consider the fact that active centers on the catalyst surface begun polymerize immediately at higher temperatures, while active centers inside catalyst begun polymerize later due to complicated reaction with TEA and ED in presence of propene. As a result of this fact, catalyst is much more susceptible to fragmentation and higher porosity and poorer activities are obtained.

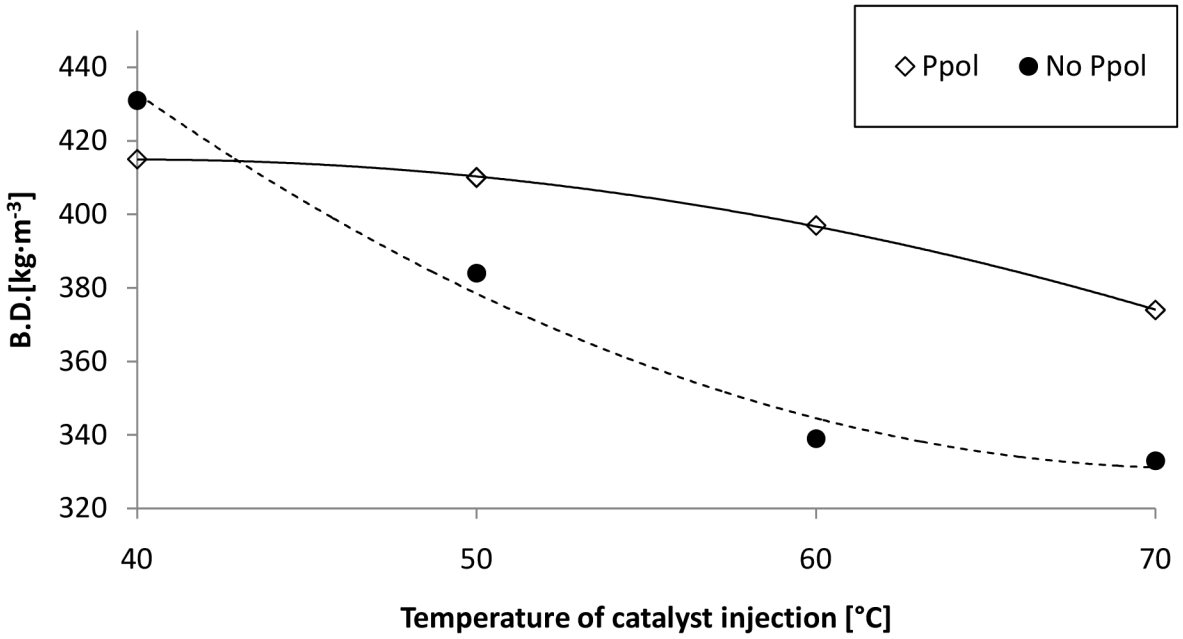

Figure 3.7.5: *Dependence of bulk density on temperature of catalyst injections for pre–polymerized and not pre–polymerized catalysts.*

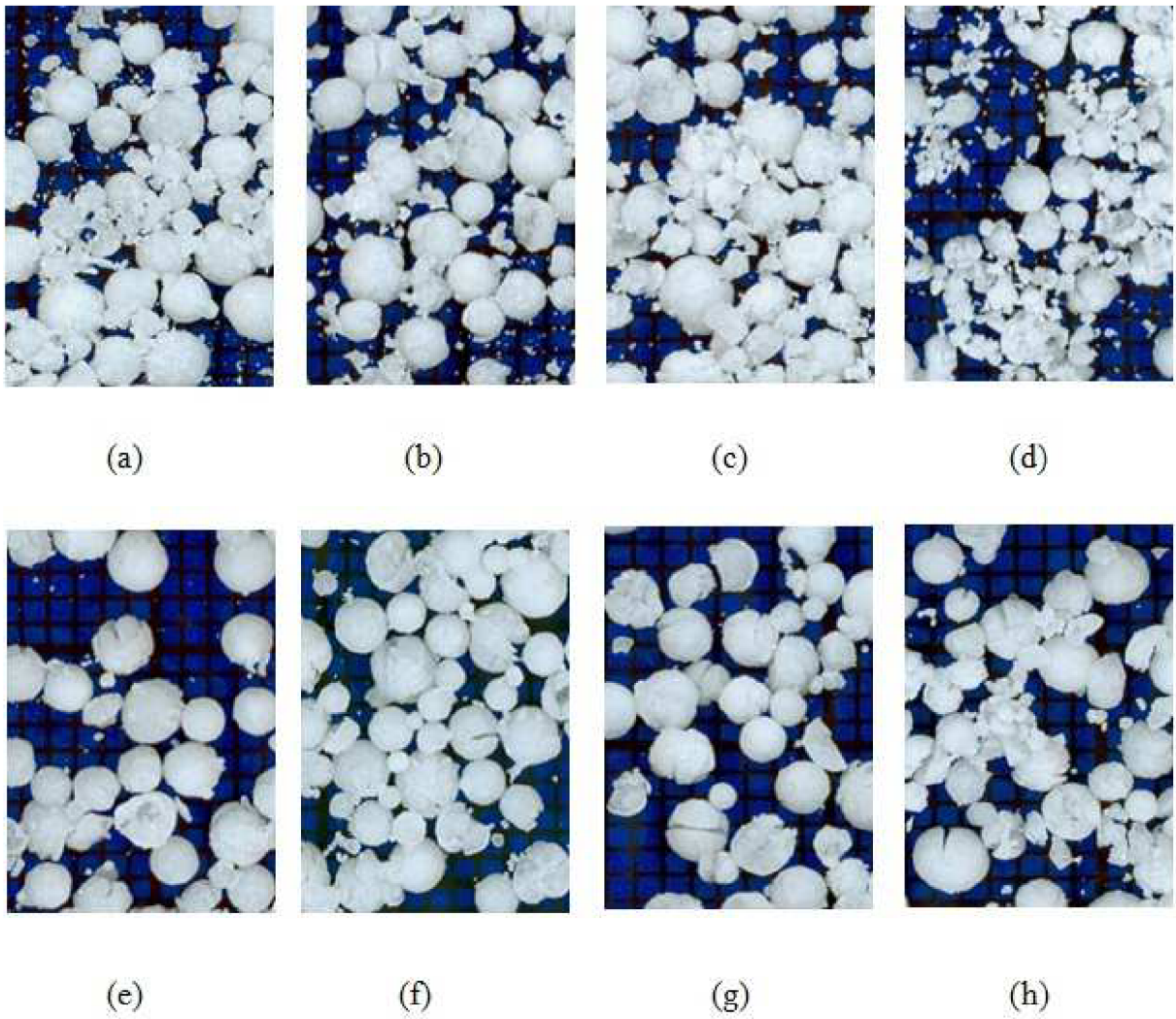

Figure 3.7.6: *Pictures of polymer powders prepared in main polymerization on catalyst, which was not pre-polymerized and injected into reactor at temperature a) 40 °C, b) 50 °C, c) 60 °C, d) 70 °C and compared with polymer powders produced with pre–polymerized catalysts, which were also injected into reactor at temperature e) 40 °C, f) 50 °C, g) 60 °C, h) 70 °C.*

Figure 3.7.7 shows sharp increase of final polymer particle porosity with increasing injection temperature. The most significant increase of porosity was observed with the not pre–polymerized catalyst. The results indicate that the increase of polymer particle porosity is related to the level of polymer particle fragmentation.

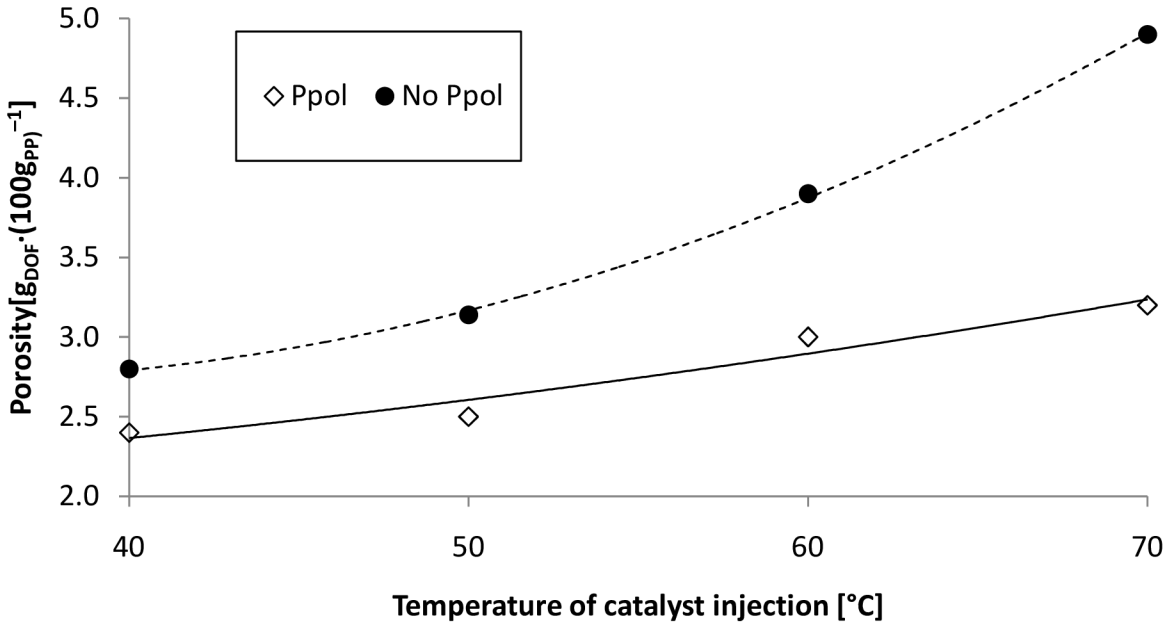

Figure 3.7.7: *Dependence of porosity on temperature of catalyst injections for pre–polymerized and not pre–polymerized catalysts.*

The observed change of polymer particle morphology with increasing temperature of catalyst injection is further supported by PSD analysis. In **Figure 3.7.8** and **Table 3.7.2** is shown the comparison of PSD profiles determined on polymer powders prepared with pre–polymerized and not pre–polymerized catalysts injected into the reactor at 40 and 70 °C.

The not pre–polymerized catalyst injected at 70 °C shows higher amount of polymer particle fragments with diameter lower than 0.5 mm. The comparison of final polymer particles of the catalysts injected at 40 °C shows that with the pre–polymerized catalyst significantly lower quantity of fragments with diameter lower than 0.5 mm was produced. On the other side, with the pre–polymerized catalyst injected at 40 °C the highest quantity of particles with diameter higher than 2.0 mm. i.e. well shaped polymer particles, was produced. The highest amount of polymer particles with diameter about 1.5 mm which were determined in the case of polymer powder prepared with pre–polymerized catalyst injected at 70 °C, indicates that the pre–polymerization step could prevent the fragmentation only partially (the biggest polymer particles still broke down to fragments despite the catalyst was pre–polymerized).

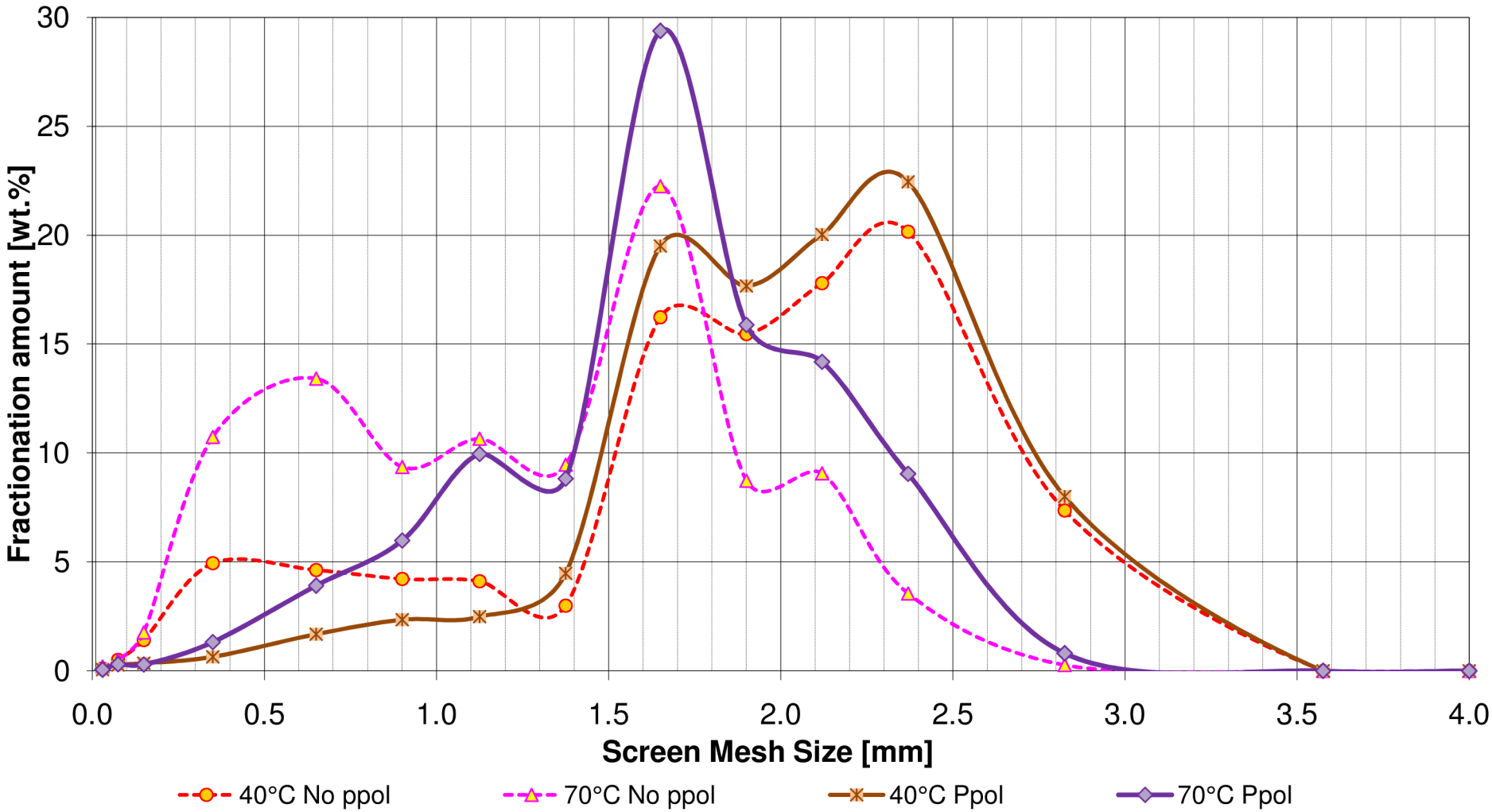

Figure 3.7.8: *Particle size distribution of polymer powders prepared with pre-–-polymerized and not pre–polymerized catalysts. Comparison at injection temperature 40 and 70 °C.*

Figure 3.7.9 expresses the dependence of MFR on temperature of catalyst injection. It is obvious that with increasing temperature of catalyst injection also slight increase of final polymer MFR was observed with not pre–polymerized and also pre–polymerized catalyst. In both cases, the increase of MFR was related to polymer particle fragmentation. The explanation of this phenomenon was already mentioned in Chapter 3.2.

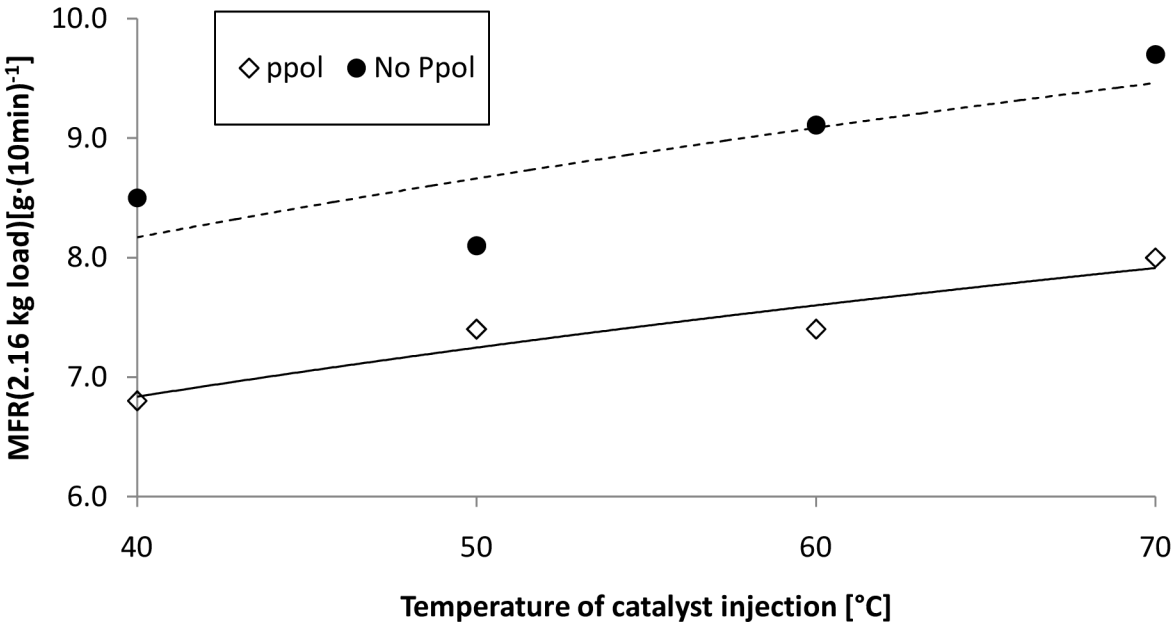

Figure 3.7.9: *Dependence of MFR on temperature of catalyst injections for pre–polymerized and not pre–polymerized catalysts.*

Figure 3.7.10 shows the dependence of X.S. on temperature of catalyst injection. Also, in this case the noticeable influence of catalyst injection temperature was observed. The increase of X.S. values was more significant with the not pre–polymerized catalyst. It is evident that the pre–polymerized catalyst produced PP with lower amount of atactic PP. The results again verified positive effect of pre–polymerization on catalyst performance in gas–phase polymerization. It is obvious that the catalyst activated and pre–polymerized under the mild conditions has the active centers more stereospecific.

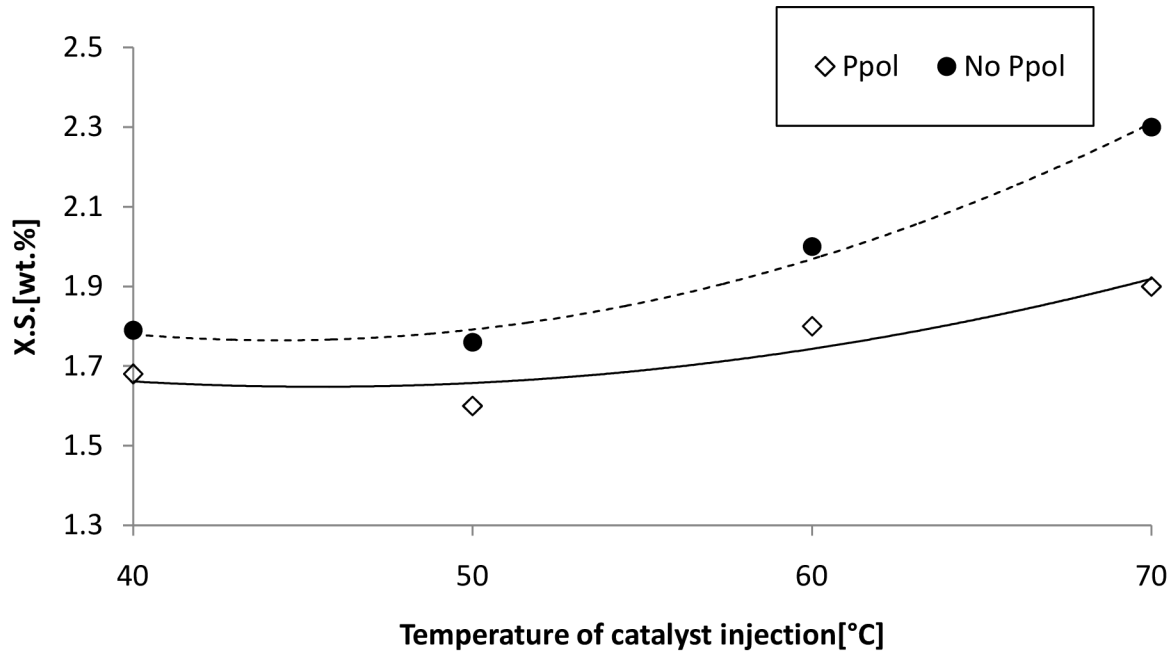

Figure 3.7.10: *Dependence of X.S. on temperature of catalyst injections for pre–polymerized and not pre–polymerized catalysts.*

3.8 Effect of 2nd Catalyst Injection

The method based on the injection of 2nd dose of catalyst into the reactor, where already polymerizing bed of polymer powder is present, was utilized for the simulation of industrial conditions of gas–phase polymerization process. The description of this method is mentioned in **Chapter 2.3.3**. The main focus of this study was to evaluate the effect of the pre–polymerization step on the catalyst performance and polymer particle morphology under the conditions close to industrial gas–phase conditions. All the experiments performed within this study and final polymer powder properties are shown in **Table 3.8.1**.

Table 3.8.1: *Effect of 2nd injection of pre–polymerized catalyst on final polymer powder properties. Pre–polymerization conditions: TEA/Ti = 3.0 mol·mol^{-1}, DIBDMS/Ti = 0.15 mol·mol^{-1}, DPP = 3.0 g_{PP}·g_{cat}^{-1}, 1 min activation, 30 min ageing, temperature of pre–polymerization 23 °C, pressure 1 bar*

No	1nd dose catalyst	2nd dose catalyst	Activity 1st dose 100 min [kg·g^{-1}·h^{-1}]	Activity 2nd dose 60 min [kg·g^{-1}·h^{-1}]	B.D [kg·m^{-3}]	MFR (2.16 kg load) [g·(10 min)$^{-1}$]	X.S [wt.%]
1	No ppol	–	33.7	–	410	8.3	1.73
2	No ppol	No ppol	33.6	19.1	435	8.1	1.81
3	Ppol	–	31.1	–	420	7.7	1.77
4	Ppol	Ppol	31.1	11.6	422	8.7	1.88

The comparison of experiments, where only not pre–polymerized catalyst was used (i.e. No. 1 and No. 2), shows noticeable increase of B.D. in the case of experiment No.2. According to **Figure 3.8.1**, where the pictures of polymer particles are shown, we can say that

the catalyst injected into the reactor as 2nd dose underwent significant fragmentation during polymerization. In the case of experiments No. 3 and No. 4, where only pre–polymerized catalysts were used, no differences in B.D. as well as in polymer morphology were observed. It is interesting that pre–polymerized catalyst shows lower activity in 2nd injection in comparison with the not pre–polymerized one. The possible explanation could be related to the heat transfer. The not pre–polymerized catalyst underwent early fragmentation, which increased total polymer particles surface. Due to the higher particle surface the heat removal was more efficient and the deactivation of active centers by overheating was lower. On contrary, in the case of pre–polymerized catalyst the fragmentation did not occurred, so the heat transfer was not sufficient and catalyst particles were overheated and active centers deactivated. However, it is obvious that the pre–polymerized catalyst system is more resistant against fragmentation, thus it is more suitable for industrial gas–phase processes.

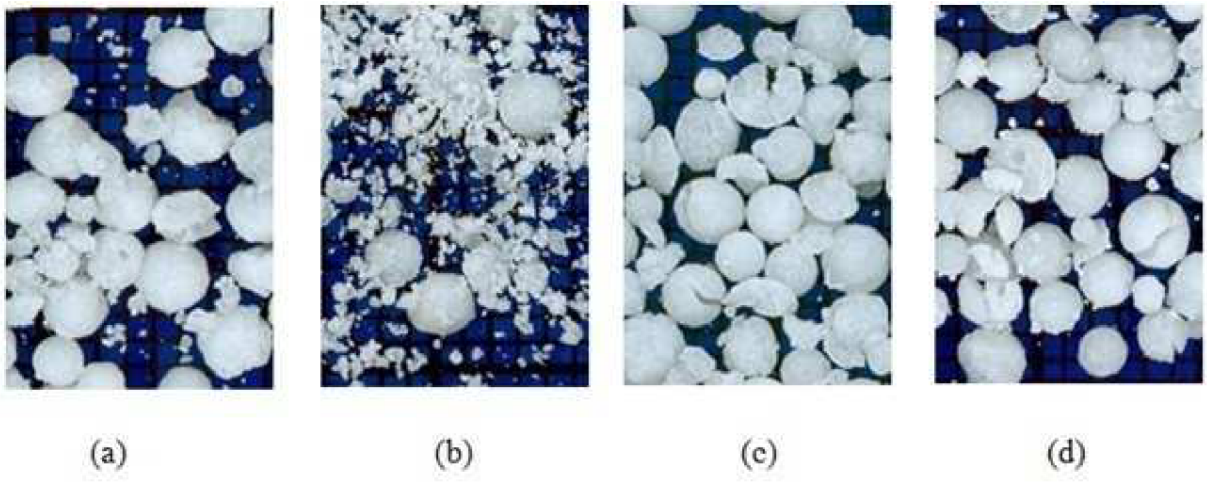

Figure 3.8.1: *Pictures of polymer powders: a) No.1: no ppol, b) No.2: no ppol–no ppol, c)No.3: ppol and d)No.4: ppol–ppol.*

4. Conclusions

The effect of the pre–polymerization step on the catalyst performance in the main gas–phase polymerization and final polymer powder properties was studied. For the better understanding of this step, the selected Ziegler–Natta catalyst was pre–polymerized and subsequently injected into the 2–litre stainless steel laboratory reactor. The main interest was focused on the effect of following variables: pre–polymerization degree, time of catalyst activation, pre–polymerized catalyst ageing, TEA/Ti and DIBDMS/Ti molar ratio applied in pre–polymerization and temperature of pre–polymerized catalyst injection into main polymerization reactor. The main conclusions resulting from this study could be summarized in the following points:

- The stirring bars are not suitable for the mixing of the catalyst with TEA and DIBDMS and subsequent pre–polymerization, because significant fragmentation of the catalyst particles was observed. It was found out that the stirring by the shaker without stirring bar is the most efficient procedure for the simulation of the pre–polymerization step.
- The catalyst activation longer than 5 min led to the adverse reaction of the catalyst active centers with TEA, which resulted in lower polymerization activity and poorer isotacticity of produced PP.
- The pre–polymerization as well as the activation led to the production of the polymer particles with evidently better morphology in comparison with not activated and pre–polymerized catalyst system.
- The degree of pre–polymerization has noticeable influence on the catalyst activity and initial polymerization rate. No significant effect of the pre–polymerization degree on the final polymer powder properties was observed.
- The pre–polymerized catalyst should be injected into the main reactor as soon as possible due to adverse reaction causing active centers deactivation, i.e. the ageing of the pre–polymerized catalyst should be minimized.
- It was found out that the most suitable TEA/Ti molar ratio is 1.0. Higher molar ratios led to adverse reactions, which deactivated the active centers and caused decrease of catalyst activity and PP isotacticity. The polymer particle morphology and powder bulk density was not affected.
- Within the studied range the external donor DIBDMS/Ti molar ratio did not have significant influence on catalyst activity as well as on polymerization kinetics. The noticeable influence of DIBDMS/Ti molar ratio applied in the pre–polymerization step was observed in the case of polymer particle porosity.
- It was observed that the pre–polymerized catalyst is more resistant against overheating, thus it was possible to apply it into the reactor at higher temperatures without significant change in activity and polymer particles morphology.

5. References

[1]. SEYMOUR, R. B.: *History of polyolefins: the world's most widely used polymers* [online]. Hingham, MA, U.S.A.: Sold and distributed in the U.S.A. and Canada by Kluwer Academic Publishers, c1986 [ref. 2017-09-13]. ISBN 90-277-2128-9.

[2]. KISSIN, Y. V.: *Polyethylene: end-use properties and their physical meaning*. Cincinnati: Hanser Publishers, 2013. ISBN 978-1-56990-520-3.PASQUINI, N. and ADDEO A. *Polypropylene handbook: the world's most widely used polymers* [online]. 2nd ed. /. Cincinnati: Hanser, c2005 [ref. 2017-09-13]. ISBN 34-462-2978-7.

[3]. PASQUINI, N.. and A. ADDEO. *Polypropylene handbook: the world's most widely used polymers* [online]. 2nd ed. /. Cincinnati: Hanser, c2005 [ref. 2017-09-13]. ISBN 34-462-2978-7.

[4]. KAMINSKY W. and H. SINN: *Transition Metals and Organometallics as Catalysts for Olefin Polymerization*. Berlin, Heidelberg: Springer Berlin Heidelberg, 1988. ISBN 978-364-2832-765.

[5]. COSSEE, P.: Ziegler-Natta catalysis I. Mechanism of polymerization of α-olefins with Ziegler-Natta catalysts. *Journal of Catalysis* [online]. 1964, **3**(1), 80-88 [ref. 2017-10-31]. DOI: 10.1016/0021-9517(64)90095-8. ISSN 00219517. Available: http://linkinghub.elsevier.com/retrieve/pii/0021951764900958

[6]. FINK G., R. MÜLHAUPT and H. H. BRINTZINGER: *Ziegler Catalysts Recent Scientific Innovations and Technological Improvements*. Berlin, Heidelberg: Springer Berlin Heidelberg, 1995. ISBN 978-364-2791-369.

[7]. RODRIGUEZ, L. A. M. and H. M. VAN LOOY: Studies on Ziegler-Natta catalysts. Part V. Stereospecificity of the active center. *Journal of Polymer Science Part A-1: Polymer Chemistry* [online]. **4**(8), 1971-1992 [ref. 2018-01-05]. DOI: 10.1002/pol.1966.150040805. ISSN 0449296x. Available: http://doi.wiley.com/10.1002/pol.1966.150040805

[8]. FERREIRA, M. L., D. E. DAMIANI and Y. DOI: Effect of different donors on kinetics of Zn catalysts and molecular weight of the obtained polypropylene. *Journal of Molecular Catalysis A: Chemical* [online]. 1999, **150**(1-2), 53-69 [ref. 2017-09-20]. DOI: 10.1016/S1381-1169(99)00208-3. ISSN 13811169. Available: http://linkinghub.elsevier.com/retrieve/pii/S1381116999002083

[9]. NATTA, G., P. PINO, G. MAZZANTI, U. GIANNINI, E. MANTICA and M. PERALDO.: The nature of some soluble catalysts for low pressure ethylene polymerization. *Journal of Polymer Science* [online]. **26**(112), 120-123 [ref. 2017-09-24]. DOI: 10.1002/pol.1957.1202611216. ISSN 00223832. Available: http://doi.wiley.com/10.1002/pol.1957.1202611216

[10]. BRESLOW, D. S. and N. R. NEWBURG: *Bis-(cyclopentadienyl)-titatium dichloride —alkylaluminum complexe as catalysts for the polymeriaztion of ethylene* [online]. [ref. 2017-09-24]. DOI: 10.1021/ja01575a066. ISBN 10.1021/ja01575a066. Available: http://pubs.acs.org/doi/abs/10.1021/ja01575a066

[11]. KAMINSKY, W. and N.R. NEWBURG: The discovery of metallocene catalysts and their present state of the art. *Journal of Polymer Science Part A: Polymer Chemistry* [online]. 2004, **42**(16), 3911-3921 [ref. 2017-09-24]. DOI: 10.1002/pola.20292. ISBN 10.1021/ja01575a066. ISSN 0887-624x. Available: http://doi.wiley.com/10.1002/pola.20292

[12]. ZIJLSTRA, H. S. and S. HARDER.: Methylalumoxane - History, Production, Properties, and Applications. *European Journal of Inorganic Chemistry* [online]. 2015, **2015**(1), 19-43 [ref. 2017-09-26]. DOI: 10.1002/ejic.201402978. ISSN 14341948. Available: http://doi.wiley.com/10.1002/ejic.201402978

[13]. BRINTZINGER, H. H. and H. FISCHER: Development of ansa-Metallocene Catalysts for Isotactic Olefin Polymerization: Mechanistic insights from metallocenesystems. *Progress in Polymer Science* [online]. 1995, **20**(3), 459-526 [ref. 2017-09-26]. DOI: 10.1007/12_2013_215. ISBN 10.1007/12_2013_215. ISSN 00796700. Available: http://link.springer.com/10.1007/12_2013_215

[14]. HUANG, J.: Ziegler-Natta catalysts for olefin polymerization: Mechanistic insights from metallocene systems. *Progress in Polymer Science* [online]. 1995, **20**(3), 459-526 [ref. 2017-09-26]. DOI: 10.1016/0079-6700(94)00039-5. ISSN 00796700. Available: http://linkinghub.elsevier.com/retrieve/pii/0079670094000395

[15]. NATTA, G., P. CORRADINI, G. ALLEGRA, G. HUSSAIN, W. KAMINSKY, P. ARAVIND and W. YEHYE: The different crystalline modifications of $TiCl_3$, a catalyst component for the polymerization of α-olefins. I: α-, β-, γ-$TiCl_3$. II. *Journal of Polymer Science* [online]. Weinheim, Germany: Wiley-VCH Verlag, 2000, **51**(156), 399-410 [ref. 2017-10-01]. DOI: 10.1002/pol.1961.1205115602. ISBN 9783527306732. ISSN 00223832. Available: http://doi.wiley.com/10.1002/pol.1961.1205115602

[16]. GAHLEITNER, M., Ch. PAULIK, S. JAHAN, M. HUSSAIN, W. KAMINSKY, P. ARAVIND and W. YEHYE: Polypropylene. *Ullmann'sEncyclopedia of Industrial Chemistry* [online]. Weinheim, Germany: Wiley-VCH Verlag, 2000, **7**(7), 1 [ref. 2017-10-01]. DOI: 10.1002/14356007.o21_o04.pub2. ISBN 9783527306732. ISSN 1996-1944. Available: http://doi.wiley.com/10.1002/14356007.o21_o04.pub2

[17]. NATTA, G., I. PASQUON, A. ZAMBELLI, G. GATTI, W. KAMINSKY, P.ARAVIND and W. YEHYE: Highly stereospecific catalytic systems for the polymerization of α-olefins to isotactic polymers: α-, β-, γ-$TiCl_3$. II. *Journal of Polymer Science* [online]. Weinheim, Germany: Wiley-VCH Verlag, 2000, **51**(156), 387-398 [ref. 2017-10-01]. DOI: 10.1002/pol.1961.1205115601. ISBN 9783527306732. ISSN 00223832. Available: http://doi.wiley.com/10.1002/pol.1961.1205115601

[18]. HERMANS, J and P. HENRIOULLE: *Process for the preparation of a Ziegler-Natta type catalyst*. 1973. USA patent US3769233DA. Granted on 24thMarch 1971. Submitted on 30th October 1973

[19]. KASHIWA, N.: The discovery and progress of $MgCl_2$-supported $TiCl_4$ catalysts. *Journal of Polymer Science Part A: Polymer Chemistry* [online].

2004, **42**(1), 1-8 [ref. 2017-10-03]. DOI: 10.1002/pola.10962. ISSN 0887-624x. Available: http://doi.wiley.com/10.1002/pola.10962

[20]. PIRINEN, S., K. JAYARATNE, P. DENIFL and T. T. PAKKANEN: Ziegler–Natta catalysts supported on crystalline and amorphous $MgCl_2$/THF complexes. *Journal of Molecular Catalysis A: Chemical* [online]. 2014, **395**, 434-439 [ref. 2017-10-03]. DOI: 10.1016/j.molcata.2014.09.013. ISSN 13811169. Available: http://linkinghub.elsevier.com/retrieve/pii/S1381116914004166

[21]. KIM, S. H., C. R. TEWELL and G. A. SOMORJAI: Surface Characterization of the $TiCl_x$ /$MgCl_2$ Model Ziegler−Natta Polymerization Catalysts: Adsorption Site Studies Using Mesitylene Thermal Desorption. *Langmuir* [online]. 2000, **16**(24), 9414-9420 [ref. 2018-01-11]. DOI: 10.1021/la000194w. ISSN 0743-7463. Available: http://pubs.acs.org/doi/abs/10.1021/la000194w

[22]. UTKO, J.,P. SOBOTA, T. LIS and K. MAJEWSKA: Reaction of $MgCl_2$ with $AlCl_3$ in ethyl acetate. The crystal structure of $[Mg(CH_3OCOC_2H_5)_6][AlCl_4]_2$. *Journal of Organometallic Chemistry* [online]. 1989, **359**(3), 295-300 [ref. 2017-10-03]. DOI: 10.1016/0022-328X(89)88093-3. ISSN 0022328x. Available: http://linkinghub.elsevier.com/retrieve/pii/0022328X89880933

[23]. MA, Z., L. WANG, W. WANG, L. FENG and X. GU: Study of propylene polymerization catalyzed by a spherical $MgCl_2$-supported Ziegler-Natta catalyst system: The effects of external donors. *Journal of Applied Polymer Science* [online]. 2005, **95**(3), 738-742 [ref. 2017-10-04]. DOI: 10.1002/app.21247. ISSN 0021-8995. Available: http://doi.wiley.com/10.1002/app.21247

[24]. ALBIZZATI, E., E GIANNETTI and U. GIANNINI: *Die Makromolekulare Chemie, Rapid Communications* [online]. **5**(10), 673-677 [ref. 2017-10-16]. DOI:10.1002/marc.1984.030051013. ISSN 01732803. Available: http://doi.wiley.com/10.1002/marc.1984.030051013REDZIC

[25]. GAROFF E.T., C. C. MARDARE, M. LIST, G. HESSER, L. MAYRHOFER, A. W. HASSEL and C. PAULIK: Heterogeneous Ziegler–Natta catalysts with various sizes of $MgCl_2$ crystallites: synthesis and characterization. *Iranian Polymer Journal* [online]. 2016, **25**(4), 321-337 [ref. 2017-10-11]. DOI: 10.1007/s13726-016-0424-x. ISSN 1026-1265. Available: http://link.springer.com/10.1007/s13726-016-0424-x

[26]. TRISCHLER, H., T. HÖCHFURTNER, M. RUFF and C. PAULIK: Influence of the aluminum alkyl co-catalyst type in Ziegler-Natta ethene polymerization on the formation of active sites, polymerization rate, and molecular weight. *Kinetics and Catalysis* [online]. 2013, **54**(5), 559-565 [ref. 2017-10-17]. DOI: 10.1134/S0023158413050170. ISSN 0023-1584. Available: http://link.springer.com/10.1134/S0023158413050170

[27]. CHADWICK, J., G. MORINI, G. BALBONTIN, I. CAMURATI, J. R. HEERE, I. MINGOZZI, F. TESTONI: Effects of Internal and External Donors on the Regio- and Stereoselectivity of Active Species in $MgCl_2$-Supported Catalysts for Propene Polymerization. Macromolecular Chemistry and Physics. 202. 1995 - 2002.

[28]. BOERO, M., PARRINELLO, S. HÜFFER and H. WEISS: First Principles Study of Propene Polymerization in Ziegler−Natta Heterogeneous Catalysis. *Journal of the American Chemical Society* [online]. 2000, **122**(3), 501-509 [ref. 2017-10-17]. DOI: 10.1021/ja990913x. ISSN 0002-7863. Available: http://pubs.acs.org/doi/abs/10.1021/ja990913x

[29]. P. C. BARBÉ, G. CECCHIN and L. NORISTI: *The catalytic system Ti-complex/$MgCl_2$* [online]. [ref. 2017-10-23]. DOI: 10.1007/BFb0037612. ISBN 10.1007/BFb0037612. Available: http://www.springerlink.com/index/10.1007/BFb0037612

[30]. FORTE, M., F. M. D. COUTINHO and L. NORISTI: *Highly active magnesium chloride supported Ziegler-Natta catalysts with controlled morphology* [online]. [ref. 2017-10-23]. DOI: 10.1016/0014-3057(95)00124-7. ISBN 10.1016/0014-3057(95)00124-7. Available: http://linkinghub.elsevier.com/retrieve/pii/0014305795001247

[31]. SACCHI, M. C., F. FORLINI, I. TRITTO, R. MENDICHI, G. ZANNONI and L. NORISTI: *Activation effect of alkoxysilanes as external donors in magnesium chloride-supported Ziegler-Natta catalysts* [online]. [ref. 2017-10-23]. DOI: 10.1021/ma00048a009. ISBN 10.1021/ma00048a009. Available: http://pubs.acs.org/doi/abs/10.1021/ma00048a009

[32]. TOTO, M., G. MORINI, G. GUERRA, P. CORRADINI and L. CAVALLO: Influence of 1,3-Diethers on the Stereospecificity of Propene Polymerization by Supported Ziegler−Natta Catalysts. A Theoretical Investigation on Their Adsorption on (110) and (100) Lateral Cuts of $MgCl_2$ Platelets. *Macromolecules* [online]. 2000, **33**(4), 1134-1140 [ref. 2017-10-24]. DOI: 10.1021/ma990959a. ISSN 0024-9297. Available: http://pubs.acs.org/doi/abs/10.1021/ma990959a

[33]. BARINO, L., R. SCORDAMAGLIA, G. GUERRA, P. CORRADINI and L. CAVALLO: Conformational aspects of physical phenomena in polymeric materials. *Analytica Chimica Acta* [online]. 1990, **235**(4), 229-237 [ref. 2017-10-24]. DOI: 10.1016/S0003-2670(00)82079-6. ISSN 00032670. Available: http://linkinghub.elsevier.com/retrieve/pii/S0003267000820796

[34]. KAKKONEN, H. J., J. PURSIAINEN, A. T. PAKKANEN, M. AHLGRÉN and E. IISKOLA: $TiCl_4$ diester complexes: Relationships between the crystal structures and properties of Ziegler-Natta catalysts. *Journal of Organometallic Chemistry* [online]. 1993, **453**(2), 175-184 [ref. 2017-10-24]. DOI: 10.1016/0022-328X(93)83108-8. ISSN 0022328x. Available: http://linkinghub.elsevier.com/retrieve/pii/0022328X93831088

[35]. WEN, X., M. JI, Q. YI, H. NIU and J.Y. DONG: Magnesium chloride supported Ziegler-Natta catalysts containing succinate internal electron donors for the polymerization of propylene: Relationships between the crystal structures and properties of Ziegler-Natta catalysts. *Journal of Organometallic Chemistry* [online]. 1993, **453**(2), 175-184 [ref. 2017-10-24]. DOI: 10.1002/app.32558. ISBN 10.1002/app.32558. ISSN 0022328x. Available: http://doi.wiley.com/10.1002/app.32558

[36]. MORI, H., H. IGUCHI, K. HASEBE and M. TERANO: Kinetic study of isospecific active sites formed by various alkylaluminiums on $MgCl_2$-supported Ziegler catalyst at the initial stage of propene polymerization. *Macromolecular Chemistry and Physics* [online]. **198**(4), 1249-1255 [ref. 2018-01-04]. DOI: 10.1002/macp.1997.021980426. ISSN 10221352. Available: http://doi.wiley.com/10.1002/macp.1997.021980426

[37]. MCKENZIE, I. D., P. J. T. TAIT and D. R. BURFIELD: Ziegler-Natta catalysis: 2. A kinetic investigation. *Polymer* [online]. Berlin, Heidelberg: Springer Berlin Heidelberg, 1972, **13**(7), 97-103 [ref. 2018-01-05]. DOI: 10.1016/0032-3861(72)90096-1. ISBN 978-3-642-64292-0. ISSN 00323861. Available: http://linkinghub.elsevier.com/retrieve/pii/0032386172900961

[38]. MORI, H., H. IGUCHI, K. HASEBE and M. TERANO: Kinetic study of isospecific active sites formed by various alkylaluminiums on $MgCl_2$-supported Ziegler catalyst at the initial stage of propene polymerization. *Macromolecular Chemistry and Physics* [online]. **198**(4), - [ref. 2018-01-04]. DOI: 10.1002/(SICI)1521-3935(20000201)201:3<289::AID-MACP289>3.0.CO;2-M. ISSN 10221352. Available: http://doi.wiley.com/10.1002/macp.1997.021980426

[39]. MOORE, E. P.: *Polypropylene handbook: polymerization, characterization, properties, processing, applications*. Cincinnati: Hanser/Gardner Publications, c1996. ISBN 978-156-9902-080.

[40]. SEPPÄLÄ, J. V. and M. AUER: Factors affecting kinetics in slurry type coordination polymerization. *Progress in Polymer Science* [online]. 1990, **15**(1), 147-176 [ref. 2018-01-04]. DOI: 10.1016/0079-6700(90)90018-V. ISSN 00796700. Available: http://linkinghub.elsevier.com/retrieve/pii/007967009090018V

[41]. CHIEN, J. C. W., S. WEBER and Y. HU. Magnesium chloride supported catalysts for olefin polymerization. XIX. Titanium oxidation states, catalyst deactivation, and active site structure. *Journal of Polymer Science Part A: Polymer Chemistry* [online]. **27**(5), 1499-1514 [ref. 2018-05-01]. DOI: 10.1002/pola.1989.080270504. ISSN 0887624X. Dostupné z: http://doi.wiley.com/10.1002/pola.1989.080270504

[42]. KEII, T., E. SUZUKI, M. TAMURA, M. MURATA and Y. DOI: Propene polymerization with a magnesium chloride-supported ziegler catalyst, 1. Principal kinetics. *Die MakromolekulareChemie* [online]. 1990, **183**(10), 2285-2304 [ref. 2018-01-04]. DOI: 10.1002/macp.1982.021831001. ISSN 0025116x. Available: http://doi.wiley.com/10.1002/macp.1982.021831001

[43]. BUSICO, V., P. CORRADINI, A. FERRARO, A. PROTO and Y. DOI: Polymerization of propene in the presence of $MgCl_2$-supported Ziegler-Natta catalysts, III. Catalyst deactivation. *Die Makromolekulare Chemie* [online]. 1990, **187**(5), 1125-1130 [ref. 2018-01-04]. DOI: 10.1002/macp.1986.021870509. ISSN 0025116x. Available: http://doi.wiley.com/10.1002/macp.1986.021870509

[44]. OSTROVSKII, N. M. and D. STOILJKOVIĆ: Evaluation of the effect of reaction and mass transfer on the growth of polymer particles in olefin polymerization. *Theoretical Foundations of Chemical Engineering* [online].

2011, **45**(1), 40-52 [ref. 2018-01-05]. DOI: 10.1134/S0040579511010076. ISSN 0040-5795. Available: http://link.springer.com/10.1134/S0040579511010076

[45]. BUSICO, V., V. CIPULLO and P. CORRADINI: Ziegler-Natta oligomerization of 1-alkenes: A catalyst's "fingerprint", II. Preliminary results of propene hydrooligomerization in the presence of the homogeneous isospecific catalyst system rac-(EBI)ZrC_{l2}/MAO. *Die MakromolekulareChemie, Rapid Communications* [online] . **14**(2), 97-103 [ref. 2018-01-05]. DOI: 10.1002/marc.1993.030140207. ISSN 01732803. Available: http://doi.wiley.com/10.1002/marc.1993.030140207

[46]. TAN, N., L. YU, Z. TAN and B. MAO: Kinetics of the propylene polymerization with prepolymerization at high temperature using Ziegler-Natta catalyst. *Journal of Applied Polymer Science* [online]. 2015, **132**(15), [ref. 2017-11-10]. DOI: 10.1002/app.41816. ISSN 00218995. Available: http://doi.wiley.com/10.1002/app.41816

[47]. PATER, J. T. M, G. WEICKERT, J. LOOS and W. P. J. VAN SWAAIJ: *High precision prepolymerization of propylene at extremely low reaction rates—kinetics and morphology* [online]. [ref. 2017-11-14]. DOI: 10.1016/S0009-2509(01)00081-1. ISBN 10.1016/S0009-2509(01)00081-1. Available: http://linkinghub.elsevier.com/retrieve/pii/S0009250901000811

[48]. Pater, J. T. M.: *Prepolymerization and morphology. Study on the factors determining powder morphology in propylene polymerization.* Enschede: J.T.M. Pater

[49]. BUSICO, V., R. CIPULLO, J. LOOS and W. P. M. VAN SWAAIJ: Microstructure of polypropylene. *Progress in Polymer Science* [online]. 2001, **26**(3), 443-533 [ref. 2017-11-14]. DOI: 10.1016/S0079-6700(00)00046-0. ISBN 10.1016/S0009-2509(01)00081-1. ISSN 00796700. Available: http://linkinghub.elsevier.com/retrieve/pii/S0079670000000460

[50]. KAKUGO, M., H. SADATOSHI, J. SAKAI, and M. YOKOYAMA: Growth of polypropylene particles in heterogeneous Ziegler-Natta polymerization. *Macromolecules* [online]. 1989, **22**(7), 3172-3177 [ref. 2017-11-14]. DOI: 10.1021/ma00197a046. ISBN 10.1016/S0009-2509(01)00081-1. ISSN 0024-9297. Available: http://pubs.acs.org/doi/abs/10.1021/ma00197a046

[51]. FERRERO, M. A. and M. G. CHIOVETTA: Catalyst fragmentation during propylene polymerization. III: Bulk polymerization process simulation. *Polymer Engineering and Science* [online]. 1991, **31**(12), 886-903 [ref. 2017-11-15]. DOI: 10.1002/pen.760311208. ISSN 0032-3888. Available: http://doi.wiley.com/10.1002/pen.760311208

[52]. MONJI, M., S. ABEDI, S. POURMAHDIAN and F. A. TAROMI: Effect of pre–polymerization on propylene polymerization. *Journal of Applied Polymer Science* [online]. 2009, **112**(4), 1863-1867 [ref. 2017-11-22]. DOI: 10.1002/app.29692. ISSN 00218995. Available: http://doi.wiley.com/10.1002/app.29692

[53]. KISSIN, Y. V., X. LIU, D. J. POLLICK, N. L. BRUNGARD and M. CHANG: *Ziegler-Natta catalysts for propylene polymerization: Chemistry of reactions leading to the formation of active centers* [online]. [ref. 2017-11-21]. DOI:

10.1016/j.molcata.2008.02.026. ISBN 10.1016/j.molcata.2008.02.026. Available: http://linkinghub.elsevier.com/retrieve/pii/S1381116908001313

[54]. PATER, J. T. M., G. WEICKERT, W. P. M. Van SWAAIJ, and F. A. TAROMI: Polymerization of liquid propylene with a fourth-generation Ziegler-Natta catalyst: Influence of temperature, hydrogen, monomer concentration, and pre–polymerization method on powder morphology. *Journal of Applied Polymer Science* [online]. 2003, **87**(9), 1421-1435 [ref. 2017-11-22]. DOI: 10.1002/app.11570. ISSN 0021-8995. Available: http://doi.wiley.com/10.1002/app.1157

[55]. https://www.lyondellbasell.com/en/products technology/polymers/resin type/poly propylene-homopolymer/https://grace.com/en-us/capabilities/process-licensing

[56]. https://grace.com/en-us/capabilities/process-licensing

[57]. https://www.cbi.com/What We Do/Technology/Petrochemicals/Olefins http://www.townsendsolutions.com/technology_22may2016_pptechnologyreview

[58]. http://www.townsendsolutions.com/technology_22may2016_pptechnologyreview

[59]. LOEHL, T. Borstar® Case Study. In: *Https://www.gpcaresearch.com* [online]. [ref. 2018-05-01]. Available: https://www.gpcaresearch.com/wp-content/uploads/2017/03/8-Dr.-Thorsten-Loehl.pdf

[60]. https://www.ineos.com/products/?bu=INEOS+O+%26+P+Europe&f=1

[61]. GALVAN, R. and M. TIRRELL: *Molecular weight distribution predictions for heterogeneous Ziegler-Natta polymerization using a two-site model* [online]. 2000 [ref. 2018-02-11]. DOI: 10.1016/0009-2509(86)85088-6. ISBN 10.1016/0009-2509(86)850886. Available: http://linkinghub.elsevier.com/retrieve/pii/0009250986850886

[62]. HAN KIM, S., E. MAGNI and G. A. SOMORJAI: Surface science studies of model Ziegler-Natta polymerization catalysts. *12th International Congress on Catalysis, Proceedings of the 12th ICC* [online]. Elsevier, 2000, 2000, , 3861-3866 [ref. 2018-02-17]. Studies in Surface Science and Catalysis. DOI: 10.1016/S0167-2991(00)80625-4. ISBN 9780444504807. Available: http://linkinghub.elsevier.com/retrieve/pii/S0167299100806254

[63]. TANGJITUABUN, K., S. YULL KIM, Y. HIRAOKA, T. TANIIKE, M. TERANO, B. JONGSOMJIT and P. PRASERTHDAM: *Effects of various poisoning compounds on the activity and stereospecificity of heterogeneous Ziegler–Natta catalyst* [online].[ref. 2018-02-24]. DOI: 10.1088/1468-6996/9/2/024402. ISBN 10.1088/14686996/9/2/024402.Available: http://www.tandfonline.com/doi/full/10.1088/1468-6996/9/2/024402

[64]. OSTROVSKII, N. and F. KENIG: About mechanism and model of deactivation of Ziegler-Natta polymerization catalysts. *Chemical Engineering Journal* [online]. 2005, **107**(1-3), 73-77 [ref. 2018-03-17]. DOI: 10.1016/j.cej.2004.12.012. ISSN 13858947.Available: http://linkinghub.elsevier.com/retrieve/pii/S138589470400395X

[65]. COSTA, M. A. S., A. L. S. S. SILVA, F. M. B. COUTINHO and M. DE SANTA: Highly active and stereospecific catalyst based on β-TiCl3 for propylene polymerization. *Polymer* [online]. 1996, **37**(5), 73-77 [ref. 2018-03-17]. DOI:

10.1016/0032-3861(96)87267-3. ISSN 00323861. Available: https://www.sciencedirect.com/science/article/pii/0032386196872673

[66]. RÖNKKÖ, H. L., T. KORPELA, H. KNUUTTILA, T. T. PAKKANEN, P. DENIFL, T. LEINONEN, M. KEMELL and M. LESKELÄ: Particle growth and fragmentation of solid self-supported Ziegler–Natta-type catalysts in propylene polymerization. *Journal of Molecular Catalysis A: Chemical* [online]. 2009, **309**(1-2), 40-49 [ref. 2018-03-17]. DOI: 10.1016/j.molcata.2009.04.013. ISSN 13811169. Available: http://linkinghub.elsevier.com/retrieve/pii/S1381116909002106

[67]. BUSICO, V., R. CIPULLO, G. TALARICO, A. L. SEGRE, J. C. CHADWICK, T. LEINONEN, M. KEMELL and M. LESKELÄ: New Evidence on the Nature of the Active Sites in Heterogeneous Ziegler−Natta Catalysts for Propene Polymerization. *Macromolecules* [online]. 1997, **30**(16), 4786-4790 [ref. 2018-03-17]. DOI: 10.1021/ma9704673. ISSN 0024-9297. Available: http://pubs.acs.org/doi/abs/10.1021/ma9704673

[68]. CORRADINI, P., V. BUSICO and R. CIPULLO: *2. Active Sites and Mechanisms of Stereospecificity in Heterogeneous Ziegler-Natta Catalysts* [online]. Elsevier, 1994, 1994, , 21-34 [ref. 2018-03-17]. Studies in Surface Science and Catalysis. DOI: 10.1016/S0167-2991(08)63018-9. ISBN 9780444986566. Available: http://linkinghub.elsevier.com/retrieve/pii/S0167299108630189

[69]. SHEN, X., Z. FU, J. HU, Q. WANG and Z. FAN: Mechanism of Propylene Polymerization with $MgCl_2$ -Supported Ziegler–Natta Catalysts Based on Counting of Active Centers: The Role of External Electron Donor. *The Journal of Physical Chemistry C* [online]. Elsevier, 2013, 1994, **117**(29), 15174-15182 [ref. 2018-03-17]. Studies in Surface Science and Catalysis. DOI: 10.1021/jp404416n. ISBN 9780444986566. ISSN 1932-7447. Available: http://pubs.acs.org/doi/10.1021/jp404416n

[70]. ZHENG, X., M. S. PIMPLAPURE, G. WEICKERT and J. LOOS: *Influence of Porosity on the Fragmentation of Ziegler-Natta Catalyst in the Early Stages of Propylene Polymerization* [online]. [ref. 2018-04-14]. DOI: 10.1515/epoly.2006.6.1.356. ISBN 10.1515/epoly.2006.6.1.356. Available: http://www.degruyter.com/view/j/epoly.2006.6.issue1/epoly.2006.6.1.356/epoly.2006.6.1.356.xml

6. List of symbols and abbreviations

Abbreviations

AA – Al-reduced and activated
ABS – Poly-acrylonitrile-butadiene-styrene
Al – Aluminum
$AlEt_3$ – Triethylaluminum
$AlEt_2Cl$ – Di-ethylaluminum chloride
AlR_2Cl – Alkylaluminum chloride

B.D – Bulk density
C – Carbon
C_3H_6 – Propene
Cat – Catalyst
CHMDMS – Cyclohexyl methyl dimethoxysilane
Cl – Chloride
CO – Carbon monoxide
COS – Carbonyl sulfide
Cp – Cyclopentadienyl
CSTR – Continuous stirred-tank reactor
DIBDMS – Di-i-butyl dimethoxysilane
DIBP – Di-i-butyl phthalate
DPP Degree of pre–polymerization
EB – Ethyl benzoate
ED – External donor
$Et(Ind)_2ZrC1_2$ – Ethylene bisindenyl zirconium
Eq. – Equation
GC – Gas chromatography
H_2 – Hydrogen
H_2O – Water
ID – Internal donor
I.I – Index isotacticity
Ind – Indenyl
Inj. – Injection
IPP – Isothermal pre–polymerization
MAO – Methyl alumoxane
MFR – Melt mass-flow rate
$MgCl_2$ – Magnesium dichloride
MMT – Million Metric Tons
NIPP – Nonisothermal pre–polymerization
O_2 – Oxygen
P – Pressure
PC – Personal computer
PE – Polyethylene
PLC – Programmablelogicalcontroller
PP – Polypropene
PSD – Particle size distribution
PVC – Polyvinylchloride
Rp – Polymerization rate
T – Temperature
Ti – Titanium
$TiCl_3$ – Titanium tri-chloride
$TiCl_4$ – Titanium tetra-chloride

$Ti(Cp)_2Cl_2$	–	Bis(cyclopentadienyl) titaniumdichloride
X.S	–	Xylene solubles
ZN	–	Ziegler–Natta

Symbols

Cat-[]	–	Catalyst free site
ρ	–	Density

7. APPENDIX

Table 3.1.1: *Powder fractions determined by sieving on different screens (wt.% on screen with mesh size in mm).*

Screen mesh size [mm]	**4.00**	**3.15**	**2.50**	**2.24**	**2.00**	**1.80**	**1.50**	**1.25**	**1.00**	**0.80**	**0.50**	**0.20**	**0.10**	**0.05**	**frit S3**
Not pre–polymerized catalyst	0.00	0.00	7.37	20.17	17.80	15.46	16.23	3.00	4.12	4.22	4.63	4.94	1.42	0.51	0.11
Oval egg–shaped stirring bar	0.00	0.00	0.00	0.95	3.23	5.08	21.29	18.17	14.41	14.37	11.39	6.04	3.00	1.58	0.48
Octagonal–shaped stirring bar	0.00	0.00	2.50	1.03	9.61	13.47	24.51	19.28	16.65	6.14	4.58	1.85	0.25	0.10	0.05
Stirring by analytical shaker	0.00	0.00	20.97	20.82	17.69	14.59	12.81	4.31	5.92	1.33	1.10	0.23	0.06	0.06	0.11

Table 3.7.2 *Polymer powder fractions determined by sieving on different screens (wt.% on screen with mesh size in mm).*

Screen mesh size [mm]	**4.00**	**3.15**	**2.50**	**2.24**	**2.00**	**1.80**	**1.50**	**1.25**	**1.00**	**0.80**	**0.50**	**0.20**	**0.10**	**0.05**	**frit S3**
T_{inj} = 40 °C, not pre–polymerized cat.	0.00	0.00	7.37	20.17	17.80	15.46	16.23	3.00	4.12	4.22	4.63	4.94	1.42	0.51	0.11
T_{inj} = 70 °C, not pre–polymerized cat.	0.00	0.00	0.27	3.56	9.07	8.74	22.25	9.47	10.66	9.37	13.42	10.74	1.77	0.49	0.20
T_{inj} = 40 °C, pre–polymerized cat.	0.00	0.00	8.01	22.45	20.03	17.67	19.51	4.48	2.49	2.35	1.68	0.65	0.36	0.27	0.06
T_{inj} = 70 °C, pre–polymerized cat.	0.00	0.00	0.81	9.05	14.19	15.89	29.38	8.83	9.96	5.99	3.91	1.32	0.30	0.31	0.06